# Guidebook for NTU-Caltech Taiwan Field Trip, June 2008


## Special Thanks to Sponsors:

**The Sharp Venture Fund**

**National Taiwan University**


**TABLE OF CONTENTS**

## ITINERARY

### Day 1 – Monday 6/16 Taipei

Recovery from Jet lag; Visit at Dept. Geosciences
Trip introduction and lectures on general geology of Taiwan
Hotel: guesthouse of NTU

### Day 2 – Tuesday 6/17 Taipei to Taichung

(1) Deformed Quaternary Tableland and the Frontal Thrust systems.
(2) Surface rupture of the 1999 Chi-Chi earthquake.
(3) "Great Canyon" of the Ta-An chi at Cholan.
Stops: Huo-Yan-Shan, Bi-Fong Bridge, Nei-Wan. Hotel: Taichung

### Day 3 – Wednesday 6/18 Taichung to Nantou

(1) Surface rupture of the 1999 Chi-Chi earthquake.
(2) Transect of the Fold-and-thrust belt.
Stops: Pa-Kua-Shan. Hotel: Chiayi

### Day 4 – Thursday 6/19 Nantou to Tainan

(1) Fold-and-thrust belt (or accretionary wedge) in Southwestern Taiwan.
(2) Mud volcanoes and bad land.
Stops: Tian-Liao. Hotel: Tainan

### Day 5 – Friday 6/20 Tainan to Kenting

(1) Different geomorphic features in the frontal thrust zone in southwestern Taiwan: the Tainan tableland, Xiaguangshan uplift coral reef.
(2) Kenting mélange.
(3) Uplift coral reef and marine terraces.
Stops: Tai-Nan Tableland, Bao-Li-Ci. Hotel: Hengchun

### Day 6 – Saturday 6/21 Kenting to Taitung

(1) Lichi mélange.
(2) Active faults along the southernmost Longitudinal Valley.
Stops: Tai-Dong Bridge. Hotel: Taitung

**Day 7 – Sunday 6/22** **Taitung to Rueyshui**

Active faults at the plate suture along the Longitudinal Valley.
Hotel: Rueyshui

**Day 8 – Monday 6/23** **Rueyshui to Hualien**

Transect and cross section of the Coastal Range along the Hsiuguoluan River: deformed Luzon Volcanic arc and the intra-arc basins
Stops: Siou-Gu-Luan-Ci. Hotel: Hualien

**Day 9 – Tuesday 6/24** **Hualien-Taroko-Hualien**

Ductile deformation of poly-metamorphosed pre-Tertiary basement.
Stops: Shen-Mi-Gu. Hotel: Hualien

**Day 10 – Wednesday 6/25** **Hualien to Ilan**

(1) Transect of ductile deformation of the poly-metamorphosed basement and the slate belt along the Coast Road.
(2) Visit western extremity of the Okinawa Trough: the Ilan Plain.
Stops: I-Lan. Hotel: Ilan

**Day 11 – Thursday 6/26** **Ilan to Taipei**

(1) Thrust, strike-slip and rotational tectonics of the northeastern Coast.
(2) Quaternary Tatun andesite volcanoes with hot spring fumarole and solfataras.
Stops: Long-Dong, Bei-Tou. Hotel: Taipei

**Day 12 –Friday 6/27** **Taipei**

(1) Visit to IES, Academia Sinica.
(2) Cultural sight seeing in Taipei.
Hotel: Taipei

**Day 13 – Saturday 6/28** **Taipei**

Cultural sight seeing in Taipei.
Hotel: Taipei

**Day 14 – Sunday 6/29** **Taipei to LAX**

Field Trip Itinerary

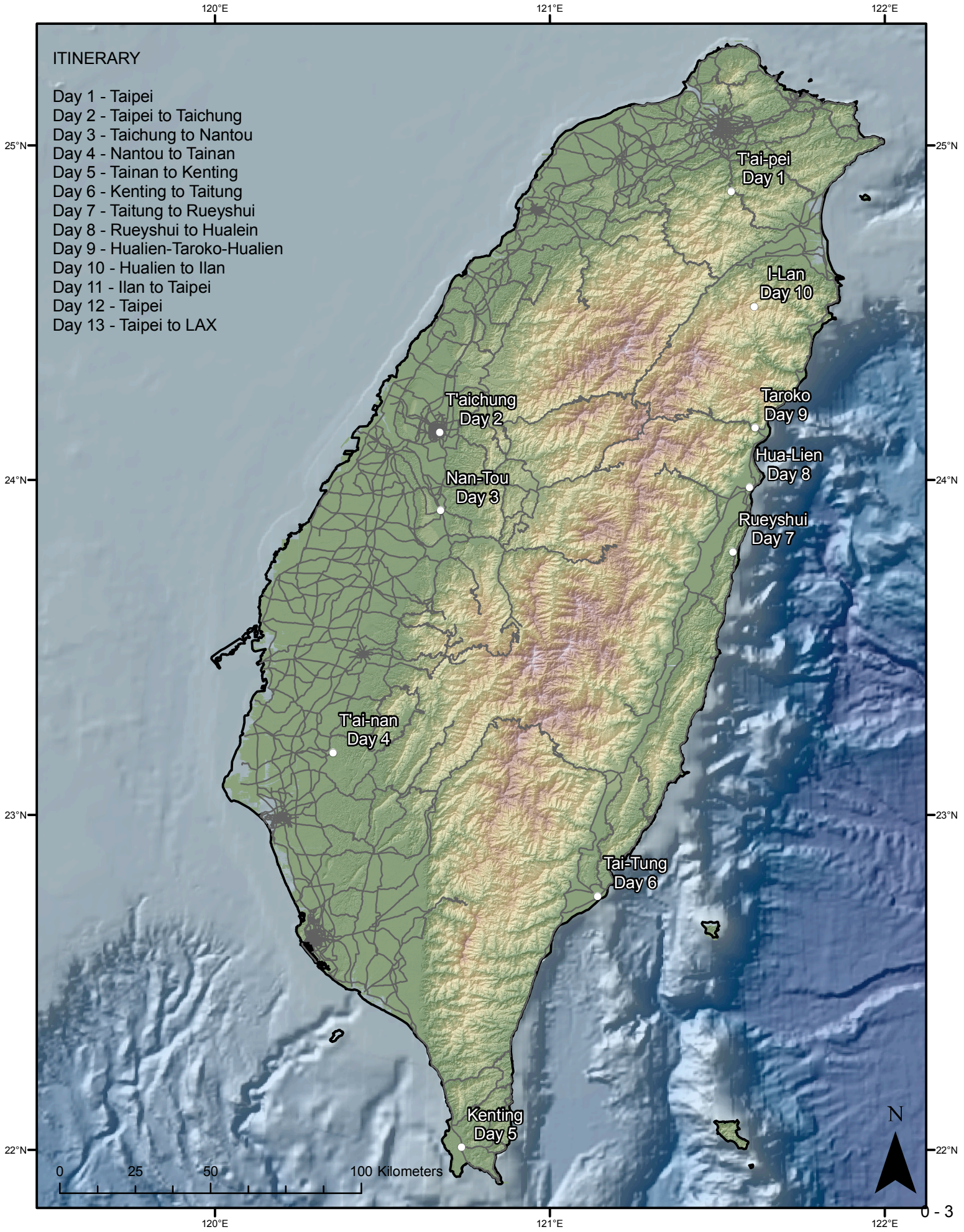

## LIST OF PARTICIPANTS

### Taiwan:

| | |
|---|---|
| Yue-Gau Chen (instructor) | ygchen@ntu.edu.tw |
| Jian-Cheng Lee (instructor) | jclee@earth.sinica.edu.tw |
| Yoko Ota (instructor) | yokoota@ntu.edu.tw |
| Bruce Shyu (instructor) | jbhs@gps.caltech.edu |
| Chia-Yu Chen | b93204038@ntu.edu.tw |
| Dung | r96224219@ntu.edu.tw |
| Chin-Wei Hsu | r96224101@ntu.edu.tw |
| Yu-Ting Kuo (organizer) | yutingkuo@ntu.edu.tw |
| I-Ching Lai | r96224101@ntu.edu.tw |
| Yen-Sheng Lin | b93204034@ntu.edu.tw |
| I-Wei Liu | lew1212@ms65.hinet.net |
| Chung-Hsiang Mu | momo@app.geo.ncu.edu.tw |
| Wei Peng | r96224113@ntu.edu.tw |

### Caltech:

| | |
|---|---|
| Jean-Philippe Avouac (instructor) | avouac@gps.caltech.edu |
| Min Chen | mchen@gps.caltech.edu |
| Gina Gage | gage@caltech.edu |
| Aimee Gillespie | aimee@caltech.edu |
| Marie Giron | giron@caltech.edu |
| Steve Kidder | kidder@gps.caltech.edu |
| Kevin Lewis | klewis@gps.caltech.edu |
| Andrew Matzen | amatzen@caltech.edu |
| Sierra Petersen | sierra.petersen@gmail.com |
| Daoyuan Sun | sdy@gps.caltech.edu |
| Xiangyan Tian | xytian@gps.caltech.edu |
| June Wicks | wicks@caltech.edu |

# Taiwan Geology - Geologic Age

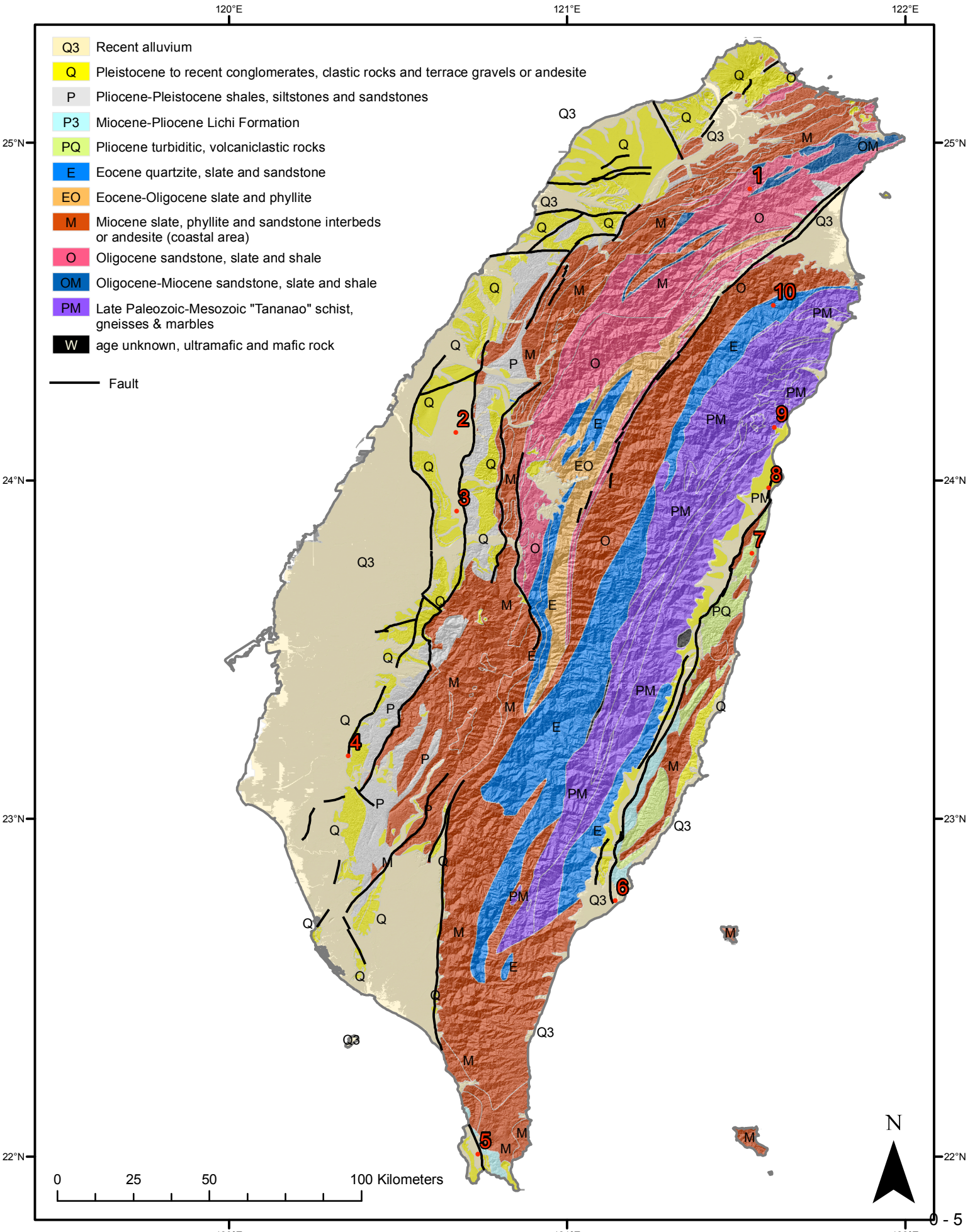

Taiwan Historical Earthquakes 1991-2000

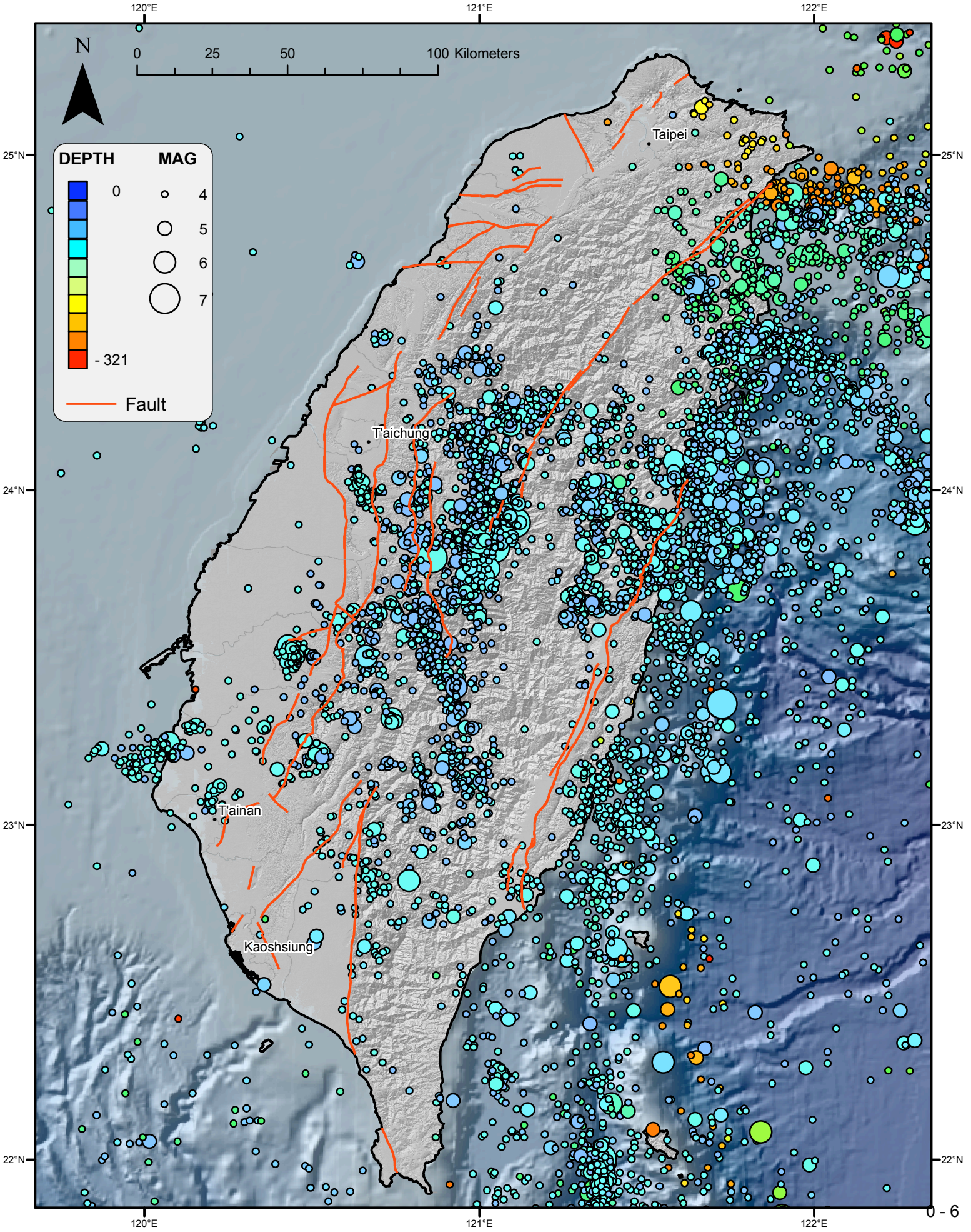


Taiwan GPS data

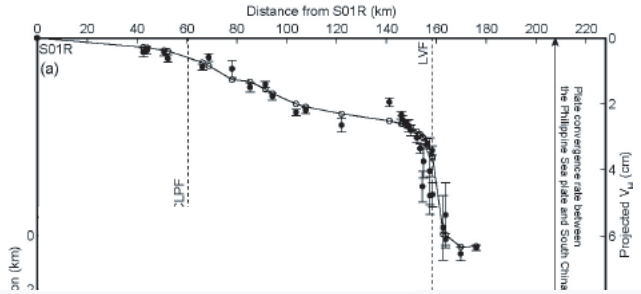


Cumulative displacement based on GPS, roughly to scale with cross section below

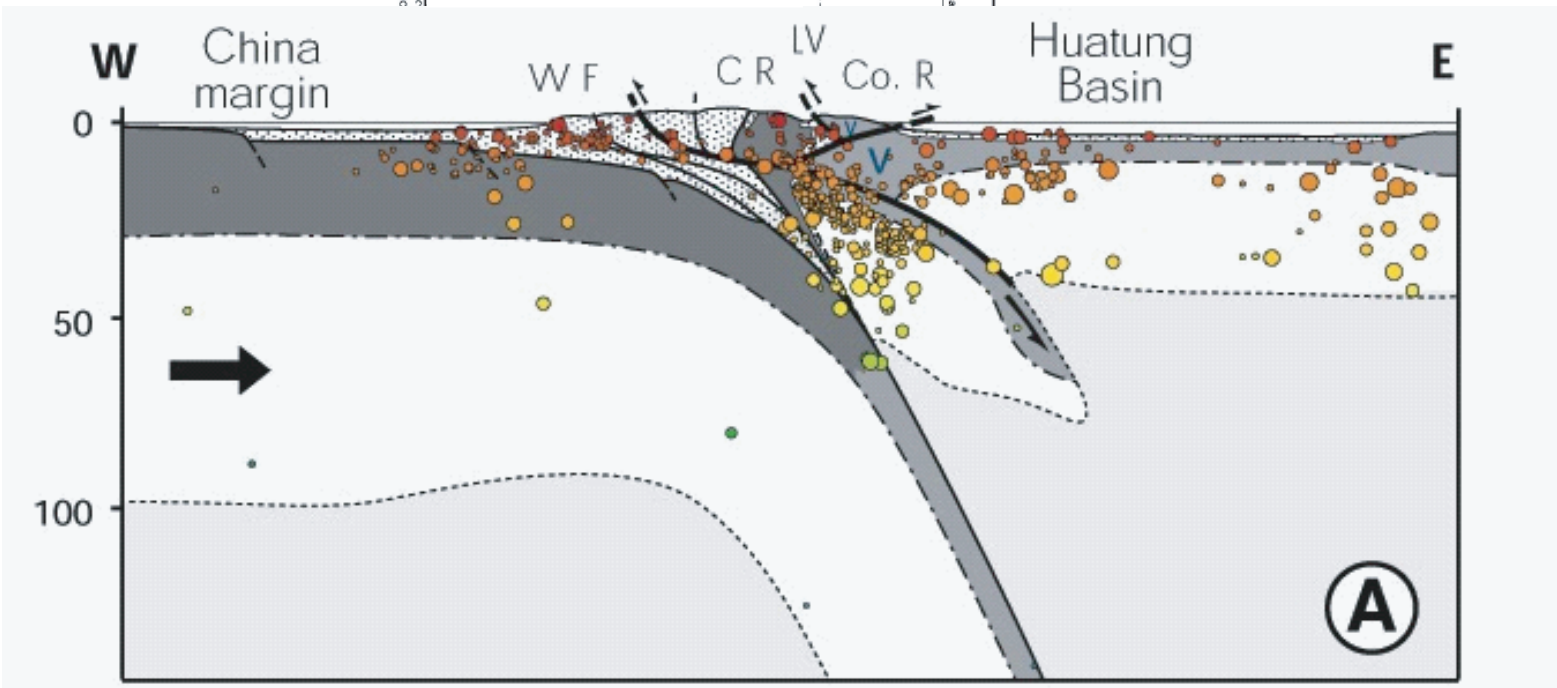

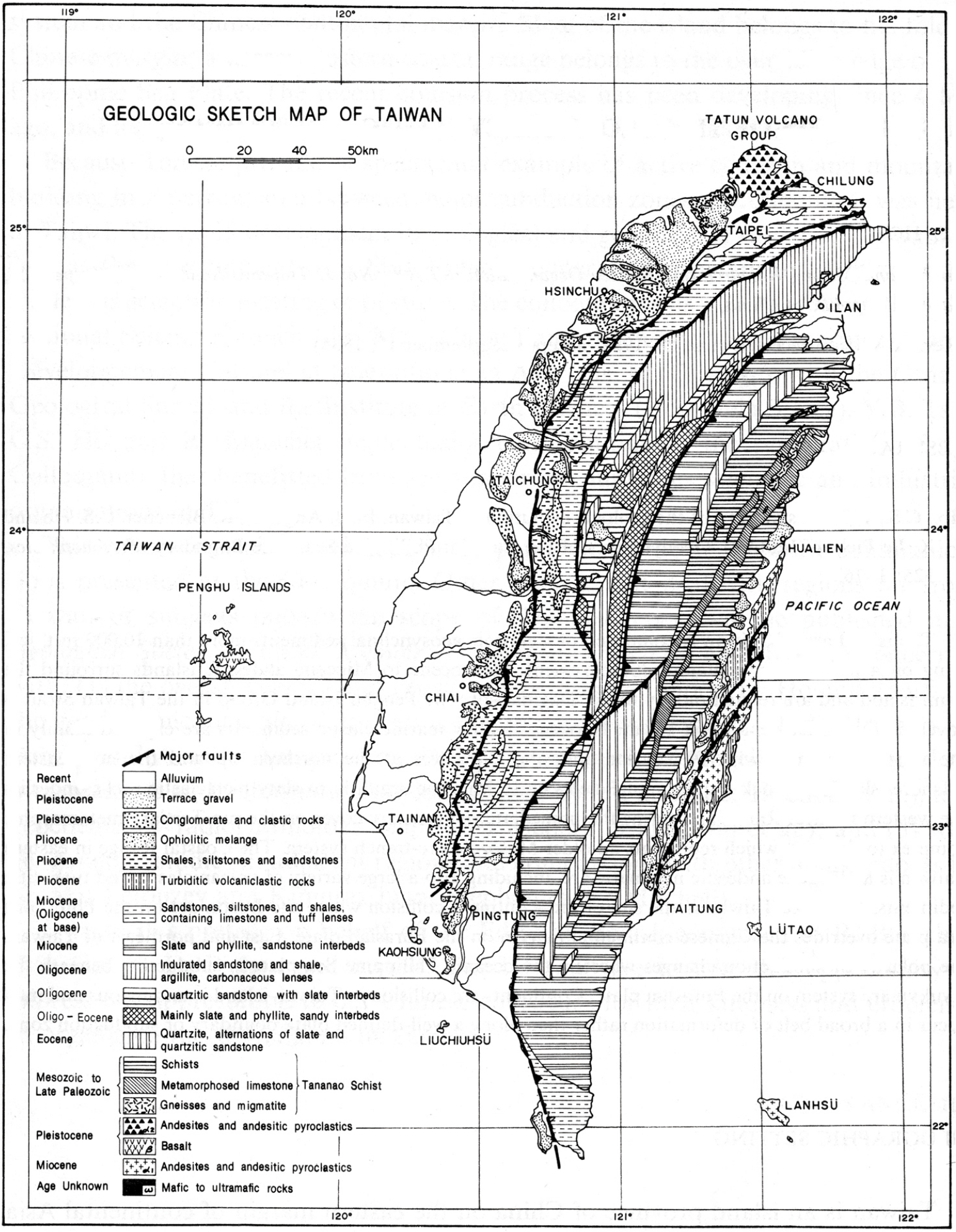


Fig. 1. Geologic sketch map of Taiwan showing age, lithology, and distribution of various stratigraphic units and the major faults or tectonic contacts. (Ho, 1986(?))

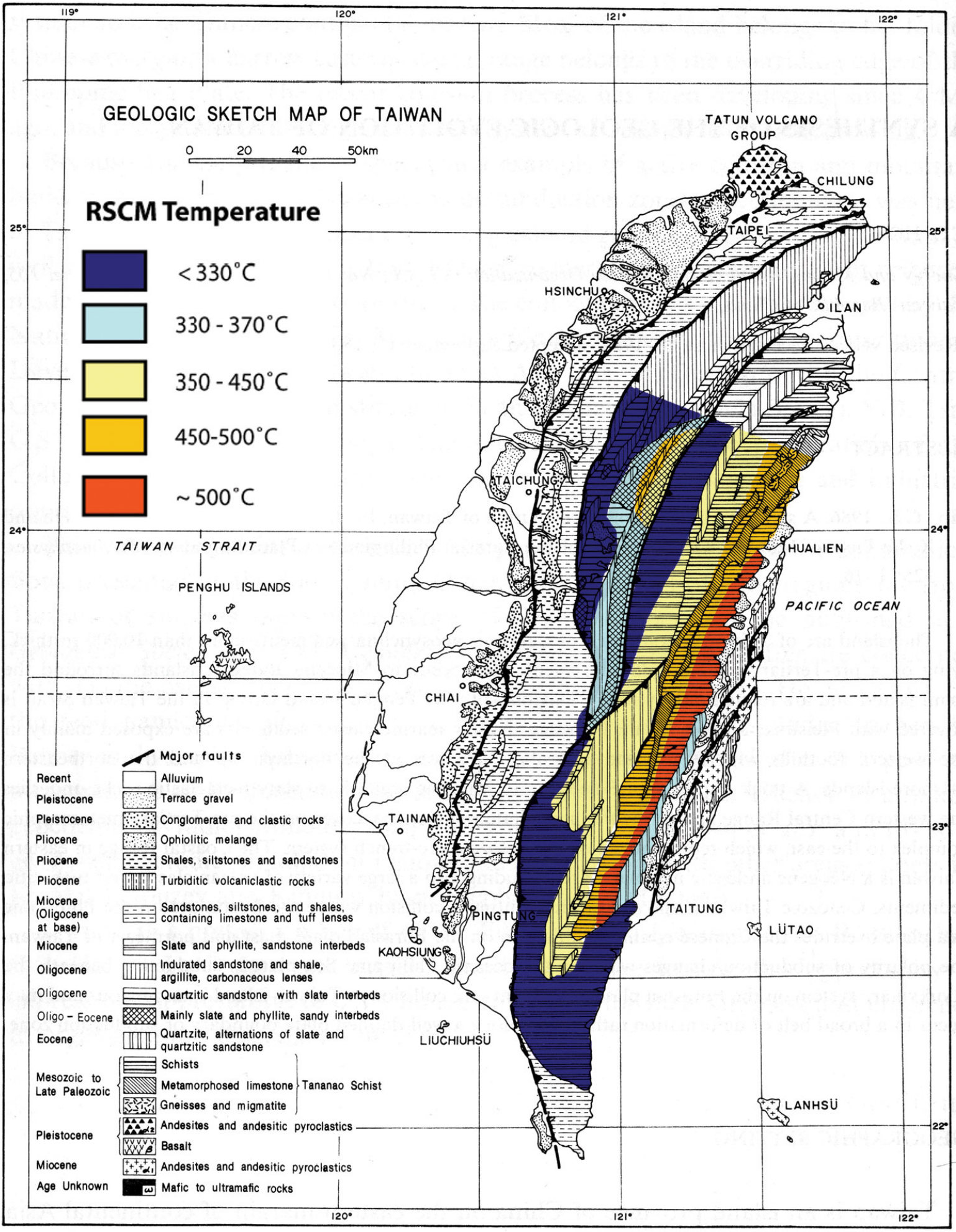


Fig. 1. Geologic sketch map of Taiwan showing age, lithology, and distribution of various stratigraphic units and the major faults or tectonic contacts. (map: Ho, 1986(?), Temperatures: Beyssac et al, 2007)

General Cross Sections across Taiwan

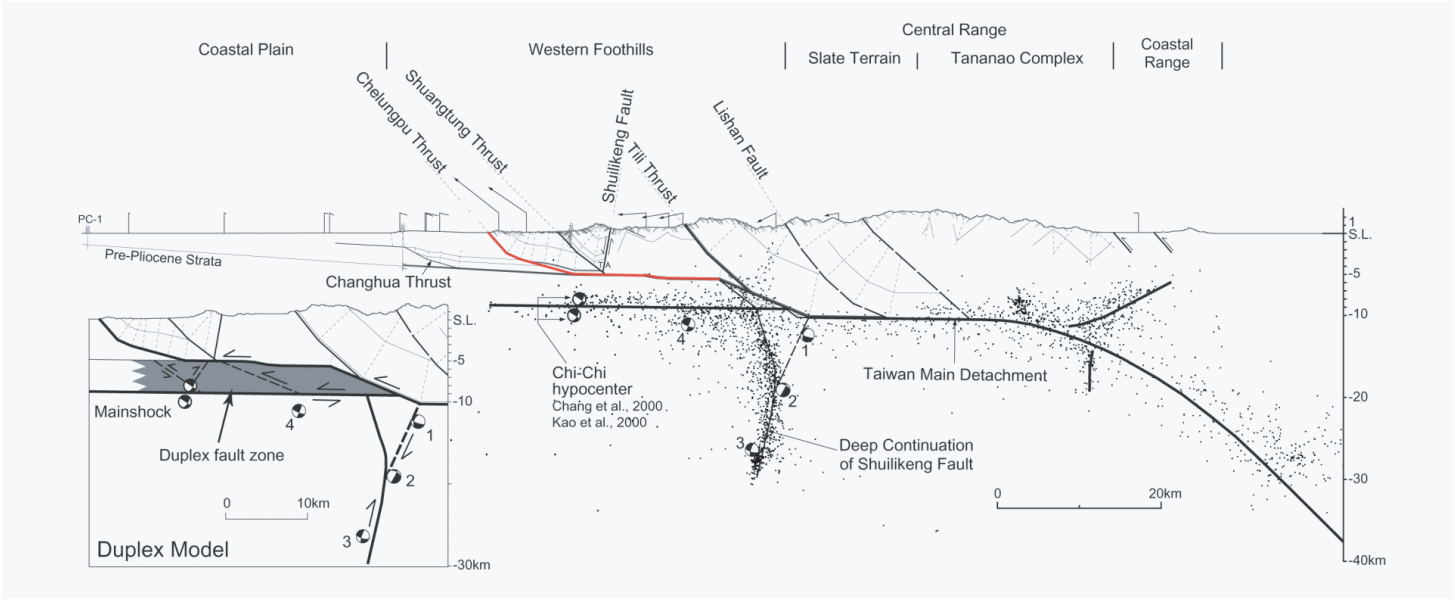


Yue, Suppe & Hung (2005)

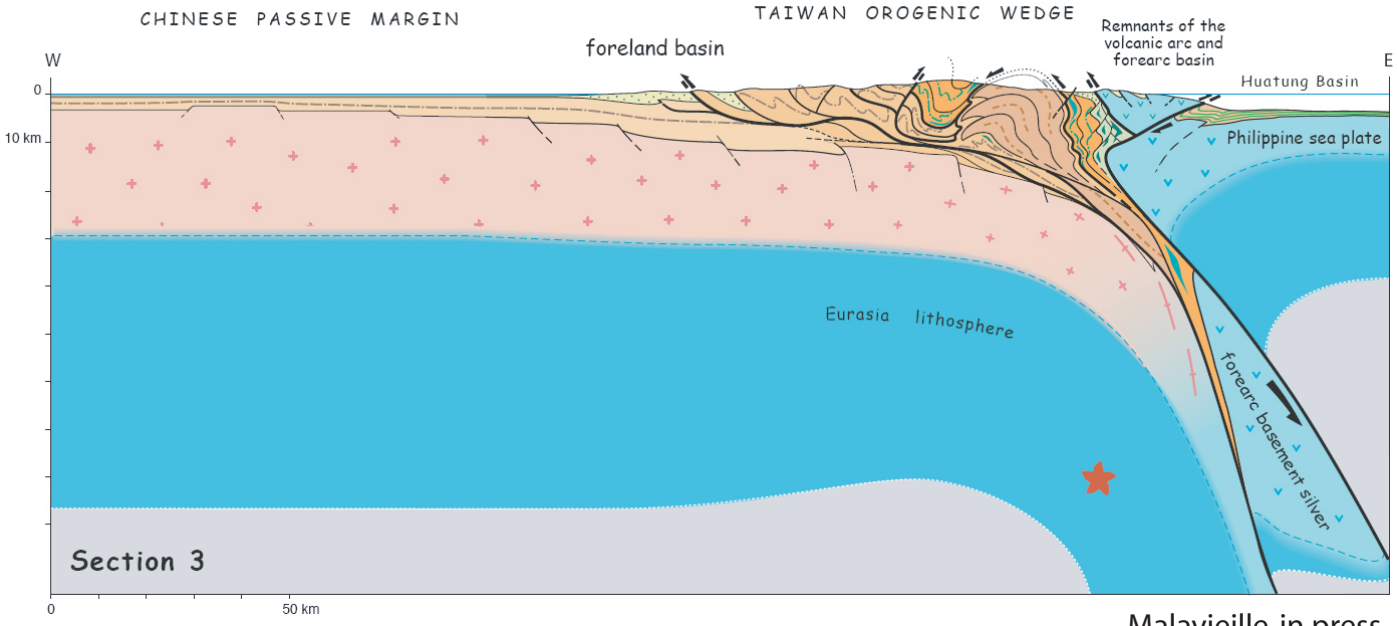


Malavieille, in press

Day Index

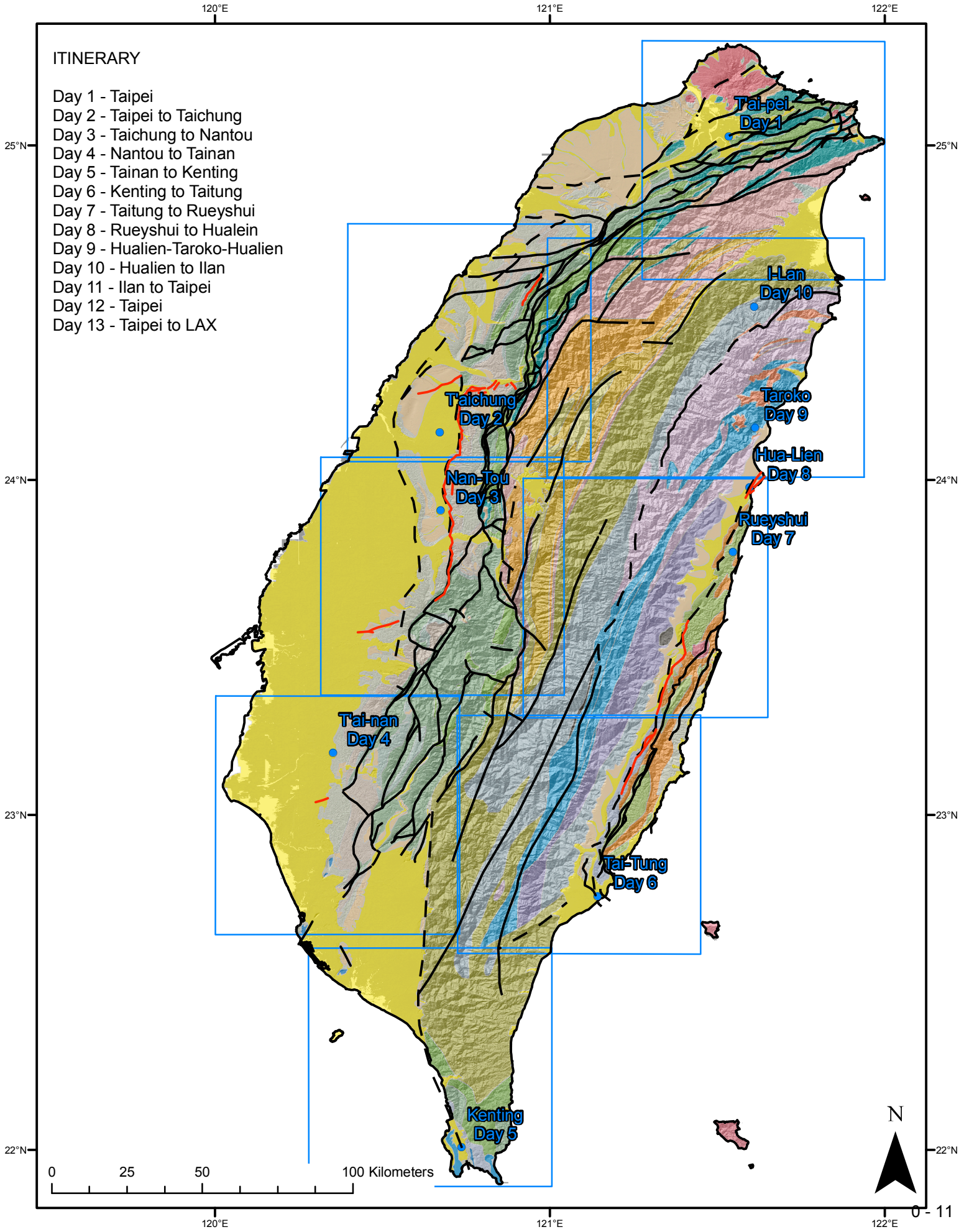
ITINERARY
Day 1 - Taipei
Day 2 - Taipei to Taichung
Day 3 - Taichung to Nantou
Day 4 - Nantou to Tainan
Day 5 - Tainan to Kenting
Day 6 - Kenting to Taitung
Day 7 - Taitung to Rueyshui
Day 8 - Rueyshui to Hualein
Day 9 - Hualien-Taroko-Hualien
Day 10 - Hualien to Ilan
Day 11 - Ilan to Taipei
Day 12 - Taipei
Day 13 - Taipei to LAX
120°E
121°E
122°E
25°N
24°N
23°N
22°N
T'ai-pei
Day 1
I-Lan
Day 10
T'aichung
Day 2
Taroko
Day 9
Hua-Lien
Day 8
Nan-Tou
Day 3
Rueyshui
Day 7
T'ai-nan
Day 4
Tai-Tung
Day 6
Kenting
Day 5
0
25
50
100 Kilometers
N

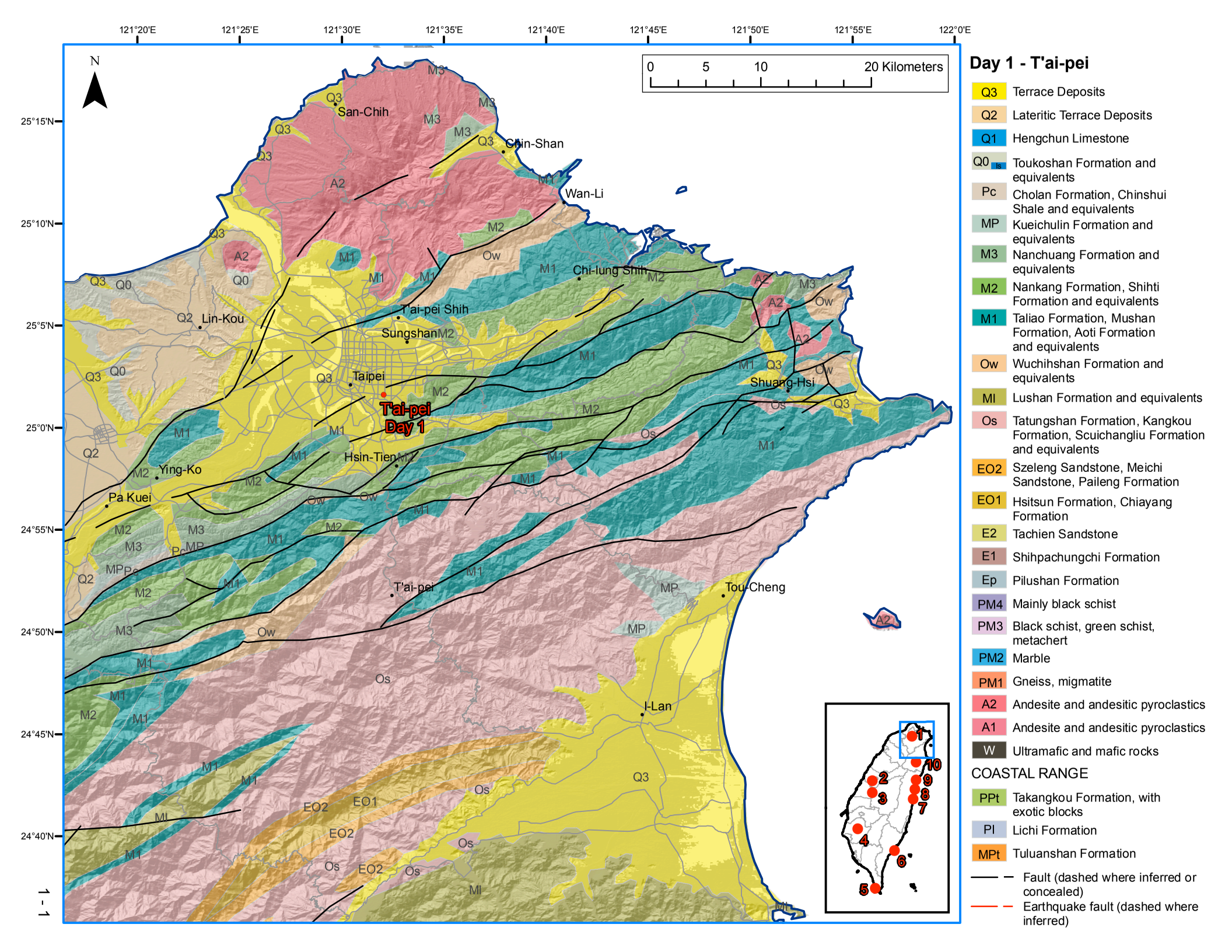
121°20'E
121°25'E
121°30'E
121°35'E
121°40'E
121°45'E
121°50'E
121°55'E
122°0'E
25°15'N
25°10'N
25°5'N
25°0'N
24°55'N
24°50'N
24°45'N
24°40'N
N
0 5 10 20 Kilometers
San-Chih
Chin-Shan
Wan-Li
Chi-lung Shih
T'ai-pei Shih
Lin-Kou
Sungshan
Taipei
T'ai-pei
Day 1
Shuang-Hsi
Hsin-Tien
Ying-Ko
Pa Kuei
T'ai-pei
Tou-Cheng
I-Lan
1 - 1
Day 1 - T'ai-pei
Q3 Terrace Deposits
Q2 Lateritic Terrace Deposits
Q1 Hengchun Limestone
Q0 ls Toukoshan Formation and equivalents
Pc Cholan Formation, Chinshui Shale and equivalents
MP Kueichulin Formation and equivalents
M3 Nanchuang Formation and equivalents
M2 Nankang Formation, Shihti Formation and equivalents
M1 Taliao Formation, Mushan Formation, Aoti Formation and equivalents
Ow Wuchihshan Formation and equivalents
Ml Lushan Formation and equivalents
Os Tatungshan Formation, Kangkou Formation, Scuichangliu Formation and equivalents
EO2 Szeleng Sandstone, Meichi Sandstone, Paileng Formation
EO1 Hsitsun Formation, Chiayang Formation
E2 Tachien Sandstone
E1 Shihpachungchi Formation
Ep Pilushan Formation
PM4 Mainly black schist
PM3 Black schist, green schist, metachert
PM2 Marble
PM1 Gneiss, migmatite
A2 Andesite and andesitic pyroclastics
A1 Andesite and andesitic pyroclastics
W Ultramafic and mafic rocks
COASTAL RANGE
PPt Takangkou Formation, with exotic blocks
Pl Lichi Formation
MPt Tuluanshan Formation
Fault (dashed where inferred or concealed)
Earthquake fault (dashed where inferred)

# DAY ONE – Monday 6/16/08

Taiwan is an exceptional area to investigate orogenic processes because of very rapid rates of deformation and erosion, as well as because of the wealth of data already available (geodynamic setting, structure of the crust, recent deformation documented by GPS and tectonic geomorphology…). The occurrence of the Mw=7.6 Chichi earthquake in 1999 allows for investigating how deformation resulting from earthquakes or from slower aseismic processes during postseismic relaxation, or during the interseismic period, contribute jointly to geological deformation over the long term.

**Taiwan finds itself in a very geodynamic setting.**

Taiwan is located at the boundary between the Philippine Sea Plate to the East and the Eurasian Plate to the West, with a convergence rate of ~ 80 mm/yr in a ~N118E direction [***Seno*, 1977**; ***Yu et al.*, 1997**]. This plate boundary is rather complex since it comprises two subduction zones of reverse polarities. To the southwest, the ongoing consumption of the oceanic crust of the South China Sea led to the collision between the Chinese Continental Margin and the Luzon Volcanic Arc ~ 6.5 Ma ago [e.g ***Lin et al.*, 2003**], that resulted in the Taiwanese mountain range.

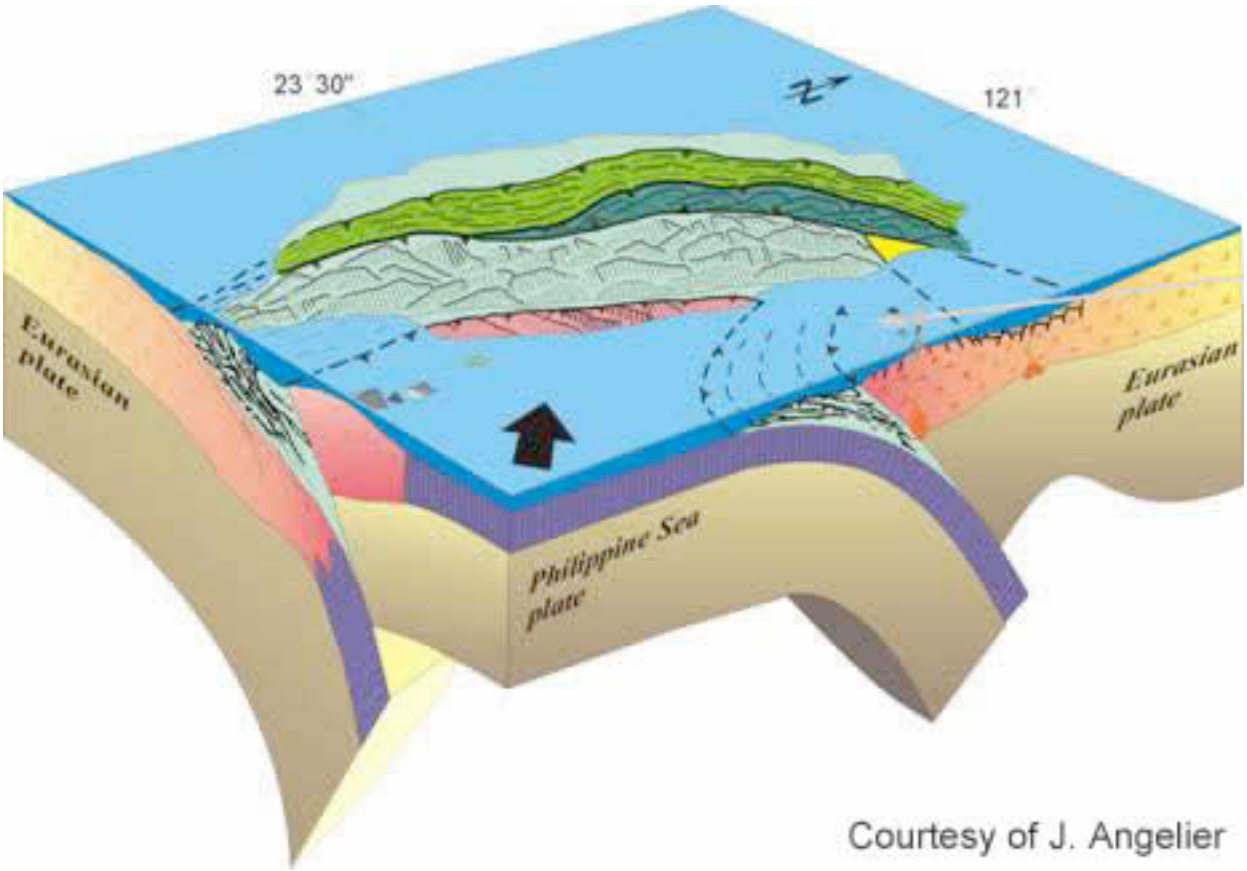


Figure 1: Geodynamic setting of the island of Taiwan.

Because of the obliquity of the convergence, the collision propagated to the south: the collision is mature and fading to the north of the island while to the south, the South China Sea is still subducting along the Manila Trench. Consequently, Taiwan is the perfect location to better understand how the transition from subduction to collision occurs.

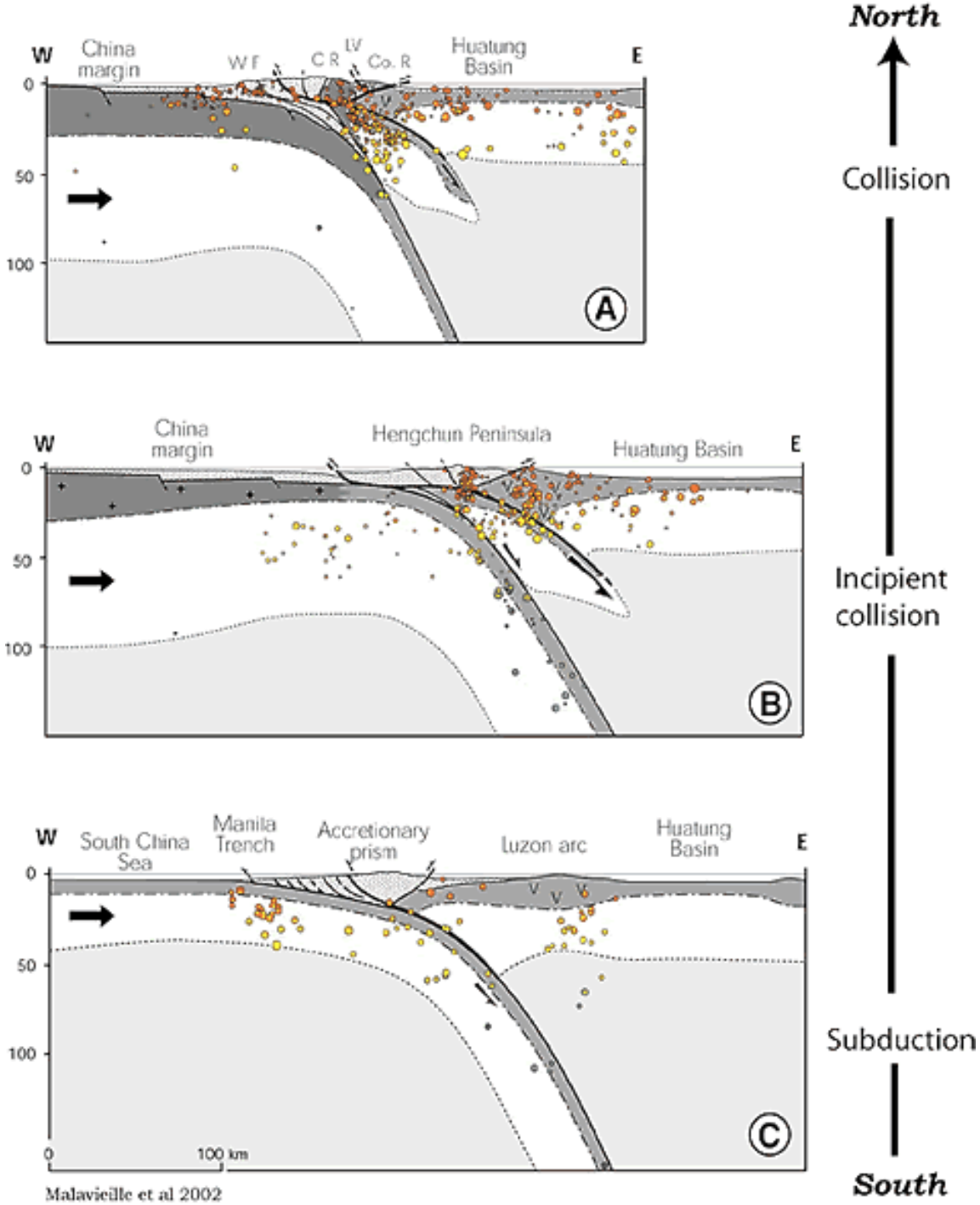


Figure 2: Transition from subduction of the oceanic crust of the South China Sea beneath the Manila Trench to the south (C), to mature collision between the Luzon volcanic arc and the Chinese passive margin in Central Taiwan (A). Incipient collision (B) occurs in the area of the Hengchun Peninsula in southernmost Taiwan. Sketches are from **[*Malavieille et al.*, 2002]**.

**The geology of Taiwan may be described in terms of different separated units.**

- **The Coastal Range** which corresponds to the accreted Luzon volcanic arc.
- **The Longitudinal Valley** which is considered as the suture zone between the Luzon arc and the Chinese continental margin.
- **The Tananao Schists** are comprised of the metamorphic pre-Tertiary basement of the Eurasian passive margin. In addition to the most recent metamorphic event, this unit has also recorded past orogenic events.
- **The Slate belt**, composed of metamorphosed and deformed sediments of the Chinese passive margin, with from East to West:
  - **The Backbone Range,** with mostly Miocene to Eocene slates, corresponds to the area of highest altitudes in the island.
  - **The Hsueshan Range**, composed of mostly Eocene and Oligocene sediments.
- **The Western Foothills**, at lower altitudes, where syn-orogenic sediments of the foreland basin have been accreted and deformed.
- **The Coastal Plain** which is part of the present foreland basin of Taiwan.

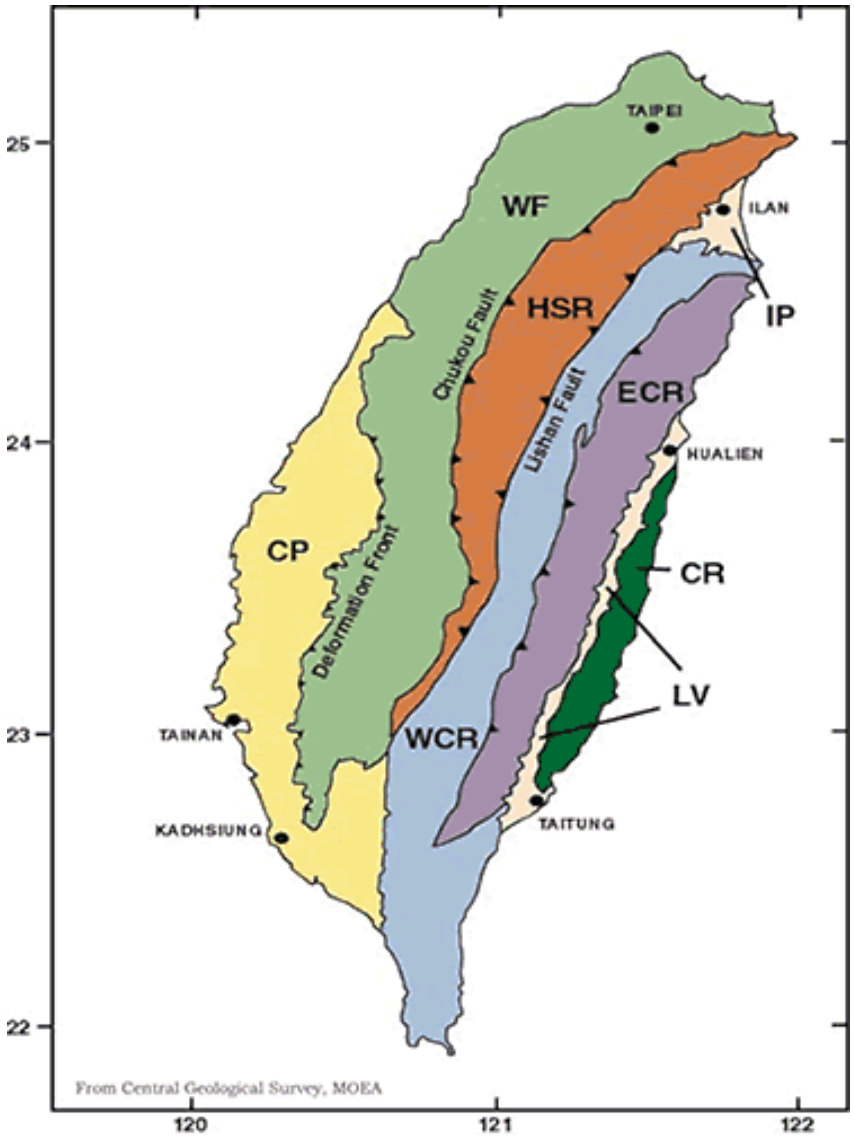


Although, the degree of metamorphism in the Slate belt cannot be easily documented due to the poor mineralogy of these rocks, it is thought that metamorphism increases from west to east across the Taiwanese range.

Figure 3: Major geological units of the Island of Taiwan. CR: Coastal Range; LV: Longitudinal Valley; ECR: East Central Range or Tananao Schist complex; WCR: West Central Range or Backbone Range; HSR: Hsueshan Range; WF: Western Foothills; CP: Coastal Plain. From Central Geological Survey of Taiwan-MOEA.

**Since the early 80's and 90's, Taiwan has been referred to as the best example of the "critical wedge" type mountain belt.**

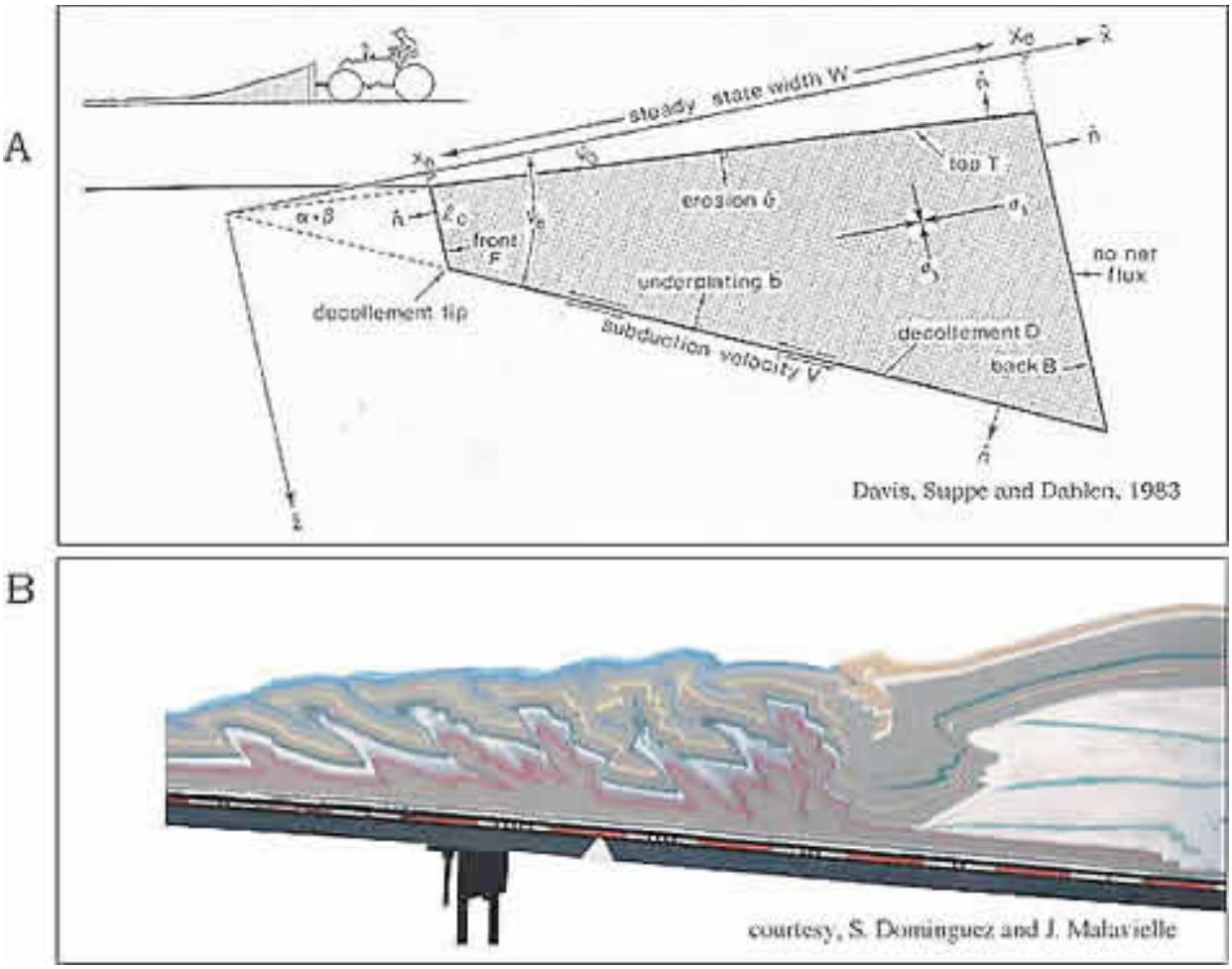


Figure 4: Critical wedge model of mountain belts. A: Basics of such model as proposed by [***Davis et al.*, 1983**]; it was refined later by [***Barr and Dahlen*, 1989**; ***Barr et al.*, 1991**; ***Dahlen and Barr*, 1989**; ***Suppe*, 1981**] for Taiwan. Rocks get to be deformed as sand would be in front of a rigid buttress overriding a rigid footwall. B: Sand-box experiment image (courtesy of J. Malavieille) illustrating this model.

In this model, a mountain belt is viewed as a deforming wedge whose geometry reflects the balance between frictional stresses at the bottom, and gravitational loads induced by the topography. The mountain belt mostly grows by frontal accretion and internal thickening. Since the wedge has to maintain its equilibrium geometry, horizontal shortening is expected to be distributed, such as the active faults that accommodate this deformation. The model successfully accounts for some aspects of the Taiwan orogen, such as its gross topography and metamorphic structure; it had been tested, given the data that were available by then. However, new constraints documenting mountain-building processes in Taiwan had been published since, and even more should result from the several TO investigations, so that this model needs be re-evaluated and tested in light of these new data.

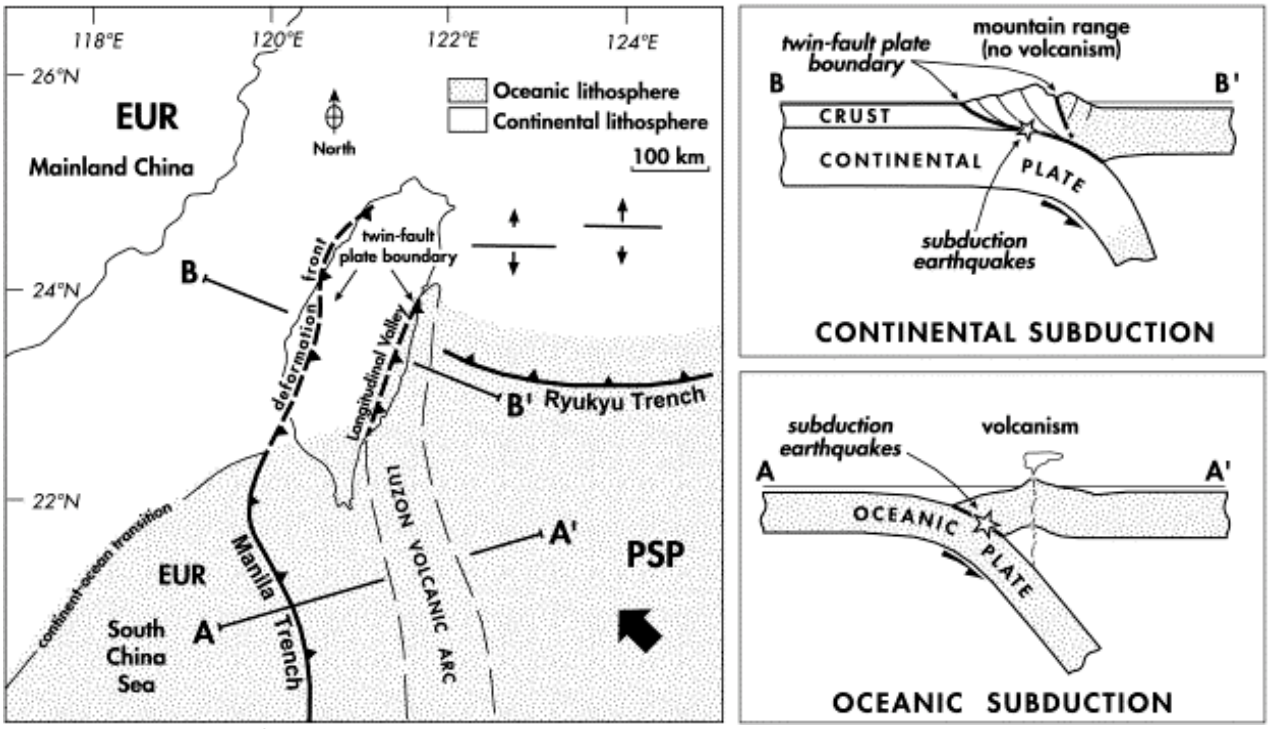


Figure 5: Location of major plate boundaries in and around Taiwan. The two schematic sections AA! and BB! are located on the map. This figure is modified from Lallemand amd Amgelier (2000b) and Lallemand (2000).

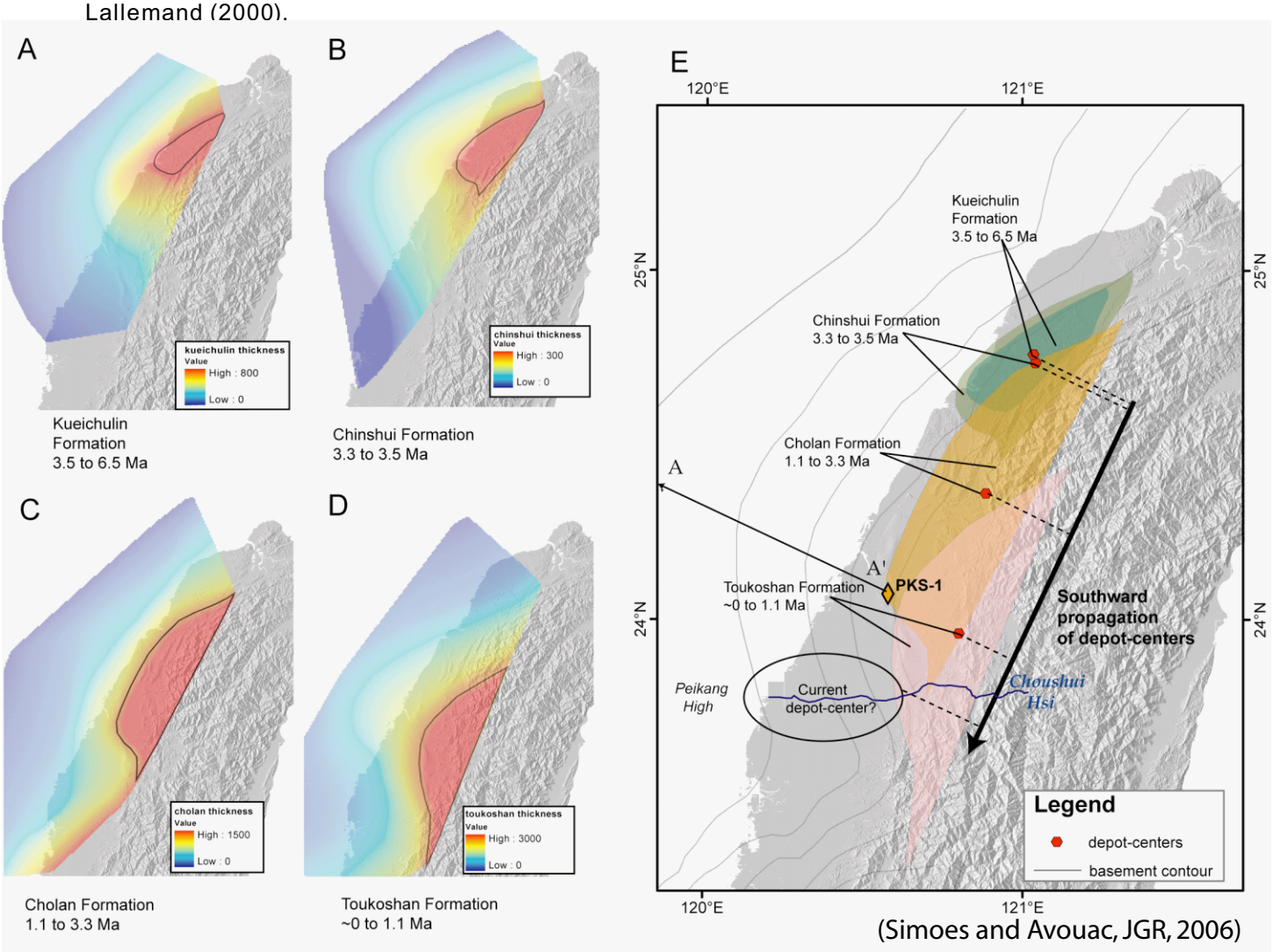


Figure: Southward propagation of the foreland basin depot centers at 31mm/yr

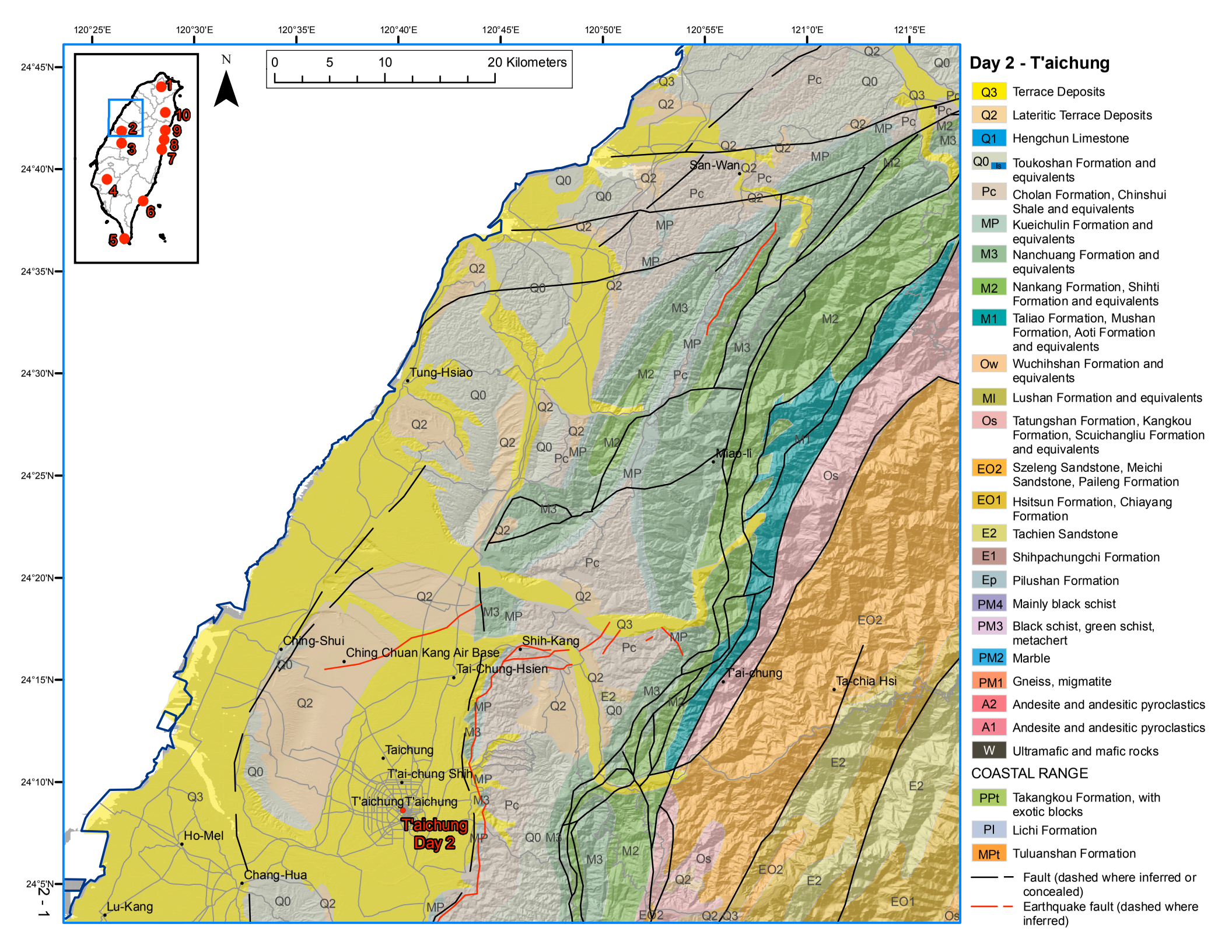
120°25'E
120°30'E
120°35'E
120°40'E
120°45'E
120°50'E
120°55'E
121°0'E
121°5'E
24°45'N
24°40'N
24°35'N
24°30'N
24°25'N
24°20'N
24°15'N
24°10'N
24°5'N
N
0 5 10 20 Kilometers
1
2
3
4
5
6
7
8
9
10
San-Wan
Tung-Hsiao
Miao-li
Ching-Shui
Ching Chuan Kang Air Base
Tai-Chung-Hsien
Shih-Kang
T'ai-chung
Ta-chia Hsi
Taichung
T'ai-chung Shih
T'aichung
T'aichung
T'aichung
Day 2
Ho-Mei
Chang-Hua
Lu-Kang
Day 2 - T'aichung
Q3 Terrace Deposits
Q2 Lateritic Terrace Deposits
Q1 Hengchun Limestone
Q0 ls Toukoshan Formation and equivalents
Pc Cholan Formation, Chinshui Shale and equivalents
MP Kueichulin Formation and equivalents
M3 Nanchuang Formation and equivalents
M2 Nankang Formation, Shihti Formation and equivalents
M1 Taliao Formation, Mushan Formation, Aoti Formation and equivalents
Ow Wuchihshan Formation and equivalents
Ml Lushan Formation and equivalents
Os Tatungshan Formation, Kangkou Formation, Scuichangliu Formation and equivalents
EO2 Szeleng Sandstone, Meichi Sandstone, Paileng Formation
EO1 Hsitsun Formation, Chiayang Formation
E2 Tachien Sandstone
E1 Shihpachungchi Formation
Ep Pilushan Formation
PM4 Mainly black schist
PM3 Black schist, green schist, metachert
PM2 Marble
PM1 Gneiss, migmatite
A2 Andesite and andesitic pyroclastics
A1 Andesite and andesitic pyroclastics
W Ultramafic and mafic rocks
COASTAL RANGE
PPt Takangkou Formation, with exotic blocks
Pl Lichi Formation
MPt Tuluanshan Formation
Fault (dashed where inferred or concealed)
Earthquake fault (dashed where inferred)

# Geomorphic evidence for prior earthquakes: Lessons from the 1999 Chichi earthquake in central Taiwan

Yue-Gau Chen*,1, Wen-Shan Chen*,1, Yuan Wang*,1, Po-Wen Lo*,1, Tsung-Kwei Liu*,1 and Jian-Cheng Lee

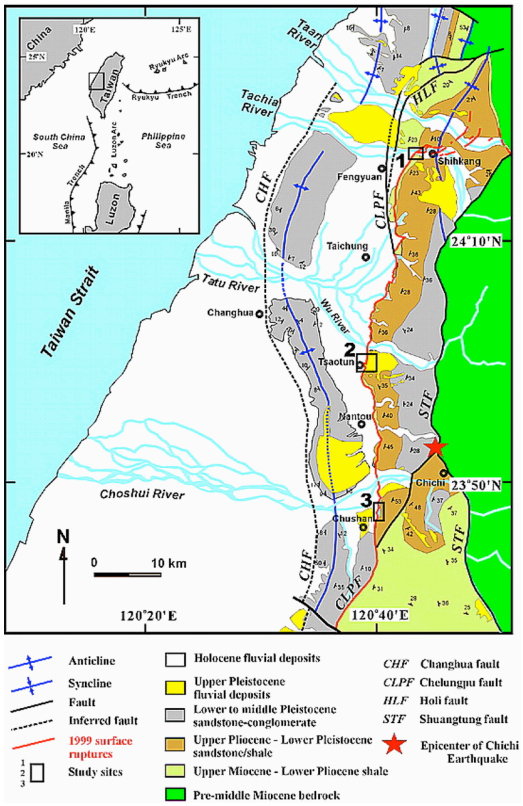


Figure 1. Geologic map of west-central Taiwan. Red line marks surface rupture associated with 1999 Chichi earthquake. Note that northern part of surface rupture cuts through hanging wall of pre- existing Chelungpu fault, and west of Shikang rupture is characterized by multiple discontinuous segments

The September 21, 1999, Mw 7.6 Chichi earthquake destroyed several thousand buildings and caused more than 2000 fatalities in central Taiwan. The earthquake occurred along the Chelungpu fault, a thrust fault on the western flank of the Taiwan fold-and- thrust belt. The surface rupture was more than 90 km long, and vertical displacements ranged from 3 to 8 m. Although pre-existing scarps were identified along the Chelungpu fault, the fault had previously been categorized as a less important active fault, owing to the lack of geochronologic evidence and the failure to recognize fault-related geomorphic features. Identifying geomorphic features at active faults in Taiwan will permit the delineation of future surface ruptures and the determination of past magnitudes of past earthquakes, thus contributing to hazard assessment.

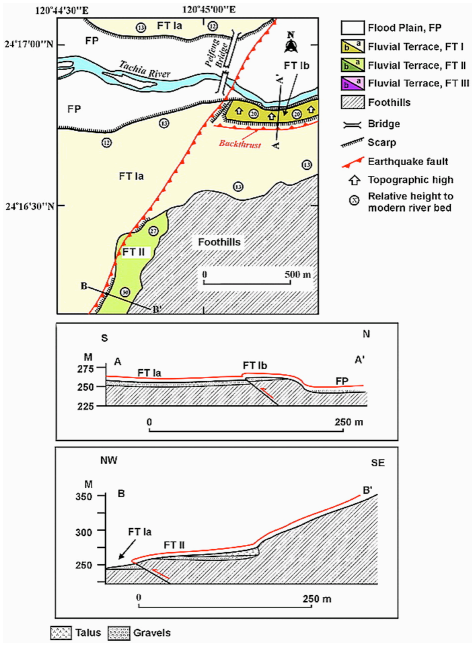


Figure 2. To east of city of Shihkang, three levels of strath terraces are identified as FT Ia, FT Ib, and FT II. Terrace 1a represents most extensive terrace level. Scarp that bounds FT II coincides with 1999 surface rupture. FT Ib scarps also coincide with 1999 rupture and backthrust fault that also broke in 1999. All relative heights labeled in map were measured before Chichi earthquake. Red lines on cross sections represent postearthquake topography

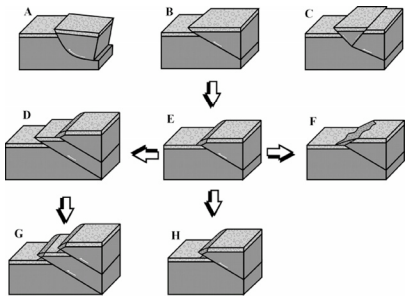


Figure 3. Block diagrams illustrating evolution of river-terrace deformation caused by coseismic offset. A–C: Fault scarp forms parallel to fault-line trace. D–E: During period of seismic quiescence, scarp will be modified and scarp-derived colluvium will be deposited adjacent to fault scarp. F: During long periods of quiescence, fault-line scarp will retreat substantially and become irregular. If recurrence interval is sufficiently short, fault-line scarp will be well preserved

## Geometry and structure of northern surface ruptures of the 1999 Mw=7.6 Chi-Chi Taiwan earthquake: influence from inherited fold belt structures

Jian-Cheng Lee[a], Hao-Tsu Chu[b], Jacques Angelier[c], Yu-Chang Chan[a], Jyr-Ching Hu[d], Chia-Yu Lu[e] and Ruey-Juin Rau[f]

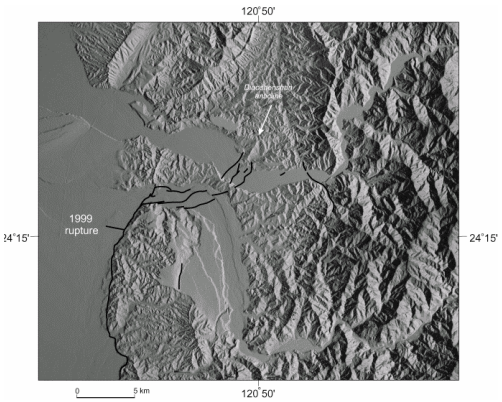


Fig. 4. 40-m DEM shading image of the northern termination area of the 1999 earthquake. Location is the same as geological map of Fig. 4. The NE–SW trending Diaoshenshan anticline fold is clearly visible in the rapidly eroded regional syncline with low topographic relief. This indicates that the Diaoshenshan anticline is an active uplift structure.

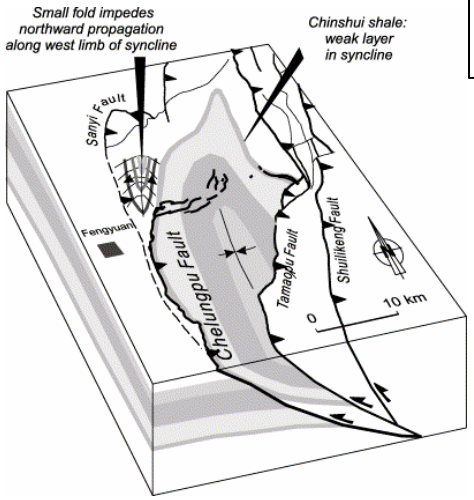


Fig. 5. Geometric configuration of the northern termination of the 1999 earthquake illustrated in a 3-D block diagram. The 1999 Chi-Chi earthquake generally ruptured along the Chelungpu fault and developed parallel to bedding of the weak zone of the Chinshui Shale at the upper 2–3 km. Geological and lithological 3-D geometry show the Chinshui Shale became shallower toward the north. The rupture surface finally emerged to the surface in the Shihkang–Shangchi fault zone and formed a spoon-like shape towards the core of the regional Pliocene syncline. This south-plunging Pliocene syncline acts as a slip guide for the new ongoing Chelungpu thrust (see text for details).

# Review of paleoseismological and active fault studies in Taiwan in the light of the Chichi earthquake of September 21, 1999

Yoko Otaa, _, _, Yue-Gau Chenb and Wen-Shan Chenb

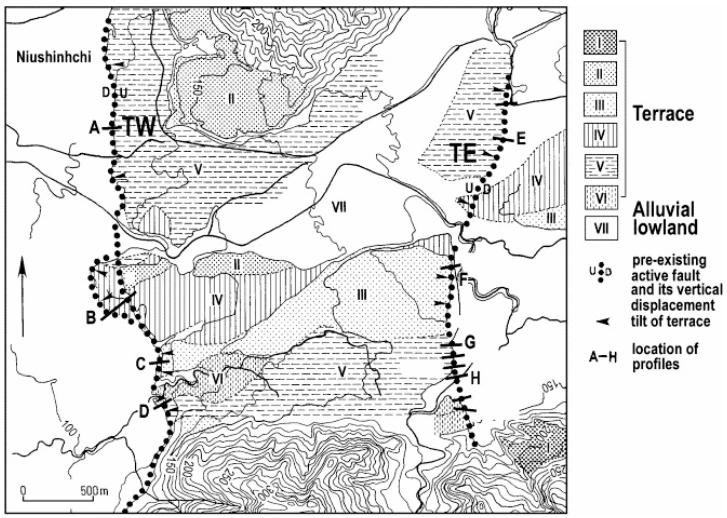


Fig. 6. Map showing the coincidence of the earthquake fault and pre-existing fault trace at the Tsaotun area. Numbers show the terrace order from the older one. Dots represent the 1999 earthquake fault and active fault, showing their close coincidence in the location (Ota, 2000). TW: Tsauton west fault (main Chelungpu fault), and TE: Tsaotun east fault as a back thrust. See Fig. 8 for the profiles.

Fig. 7. View of the flexural scarp produced by the 1999 Chichi earthquake at Kuangfu Middle School sport ground. Overriding hanging wall on the footwall, and complex deformation on the hanging wall are clearly seen (Kuangfu Middle School sport ground, photo by Ota, September, 1999).

# Structures Associated with the Northern End of the 1999 Chi-Chi Earthquake Rupture, Central Taiwan: Implications for Seismic-Hazard Assessment

Yuan-Hsi Lee1, Shih-Ting Lu2, Tung-Sheng Shih2, Meng-Long Hsieh3 and Wei-Yu Wu2

The surface rupture of the 1999 Chi-Chi earthquake (*M*w 7.6) trends more than 100 km in a north–south direction. Surface deformation at the northern end stops abruptly at an area between the Tachia River and the Taan River where a broad pop-up structure with east to northeast strike can be found that has a trend different from the north–south-striking main thrust. We combine the absolute elevation data before and after the Chi-Chi earthquake to obtain the regional vertical displacement and the magnitude of the pop-up structure. The greatest uplift could reach as high as 15–16 m. Using deformation magnitude and the area-balancing method, we measure the depth of the detachment to show the subsurface geometry of the Chelungpu fault at its northern end. This shows that the geometry of the Chelungpu fault controls termination of the surface rupture and the depth of the detachment controls the amount of deformation.

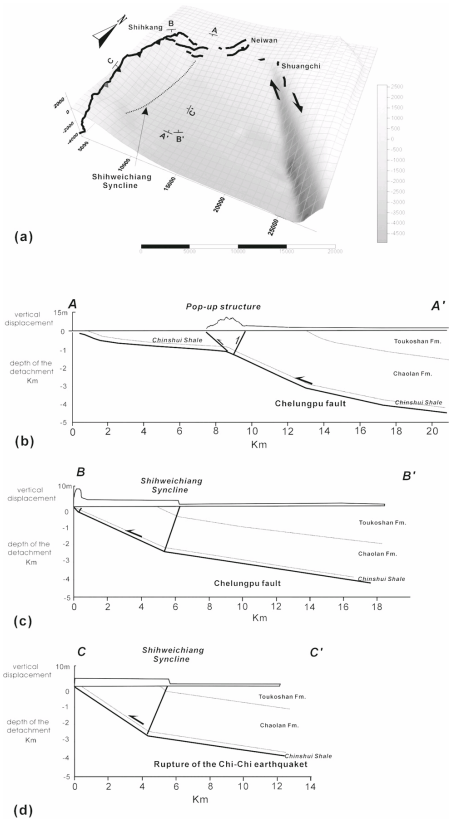


Figure 8. Subsurface structure of the Chelungpu fault in the NER. The east–west and north–south striking ramp structures have developed near the surface. The most boundary is a right lateral strike-slip fault with a steep fault plane. (b) The Chelungpu fault is active along the base of Chinshui Shale, which shows a flat-ramp structure in the north–south-trending section. We infer that the Chelungpu fault penetrates into the surface along the ramp structure. (c) Section B is in the northwest direction and along the GPS displacement direction. It also shows the ramp-flat structure; the vertical displacement is 2.99 m on the ramp plane and less than 1 m on the flat plane. The boundary of the ramp-flat structures coincides with the Shihweichiang Syncline that the vertical slip is 3 m on the ramp and 1 m on the flat.

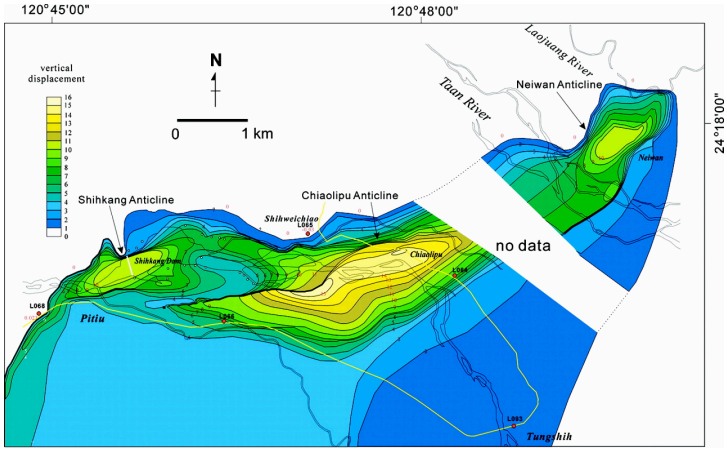


Figure 9. The uplift distribution of the NER. Around the Shihkeng Dam area, we constructed the contour based on the leveling survey of pre- and postearthquake maps at 1:2400 to 1:2500 scale. The other areas were based on total station survey results (sections DD', EE', FF', and GG'), pre- and postearthquake topographic maps at 1:5000 scale, and GPS data. Three anticlines were developed at the Shihkang Dam, Chiaolipu, and Neiwan areas. The highest vertical uplift reaches 15–16 m in the Chiaolipu area. The yellow line is the highway along which profiles C and D were measured (Fig. 2) and red dots show locations of selected GPS sites.

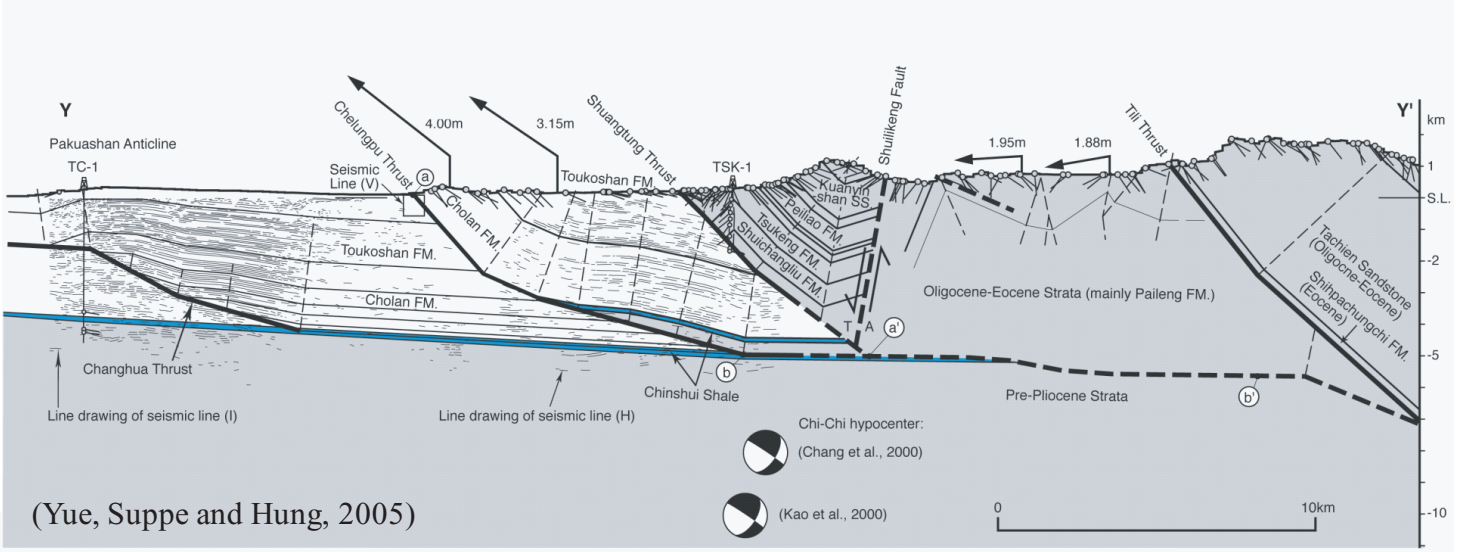


(Yue, Suppe and Hung, 2005)

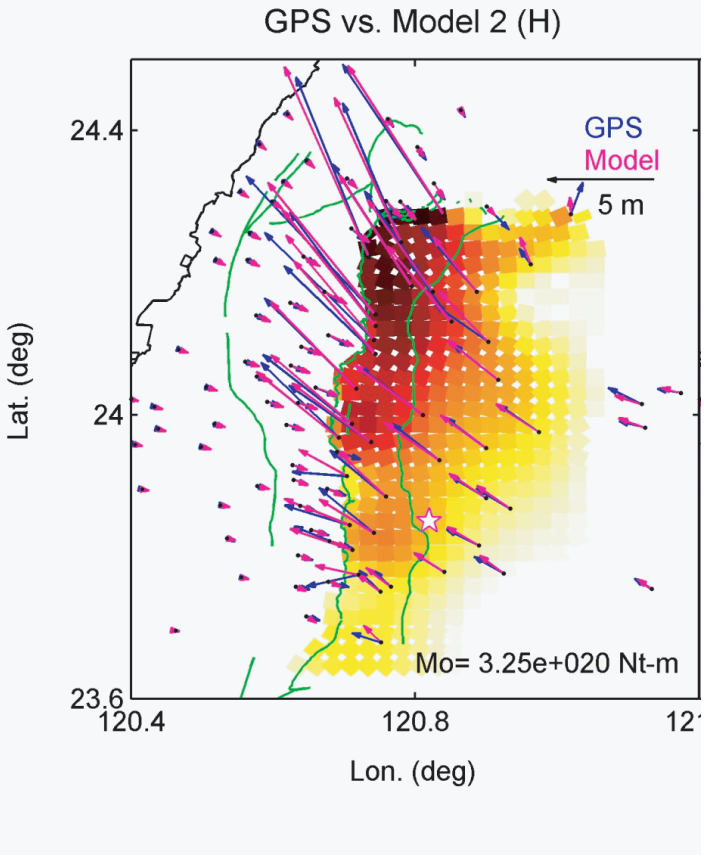


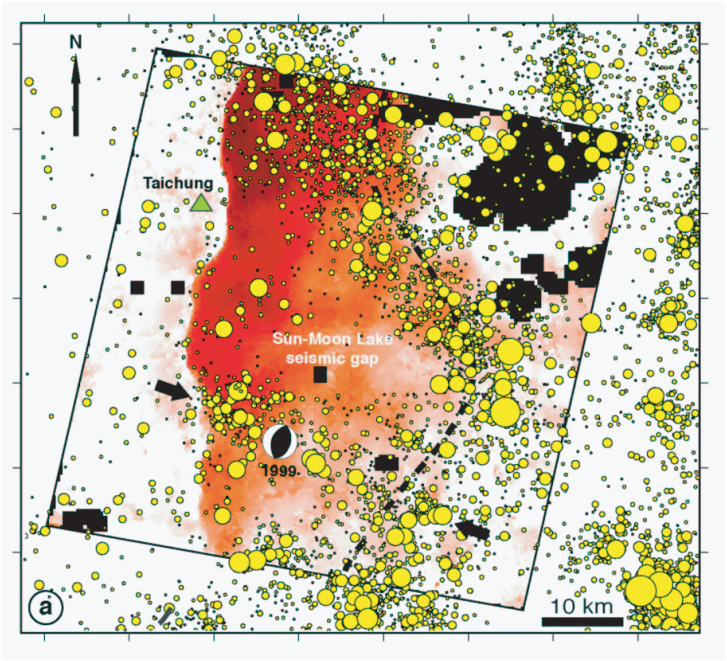


Above (color) Co-seiesmic deformation due to the 1999 Chichi EQ from SPOT images and Air photos (S. Leprince et al.)

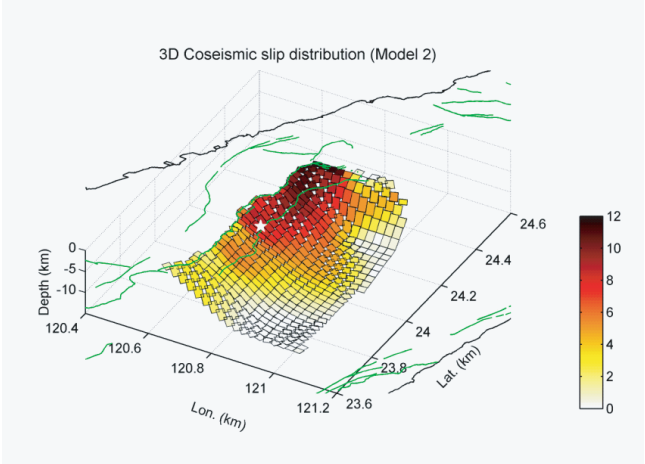


Left and upper left (color): Co-seismic slip model of Chichi EQ (Yaru Hsu)

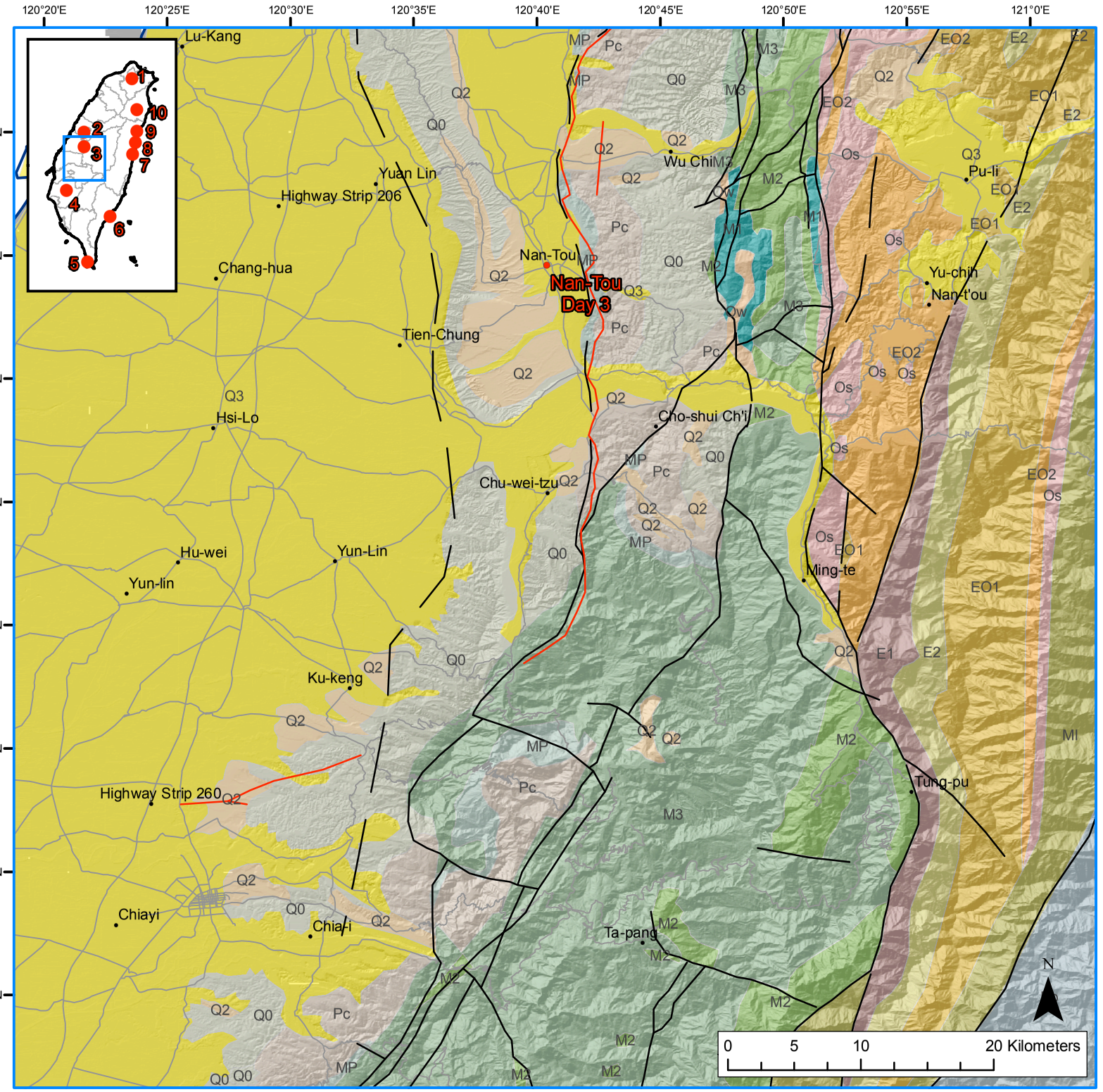


## Day 3 - Nan-Tou

- Q3 Terrace Deposits
- Q2 Lateritic Terrace Deposits
- Q1 Hengchun Limestone
- Q0 ls Toukoshan Formation and equivalents
- Pc Cholan Formation, Chinshui Shale and equivalents
- MP Kueichulin Formation and equivalents
- M3 Nanchuang Formation and equivalents
- M2 Nankang Formation, Shihti Formation and equivalents
- M1 Taliao Formation, Mushan Formation, Aoti Formation and equivalents
- Ow Wuchihshan Formation and equivalents
- Ml Lushan Formation and equivalents
- Os Tatungshan Formation, Kangkou Formation, Scuichangliu Formation and equivalents
- EO2 Szeleng Sandstone, Meichi Sandstone, Paileng Formation
- EO1 Hsitsun Formation, Chiayang Formation
- E2 Tachien Sandstone
- E1 Shihpachungchi Formation
- Ep Pilushan Formation
- PM4 Mainly black schist
- PM3 Black schist, green schist, metachert
- PM2 Marble
- PM1 Gneiss, migmatite
- A2 Andesite and andesitic pyroclastics
- A1 Andesite and andesitic pyroclastics
- W Ultramafic and mafic rocks

COASTAL RANGE

- PPt Takangkou Formation, with exotic blocks
- Pl Lichi Formation
- MPt Tuluanshan Formation

- Fault (dashed where inferred or concealed)
- Earthquake fault (dashed where inferred)

## Day 3 Taichung to Nantou

(1) Surface rupture of the 1999 Chi-Chi earthquake.
(2) Transect of the Fold-and-thrust belt.
Stops: Pa-Kua-Shan

The Pakuashan anticline is an active fault tip fold that constitutes the frontal most zone of deformation along the western piedmont of the Taiwan Range. Assessing seismic hazards associated with this fold and its contribution to crustal shortening across central Taiwan requires some understanding of the fold structure and growth rate.

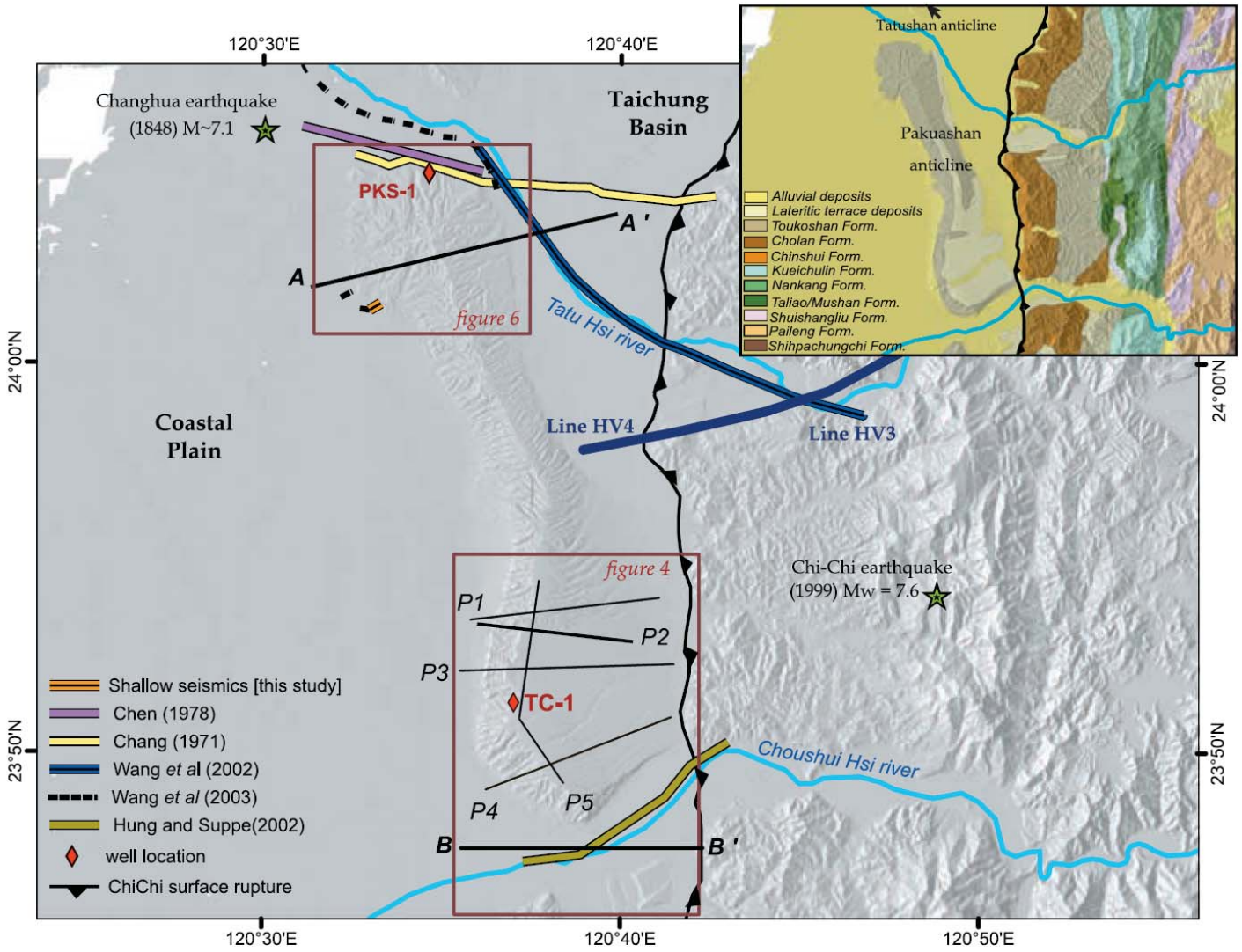


Figure1. Map of the Western Foothills of central Taiwan with locations of PKS-1 and TC-1 wells, along with available seismic lines. The Changhua blind fault marks the front of the Taiwan range in this region and is responsible for folding of the Pakuashan and Tatushan anticlines. P1 to P5 show location of topographic profiles across lateritic surfaces which cap the anticline to the south. Lines A-A0 and B-B0 indicate the N78° ± 3°E and N90° ± 5°E directions along which data are projected for northern and southern Pakuashan, respectively.

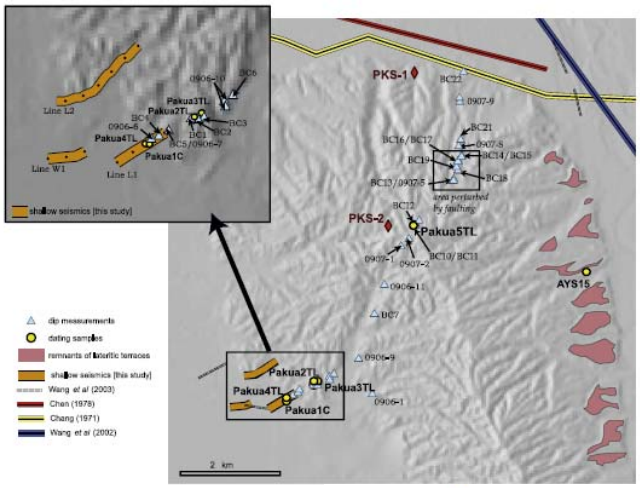


Figure 2. Map of northern Pakuashan. Age samples (bold characters on map, see Table 2) were mainly collected in the forelimb.

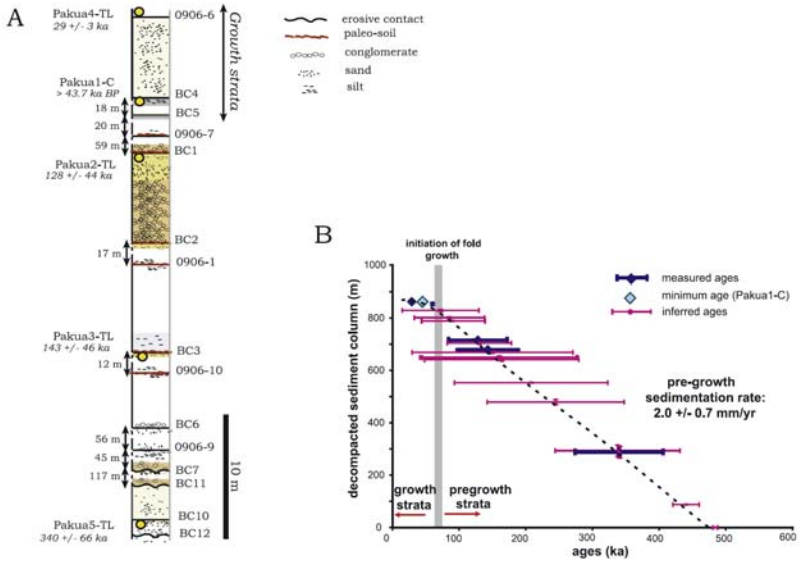


Fig. 3 (a) Stratigraphic column of the section surveyed in the forelimb of Pakuashan along highway 74 (northern transect). (b) Decompacted sediment thicknesses versus depositional ages for all samples from the forelimb of northern Pakuashan.

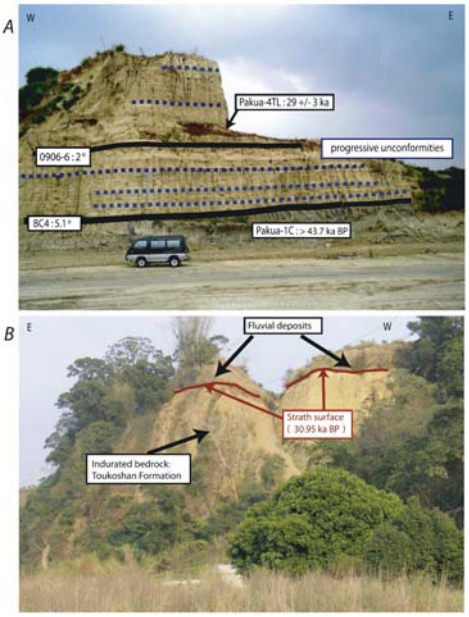


Figure 4. Pictures of the field survey. (a) Field picture locating BC4 and 0906-6 sedimentary contacts (black lines) and dating samples Pakua4-TL and Pakua1-C in northern Pakuashan. Also emphasized in this picture are the dips of successive sediment layers (blue dotted lines), showing subtle progressive unconformities. (b) Strath surface associated to the 30,950 ± 290 years old terrace south of the Pakuashan anticline. This erosive contact separates the more indurated fluvial sediments of the Toukoshan Formation and the more recent deposits that were sampled for dating.

The geometry of several deformed strata and geomorphic surfaces recorded different cumulative amounts of shortening. These units were dated to ages ranging from ~19 ka to ~340 ka. Those data together with shallow seismic profiles show that the anticline has formed as a result of pure shear with subsequent limb rotation. The cumulative shortening along the direction of tectonic transport is estimated to be 1010 ± 160 m. An analytical fold model derived from a sandbox experiment can be used to model growth strata.

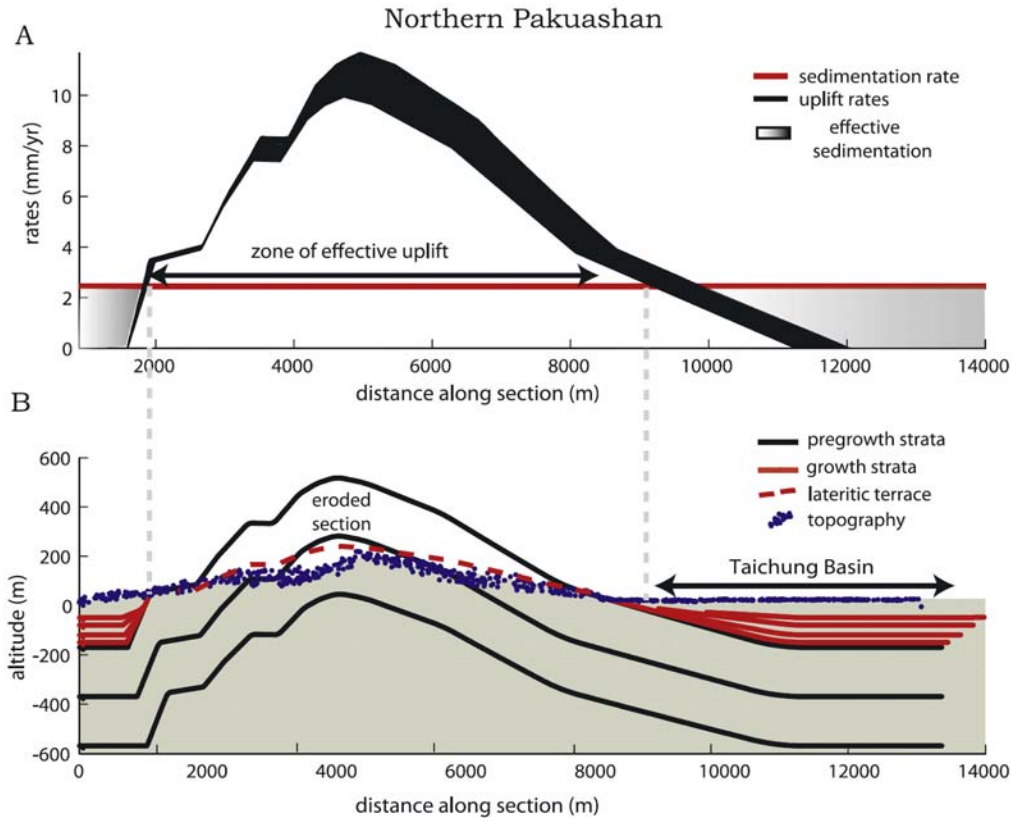


Figure 5. Fold growth and footwall subsidence predicted for northern Pakuashan. An average sedimentation rate of 2.5 mm/yr is assumed. (a) Uplift versus sedimentation rates predicted by our model. Where subsidence exceeds uplift (shaded areas), sedimentation prevails and the deposition of growth strata is possible. (b) Incremental growth of the northern Pakuashan anticline predicted by model. Finite deformation is recorded by pregrowth strata (black), while incremental shortening is documented by growth strata (red). The red dashed line across the whole fold represents the deformed geometry of a 21 ka layer, equivalent to the lateritic surfaces capping the northern Pakuashan anticline.

The deformation across Pakuashan initiated 62,200 ± 9600 years ago, with a shortening rate of 16.3 ± 4.1 mm/yr. Combined with constraints on the foreland sedimentation, the model shows how the present morphology of the Pakuashan anticline has resulted from the combination of uplift and erosion by river incision or hillslope processes.

# Principle of the approach:

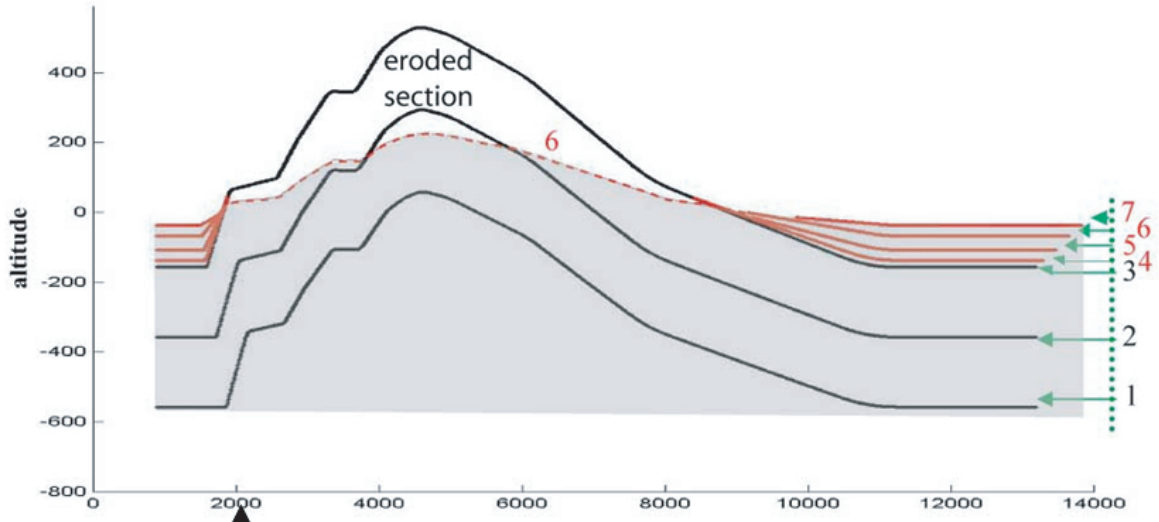


Finite shortening recorded by strata vs. incremental shortening recorded by growth strata or geomorphic markers.

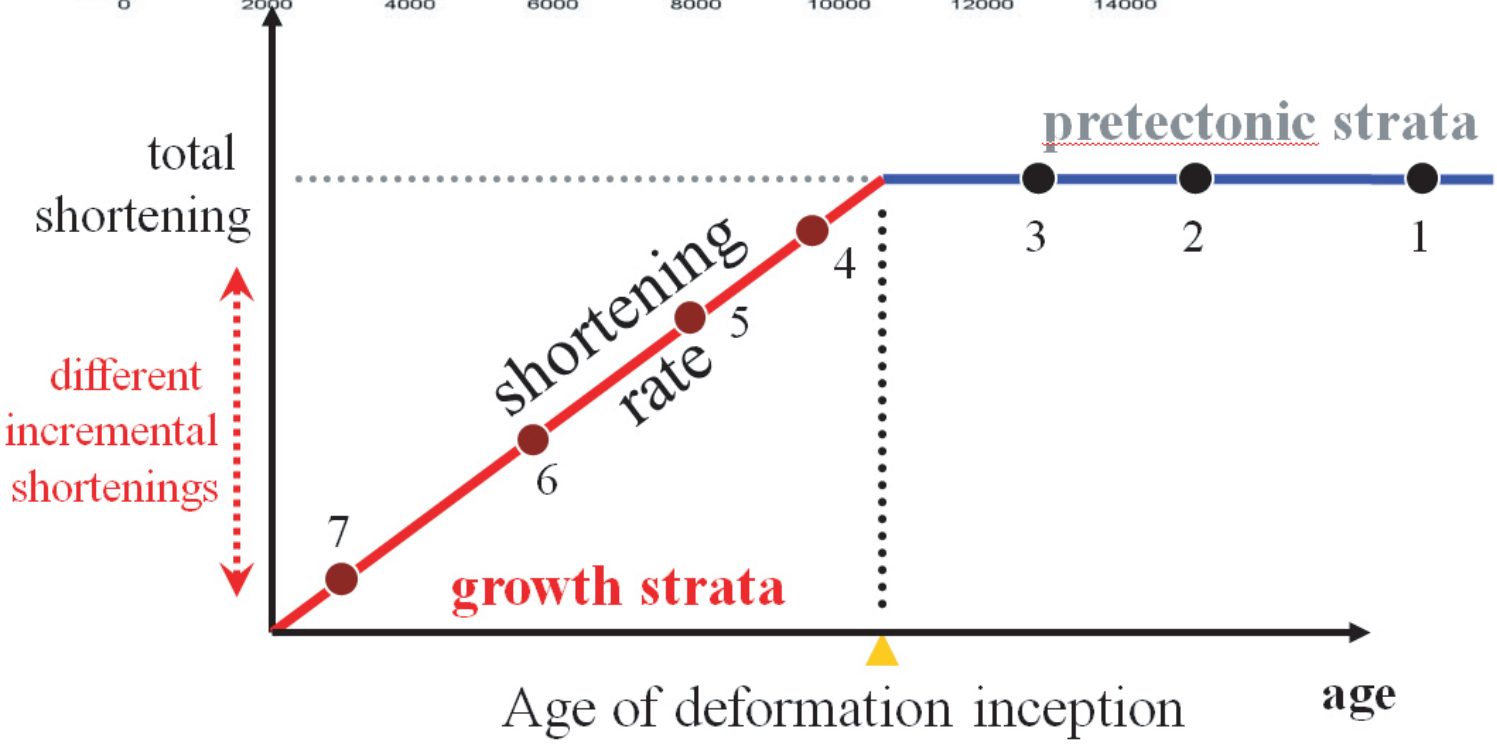

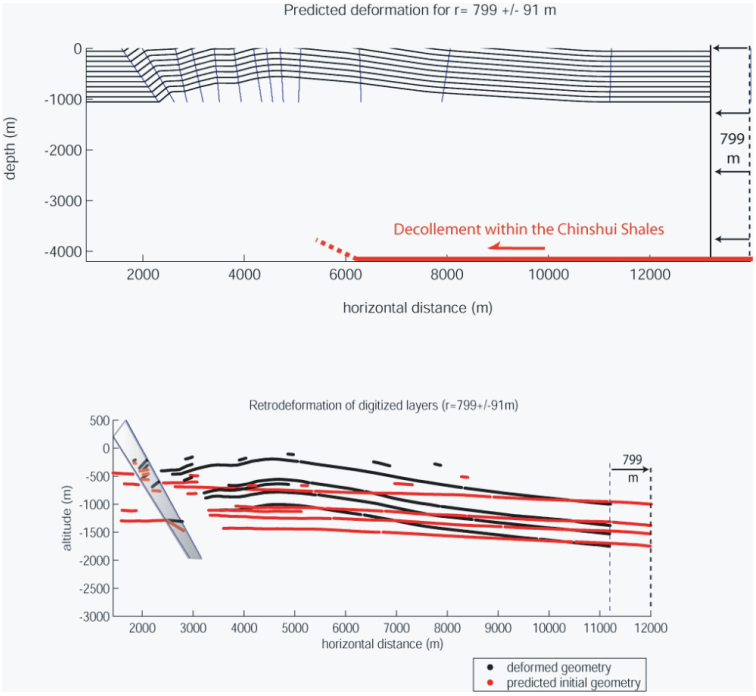


Example of analysis from northern Pakuashan: Modeling incremental growth of the fault-tip fold. Model describes quite well the finite structure of the Pakuashan anticline. We can use these calibrated formulations to translate dips measured in the field into cumulated shortening !

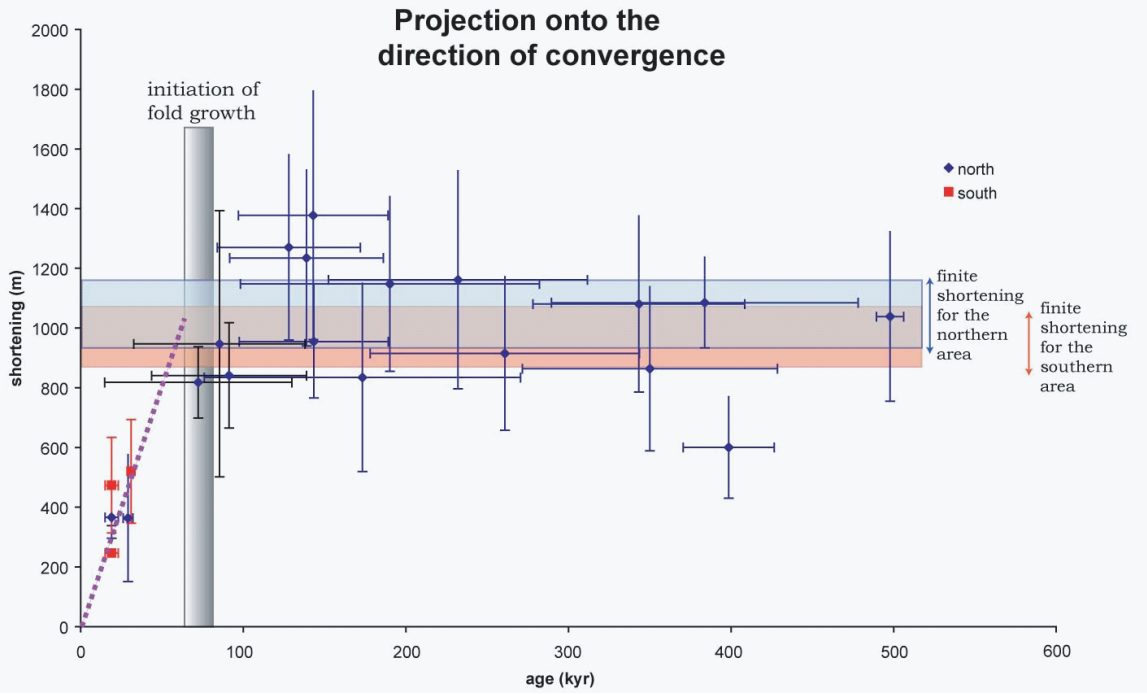


Results for northern and southern Pakuashan, along the direction of transport:

Consistent kinematics from north to south
Age of deformation initiation: 63,7 +/- 9.8 ka
Shortening rate across the Pakuashan anticline: 15.9 +/- 1.4 mm/yr

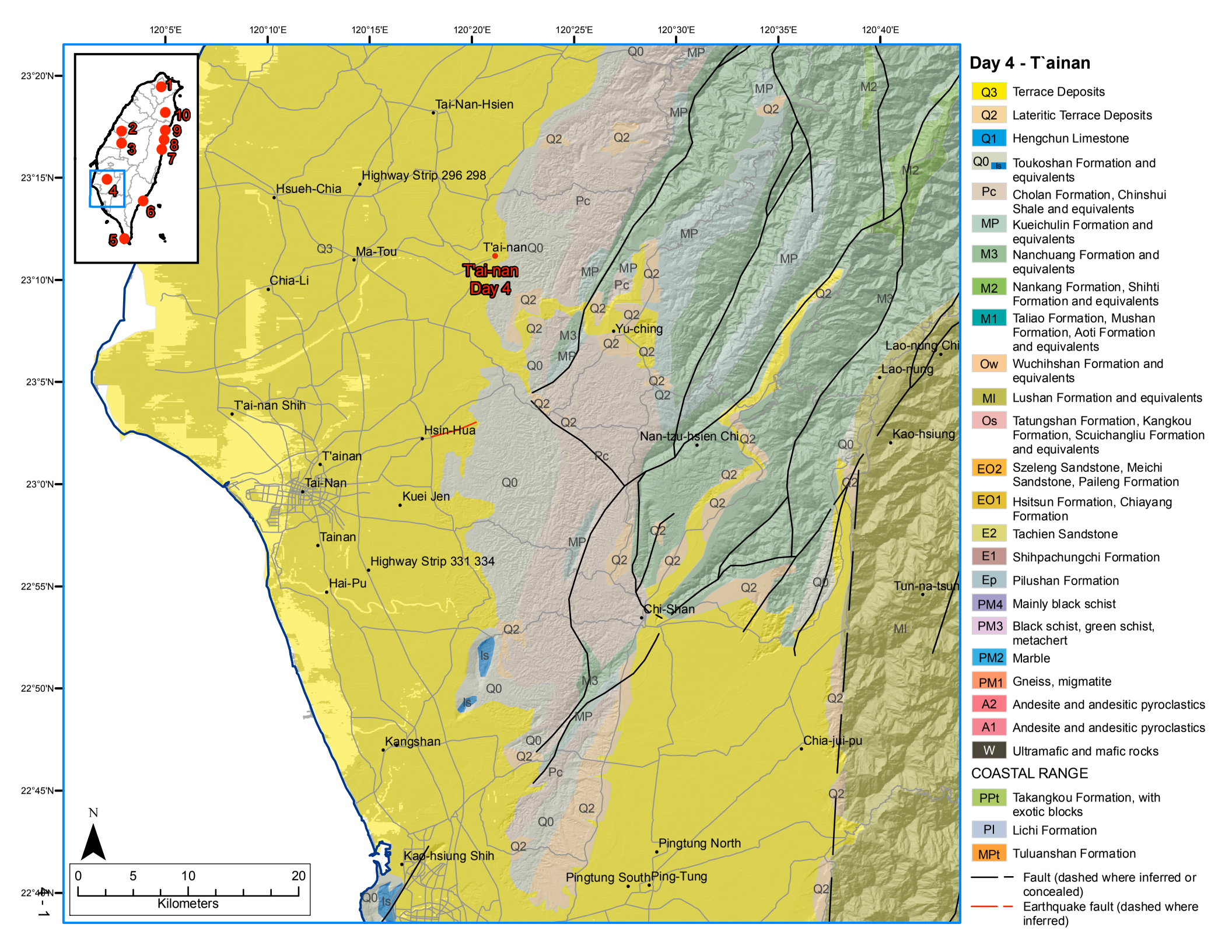
120°5'E
120°10'E
120°15'E
120°20'E
120°25'E
120°30'E
120°35'E
120°40'E
23°20'N
23°15'N
23°10'N
23°5'N
23°0'N
22°55'N
22°50'N
22°45'N
22°40'N
Tai-Nan-Hsien
Highway Strip 296 298
Hsueh-Chia
Ma-Tou
T'ai-nan
T'ai-nan
Day 4
Chia-Li
Yu-ching
T'ai-nan Shih
Hsin-Hua
T'ainan
Tai-Nan
Kuei Jen
Tainan
Highway Strip 331 334
Hai-Pu
Kangshan
Kao-hsiung Shih
Pingtung South
Ping-Tung
Pingtung North
Chia-jui-pu
Chi-Shan
Nan-tzu-hsien Chi
Lao-nung Chi
Lao-nung
Kao-hsiung
Tun-na-tsun
N
0
5
10
20
Kilometers
Day 4 - T`ainan
Q3 Terrace Deposits
Q2 Lateritic Terrace Deposits
Q1 Hengchun Limestone
Q0 Toukoshan Formation and equivalents
Pc Cholan Formation, Chinshui Shale and equivalents
MP Kueichulin Formation and equivalents
M3 Nanchuang Formation and equivalents
M2 Nankang Formation, Shihti Formation and equivalents
M1 Taliao Formation, Mushan Formation, Aoti Formation and equivalents
Ow Wuchihshan Formation and equivalents
MI Lushan Formation and equivalents
Os Tatungshan Formation, Kangkou Formation, Scuichangliu Formation and equivalents
EO2 Szeleng Sandstone, Meichi Sandstone, Paileng Formation
EO1 Hsitsun Formation, Chiayang Formation
E2 Tachien Sandstone
E1 Shihpachungchi Formation
Ep Pilushan Formation
PM4 Mainly black schist
PM3 Black schist, green schist, metachert
PM2 Marble
PM1 Gneiss, migmatite
A2 Andesite and andesitic pyroclastics
A1 Andesite and andesitic pyroclastics
W Ultramafic and mafic rocks
COASTAL RANGE
PPt Takangkou Formation, with exotic blocks
Pl Lichi Formation
MPt Tuluanshan Formation
Fault (dashed where inferred or concealed)
Earthquake fault (dashed where inferred)

## Day 4 -6/19 Nantou to Tainan Stops: Tian-Liao Hotel: Tainan

Hung, J.H., Wiltschko, D.V., Lin, H.C., Hickman, J.H., Fang, P. and Bock Y. (1999) Structure and motion of the southwestern Taiwan Fold and Thrust belt. TAO, 10, p. 543-568.

(1) Fold-and-thrust belt (or accretionary wedge) in Southwestern Taiwan.

Surface and limited seismic data have been used to construct new cross sections across the southwestern Taiwan fold and Thrust Belt.
The Chukou fault (Fault 2 in Figure 1) and its extension to the south (Lunhou fault, Fault 4 in Figure 1) are not the frontal structure in this area. The magnitudes of both velocities and strain rates increase progressively from north to south along the Chukou-Lunhou fault, which could be accounted by an oblique arc-continent collision developing progressively from north to south. The GPS observation of increasing horizontal velocity along the profile E-E' (figure 1) suggests that, contrary to previous beliefs that Chukou fault (CKF) is the major active fault responsible for earthquakes in southwestern Taiwan, the deformation is distributed in an area wider than just the CKF. The faults to the east of CKF may be active or there is a common detachment exists at depth.

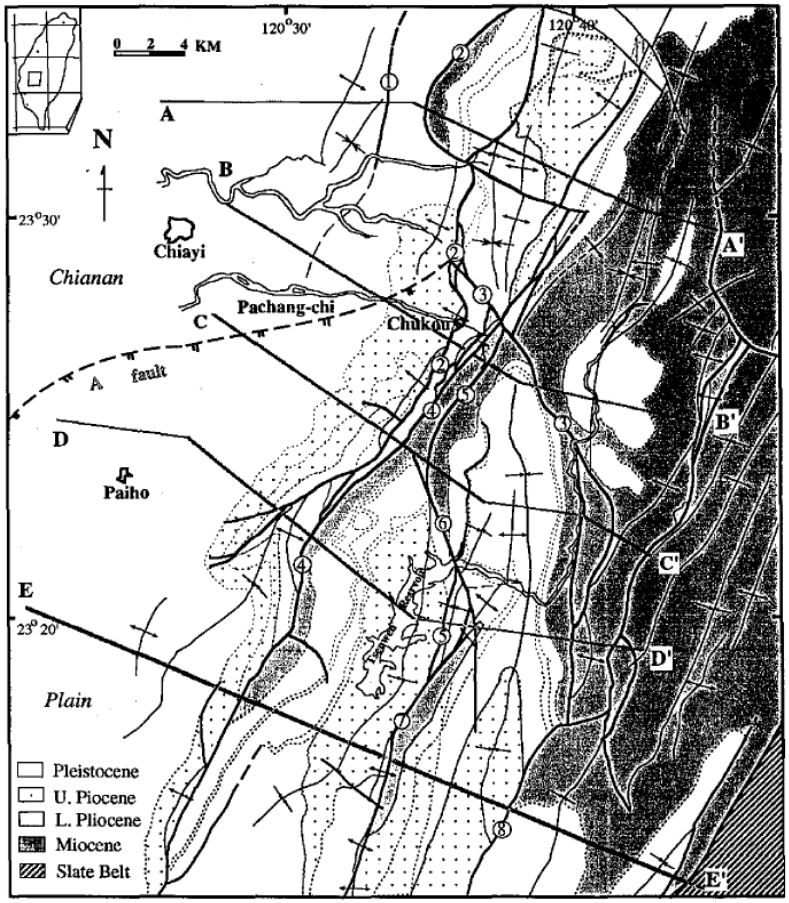


Figure 1 (right). Generalized geological map of the southwestern of Taiwan show the locations of the cross sections of A-A' to E –E' from Hung et al. (1999). 1. Chiuhsiungken, 2. Chukou, 3.Tatou, 4. Lunhou, 5.Mayoushan, 6. Tingpinglin, 7. Chutouchi, 8. Pingchi.

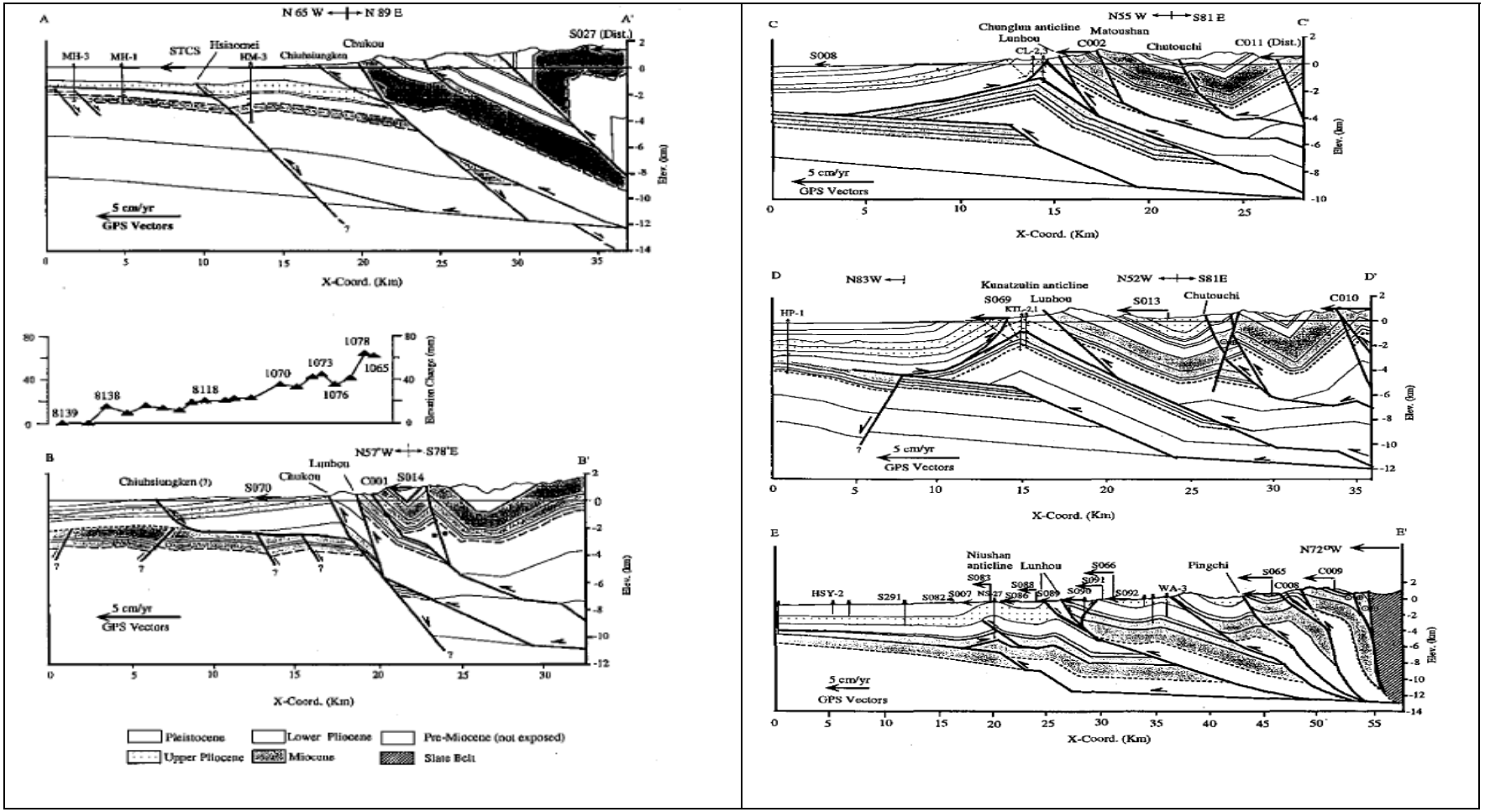


Figure 2. Five cross sections through Southwestern Foothills are assembled from the surface and subsurface geological data. Horizontal velocities of the GPS monument are projected into the line of each cross section.

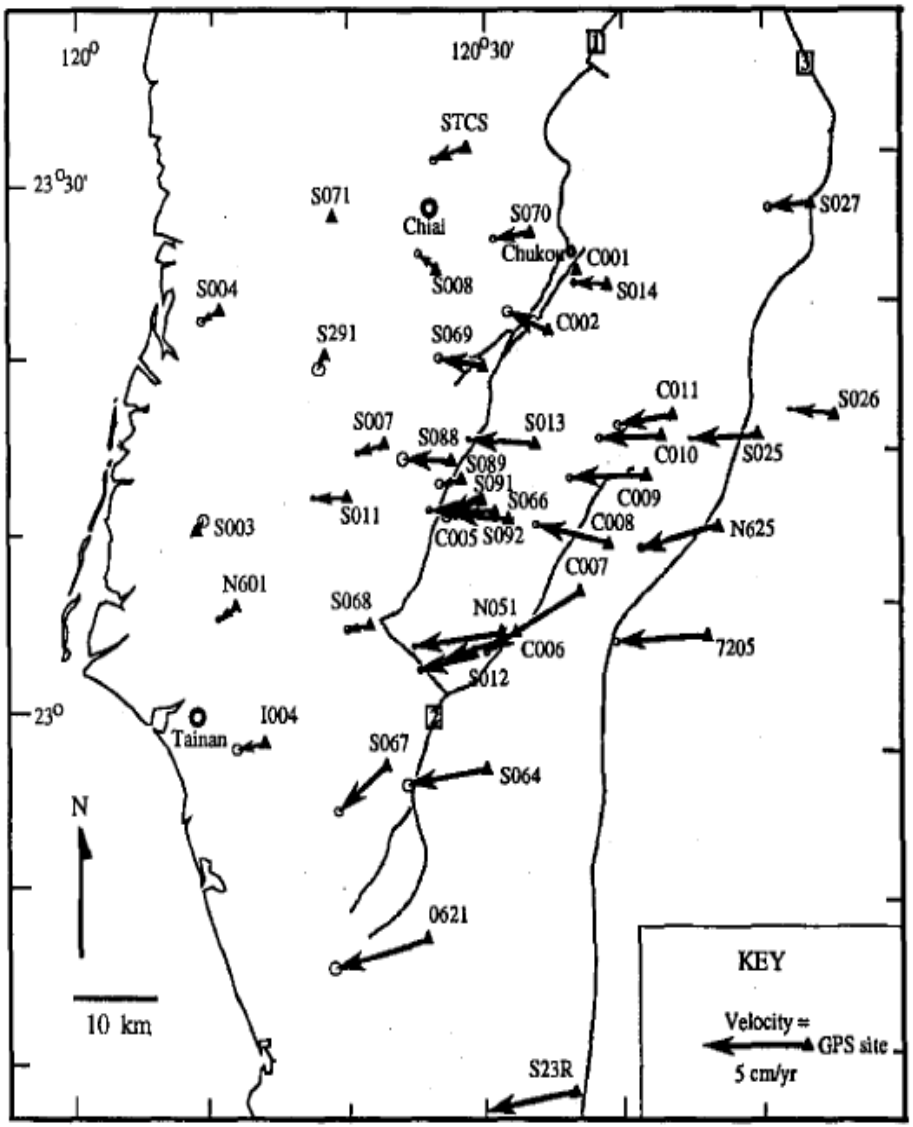


Figure 3 (left). Horizontal GPS station velocity relative to Paisha in the southwestern Taiwan. Gray lines are the major thrust faults, 1: Chukou-Lunhou, 2: Pingchi, 3: Laonungchi.

(2) Mud volcanoes and bad land.

Mud volcanoes (MVs) are commonly found in southern Taiwan. They are believed to be the products related to the accretionary prism due to the ongoing arc-continent collision between Eurasian plate and Luzon arc. The barren badland is geologically known as the mudstone, which is badly washed out. It is originally the sedimentary clay on the seabed and comes out of the earth surface after orogenesis. Since the unique landscape resembles the surface of the moon, the spot is named the Moon World (Tianliao Moon World).

Figure 4. Wushanding Mud Volcano Nature Reserve (bottom light, Photo by Steven Crook, from www.taiwanfun.com). Tianliao Moon World (bottom right, from english.kscg.gov.tw).

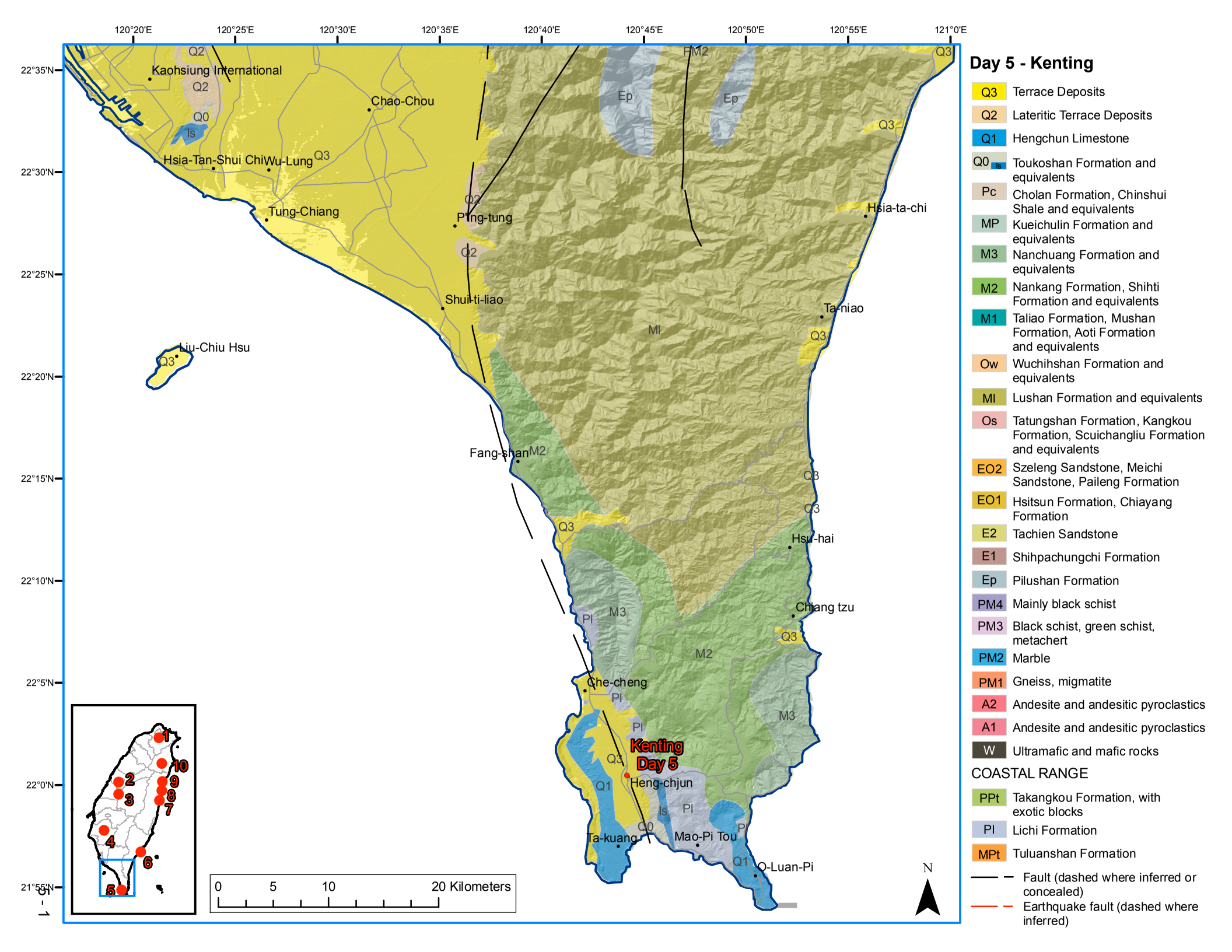
Day 5 - Kenting
Q3 Terrace Deposits
Q2 Lateritic Terrace Deposits
Q1 Hengchun Limestone
Q0 Toukoshan Formation and equivalents
Pc Cholan Formation, Chinshui Shale and equivalents
MP Kueichulin Formation and equivalents
M3 Nanchuang Formation and equivalents
M2 Nankang Formation, Shihti Formation and equivalents
M1 Taliao Formation, Mushan Formation, Aoti Formation and equivalents
Ow Wuchihshan Formation and equivalents
Ml Lushan Formation and equivalents
Os Tatungshan Formation, Kangkou Formation, Scuichangliu Formation and equivalents
EO2 Szeleng Sandstone, Meichi Sandstone, Paileng Formation
EO1 Hsitsun Formation, Chiayang Formation
E2 Tachien Sandstone
E1 Shihpachungchi Formation
Ep Pilushan Formation
PM4 Mainly black schist
PM3 Black schist, green schist, metachert
PM2 Marble
PM1 Gneiss, migmatite
A2 Andesite and andesitic pyroclastics
A1 Andesite and andesitic pyroclastics
W Ultramafic and mafic rocks
COASTAL RANGE
PPt Takangkou Formation, with exotic blocks
Pl Lichi Formation
MPt Tuluanshan Formation
Fault (dashed where inferred or concealed)
Earthquake fault (dashed where inferred)
Kaohsiung International
Chao-Chou
Hsia-Tan-Shui Chi
Wu-Lung
Tung-Chiang
P'ing-tung
Hsia-ta-chi
Shui-ti-liao
Ta-niao
Liu-Chiu Hsu
Fang-shan
Hsu-hai
Chiang tzu
Che-cheng
Kenting
Day 5
Heng-chjun
Ta-kuang
Mao-Pi Tou
O-Luan-Pi
120°20'E
120°25'E
120°30'E
120°35'E
120°40'E
120°45'E
120°50'E
120°55'E
121°0'E
22°35'N
22°30'N
22°25'N
22°20'N
22°15'N
22°10'N
22°5'N
22°0'N
21°55'N
0 5 10 20 Kilometers
N

Marie Giron

**Day 5 – 6/20**

## Geomorphic features in the frontal thrust zone in southwestern Taiwan

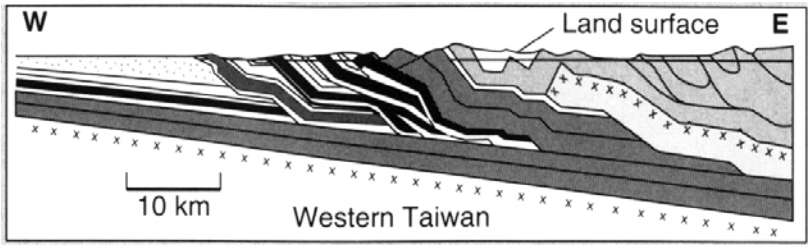


Figure 1: Cross section of fold and thrust belt in Western Taiwan

In a thrust zone, many interesting features can form from the deformation. In Taiwan, these features include the Tainan Tableland, uplift coral reefs, and the Kenting mélange.

### Tainan Tableland

Chen, Y.-G. and T.-K. Liu (2000). "Holocene uplift and subsidence along an active tectonic margin southwestern Taiwan." Quaternary Science Reviews **19**(9): 923-930.

***Abstract***

*Taiwan is located along a convergent plate boundary, where the Luzon Arc collides with the Eurasia continental margin. The Tainan Plain of southwestern Taiwan is incorporated into and deformed by a regional fold-and-thrust belt associated with this convergent plate margin. In this study we establish a tentative regional Holocene relative sea-level curve that allows us to analyze crustal uplift and subsidence rates of the Tainan Plain. The maximum Holocene uplift rates on the Tainan Plain occur on the Tainan Tableland and the Chungchou Terrace. These two areas have experienced long-term (Holocene) uplift rates of 5 and 7 mm/yr, respectively. The Tawan Lowland, located between these two areas, is subsiding at a long-term rate of about 1 mm/yr. Based on this pattern of the crustal movement, the Tainan Tableland is interpreted as a mud diapiric dome, and the Chungchou Terrace as the product of a blind thrust fault. The Holocene reference sea-level curve proposed in this study can be used to determine the pattern of crustal movements elsewhere in Taiwan. It also can suggest that the Holocene terrace development does not occur in area where the uplift rate exceeds 8 mm/yr, while late Holocene regression, the general trend around the western Pacific, is not recorded where the rate of subsidence is lower than 1 mm/yr.*

The authors believe that the Tainan Tableland is a mud diapiric dome that is actively moving today. "A **diapir** is an intrusion caused by buoyancy and pressure differentials" (Wikipedia)

## Uplift Coral Reefs and Marine Terraces

In Taiwan, there are coral reefs that are exposed and no longer in water. Famous uplifted coral reefs exist in Kenting National Park in the south of Taiwan. Some possible explanations are a change in sea level or a rise in the crust that the coral reefs lie on. The following abstract comes from a paper describing the latter.

Gong, S.Y., Wang, S.W. and Lee, T.Y. (1998) Pleistocene coral reefs associated with claystones, Southwestern Taiwan. Coral Reefs (1998) 17 : 215-222


***Abstract***

*Scleractinian coral reefs, when coexistent with siliciclastic sediments, usually occur in association with deltaic or coastal sands. Nevertheless, Pleistocene reef limestones in southwestern Taiwan are developed in association with thick claystones that were deposited in a deeper-water environment. These reef limestones are characterized by: (1) rapid transition from underlying claystones upward to reefal limestones, (2) lateral interfingering with open-shelf claystones, (3) being overlain by terrestrial deposits or exposed with no covering strata, and (4) being located in close association with anticlines. The authors propose that these reef limestones developed on anticlinal ridges raised above the adjacent sea floor by thrust-front migration in a foreland setting.*


The authors go on to say that the coral reefs must have formed in shallow water in order to survive, and they must have been on a topographic high relative to the ocean floor around it because the reefs are not covered in siliciclastics that cover adjacent rock. The suggested explanation was that the reefs formed on anticlines associated with the fault-propagation folding. The method of uplift above sea level was probably due to tectonics and not a sea level change because the sediment covering the coral reefs is terrestrial and not marine.

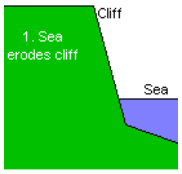


Figure 2: formation of a marine terrace

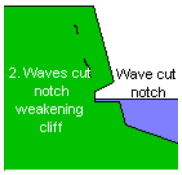


Marine terraces form from erosion of a cliff face by continual wave action. Old marine terraces are a good indicator of old sea levels. Part of the eastern coast of Taiwan is experiencing Holocene uplift of 15 m/Ma.

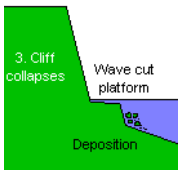

**Kenting Mélange**

**"**Mélange is a large scale breccia formed in the accretionary wedge above a subduction zone" (Wikipedia). A variety of rocks can be found in mélanges including metamorphic and sedimentary, and mélanges are sometimes referred to as garbage cans. The mélange wedge is very deformed and lacks order. During subduction, shearing flattens rocks and deforms the overall structure of them. The mélange is formed next to the subduction trench.

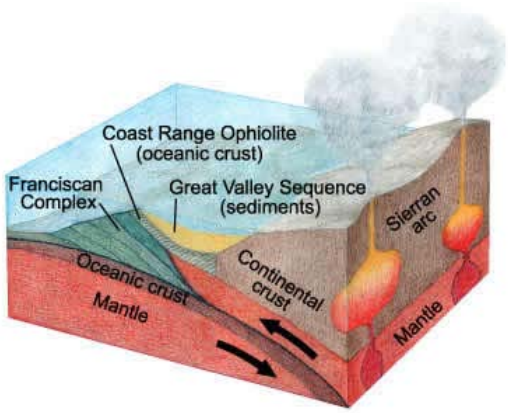


Figure 3: Subduction and mélange wedge from California where the mélange is a part of the Franciscan complex.

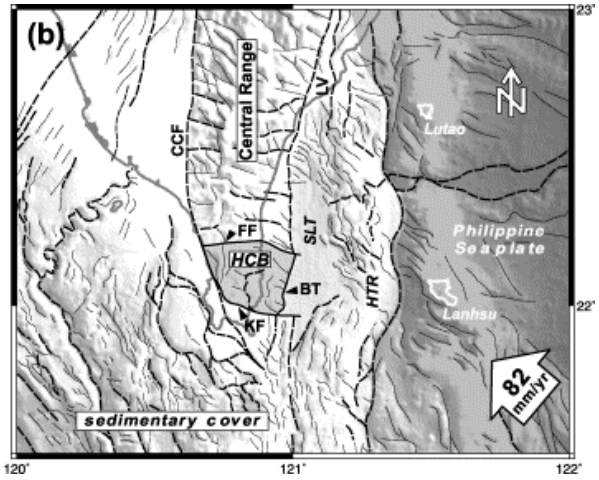


Figure 4: Kenting mélange (represented by KF) in the southern part of Taiwan.

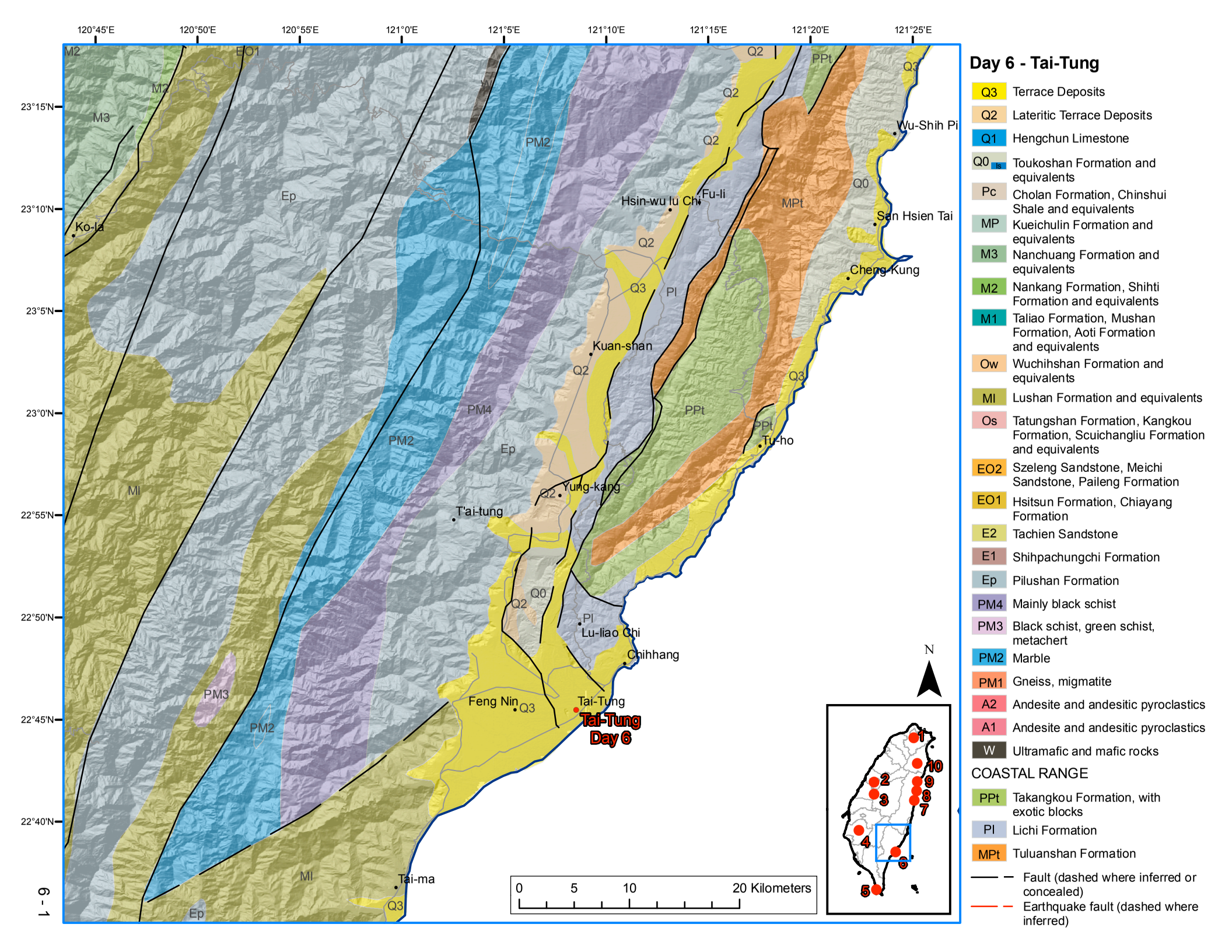


## Day 6 - Tai-Tung

- Q3 Terrace Deposits
- Q2 Lateritic Terrace Deposits
- Q1 Hengchun Limestone
- Q0 Toukoshan Formation and equivalents
- Pc Cholan Formation, Chinshui Shale and equivalents
- MP Kueichulin Formation and equivalents
- M3 Nanchuang Formation and equivalents
- M2 Nankang Formation, Shihti Formation and equivalents
- M1 Taliao Formation, Mushan Formation, Aoti Formation and equivalents
- Ow Wuchihshan Formation and equivalents
- Ml Lushan Formation and equivalents
- Os Tatungshan Formation, Kangkou Formation, Scuichangliu Formation and equivalents
- EO2 Szeleng Sandstone, Meichi Sandstone, Paileng Formation
- EO1 Hsitsun Formation, Chiayang Formation
- E2 Tachien Sandstone
- E1 Shihpachungchi Formation
- Ep Pilushan Formation
- PM4 Mainly black schist
- PM3 Black schist, green schist, metachert
- PM2 Marble
- PM1 Gneiss, migmatite
- A2 Andesite and andesitic pyroclastics
- A1 Andesite and andesitic pyroclastics
- W Ultramafic and mafic rocks

COASTAL RANGE

- PPt Takangkou Formation, with exotic blocks
- Pl Lichi Formation
- MPt Tuluanshan Formation

- Fault (dashed where inferred or concealed)
- Earthquake fault (dashed where inferred)

**Day 6 -6/21** **Kenting to Taitung**

**(1) Lichi Mélange.**
Text and figures from C.-P. Chang et al. / Tectonophysics 325 (2000) 43–62

**Abstract**
Juxtaposed against the remnant forearc basin sequences along thrust faults, the Lichi Me´lange of the Coastal Range of Taiwan is composed of exotic ophiolite and sedimentary blocks, metric to kilometric in size, and coherent turbidite beds, all embedded in a sheared scaly argillaceous[ed. substantial amount of clay] matrix. The Lichi Mélange is controversial in origin, being interpreted either as a subduction complex, or as an olistostrome [chaotic unit formed by slumping or sliding]. By separating four main deformation levels within the Lichi Me´lange and adjacent sedimentary rocks, we establish detailed geological maps and structural profiles in two key areas of the Lichi Mélange. We reconstruct also the evolution in cross-section and calculate the approximate minimum amount of shortening that corresponds to folding and thrusting in these areas. Our field studies suggest that the Lichi Mélange most likely arose from the shearing of lower forearc sequences rather than from a subduction complex or an olistostrome. This conclusion is supported by the structural analysis, the clay mineral distribution, and some interfingering sedimentary relationships between the Lichi Mélange and the lower Takangkou Formation. We also undertake a comprehensive tectonic analysis of the shear surfaces in the Lichi Mélange. The direction of the maximum compressional stress that we obtain is N100° ~120°E, compatible with that of plate convergence. During the most recent stage of collision, between the Eurasian plate (eastern Central Range of Taiwan) and the Philippine Sea plate (Coastal Range), a major fault zone developed along the innately weak zone of mélange, further increasing the shear deformation pattern of the Lichi Mélange. This Longitudinal Valley Fault separates the Eurasian plate and the Philippine Sea plate and is one of the most active faults in Taiwan. It can be considered as the present plate boundary in the Taiwan arc–continent collision terrane. According to our reconstruction, this plate boundary of the Longitudinal Valley originated as a submarine arc–prism boundary.

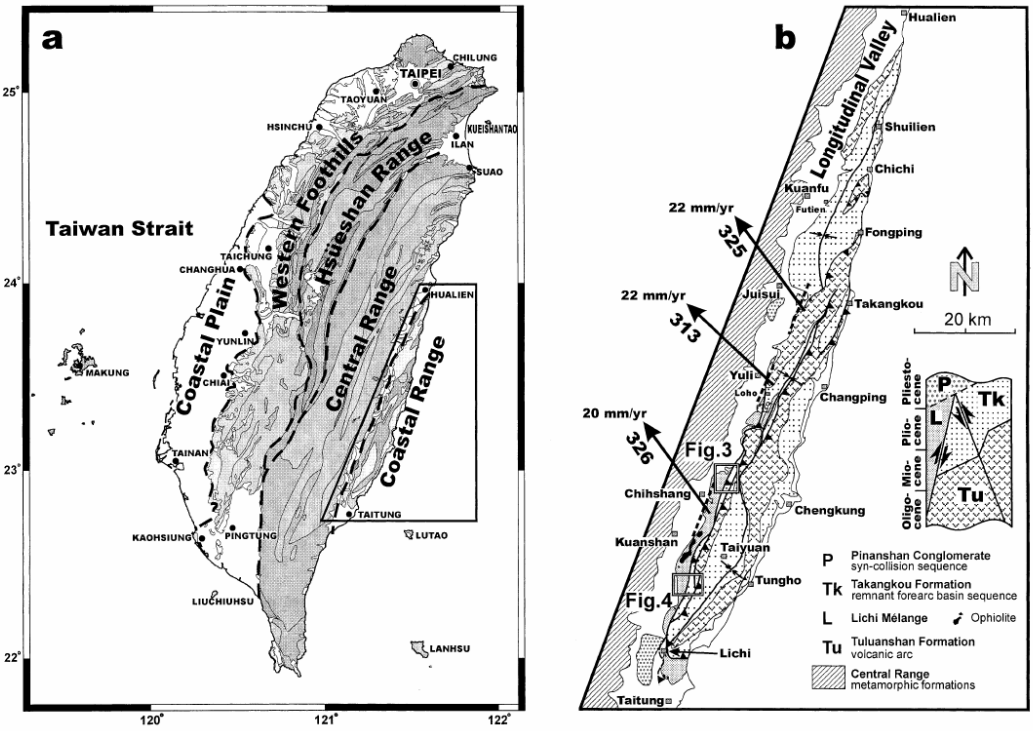


Fig. 2. (a) Main geologic units of Taiwan, with location of map (b). (b) Geologic map of the Coastal Range and present-day displacement across the Longitudinal Valley Fault Zone. Note the particular distribution of the Lichi Mélange: along the western flank of the southern Coastal Range, around the southern tip of the Coastal Range, and also near the Futien village in the northern Coastal Range (Teng, 1981), near the Fongping village in the eastern Coastal Range (Chen, 1988) and in the Loho basin of the central Coastal Range. The study areas of Figs. 3 and 4 are shown as two rectangular frames. Large arrows (after Lee and Angelier, 1993) indicate the displacement of the upthrust, eastern block of the Longitudinal Valley Fault relative to the Central Range, with computed azimuths of displacement in degrees and computed velocities in mm yr−1.



## Lithology and origin of the Lichi Mélange

The Lichi Mélange is distributed around the southwestern flank of the Coastal Range, and is composed of strongly sheared chaotic mudstones that contain many exotic blocks of various sizes and lithologies. Most of the Lichi Mélange crops out as a narrow belt with a length of about 65 km along the Longitudinal Valley, but smaller outcrops have been found in other areas of the Coastal Range (Fig. 2b). The best examples are located inside the Coastal Range, near the village of Futien in the north (Teng, 1981), near the village of Fongping to the east (Chen, 1988), and in the Loho basin of the central part of the Coastal Range (Hsu, 1956; Song, 1986). The most characteristic lithological feature of the Lichi Mélange is the presence of intensely sheared mudstones without distinctive stratification. However, layers of pebbly mudstones and coherent stratifications have been reported locally (Chang, 1967; Liou et al., 1977b; Page, 1978; Lee, 1984; Barrier and Muller, 1984; Chang, 1996). Some blocks inside the mélange may reach kilometric size and they are generally angular in shape. Most small blocks (decametric or smaller) are heavily sheared, but many large blocks remain almost intact (Teng, 1988). In terms of lithology, the exotic blocks belong to three types; (1) the ophiolitic suite, including peridotite, gabbro, and basalt; (2) the sedimentary suite, including various kinds of sedimentary clasts derived from the Takangkou Formation or other submarine sequences of shelf or continental slope environment, such as turbidites, sandstones, quartz-rich sandstone (Miocene in age),

sandstone/shale interbeds, shales, conglomerates, mudstones, and limestones; and (3) the andesitic suite, including volcanic breccias, tuffs, andesitic agglomerates, and volcaniclastic turbidites, all derived from the Tuluanshan Formation (Hsu, 1976; Liou et al., 1977a; Page and Suppe, 1981). Both the composition of the sedimentary blocks and their relationships at the contact with the matrix of the Lichi Mélange deserve particular attention, because they have the potential to highlight the origin of the Lichi Mélange. These aspects are discussed below. In fact, two kinds of sedimentary source materials coexist within the Lichi Mélange (Lin and Chen, 1986). One of these sources involves the continental materials, which are rich in illite and chlorite and were transported into the marine basin from the eastern Asian continent and/or the accretionary prism of the subduction zone (such as the ancient Central Range and its southern extension). The other source involves the volcanic arc material, which is rich in kaolinite and smectite and was transported from the volcanic arc in a tropical area (such as the Philippine islands). These two kinds of source materials were simultaneously deposited in the same sedimentary basin, that of the future Lichi Mélange. As indicated by the presence of large amounts of kaolinite in the mélange, part of the source area for the primary strata precursor of the Lichi Mélange had a humid, warm climate with much rainfall. This context fits well with the Miocene paleo-position of the Luzon arc, far to the southeast of the present location of the Lichi Mélange in Taiwan. In contrast with the Lichi Mélange, the kaolinite is rare or almost absent in the clay fractions of the adjacent Takangkou Formation. This suggests that contrary to the Lichi Mélange situation, the typical Takangkou forearc basin received much material from a continental source (like the ancient Central Range) than from a volcanic arc source (Lin and Chen, 1986; Chang, 1996). Although the contact between the Lichi Mélange and the other rock units is mainly tectonic (Hsu, 1976), interdigitation of stratigraphic origin with strata of the Takankou Formation might exist locally (Page and Suppe, 1981; Lee, 1984; Barrier and Muller, 1984; Chang, 1996). The best evidences for stratigraphic interfingering occur between the Lichi Mélange and the lower Takangkou flysch, which is lower Pliocene in age according to NN14–NN15 nannoplankton zones in the Mukenhsi area (Lee, 1984). Because of the existence of some evidence for interfingering, Page and Suppe (1981) considered that the contact between the Lichi Mélange and the Takangkou Formation is quasi-conformable in type. Our mapping confirmed the existence of such stratigraphic relationships, which result in major constraints while reconstructing the tectonic evolution of the Lichi Mélange area.

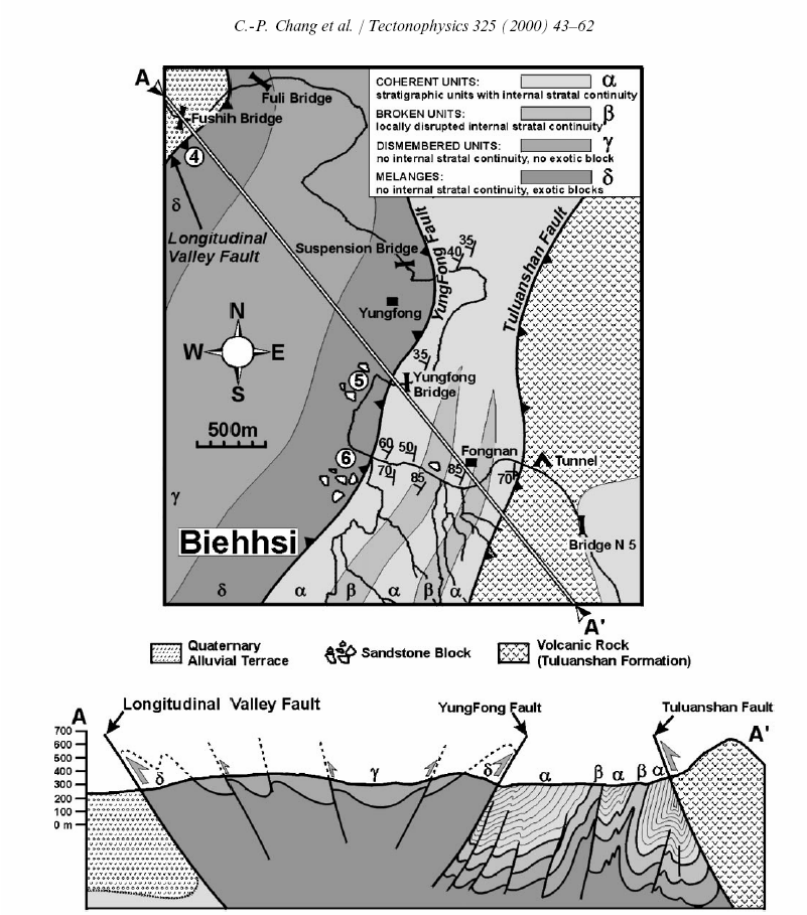


Fig. 3. Detailed geologic map of the Biehhsi valley area and geologic cross-section. Unit α can be considered as Takankou Formation, units γ and δ can be considered as Lichi Mélange and unit b is an intermediate member between Takankou Formation and Lichi Mélange (definitions and discussion in text). Circled numbers 4, 5 and 6 refer to sites of brittle tectonic analysis in the Lichi Mélange (stereoplots in Fig. 7).

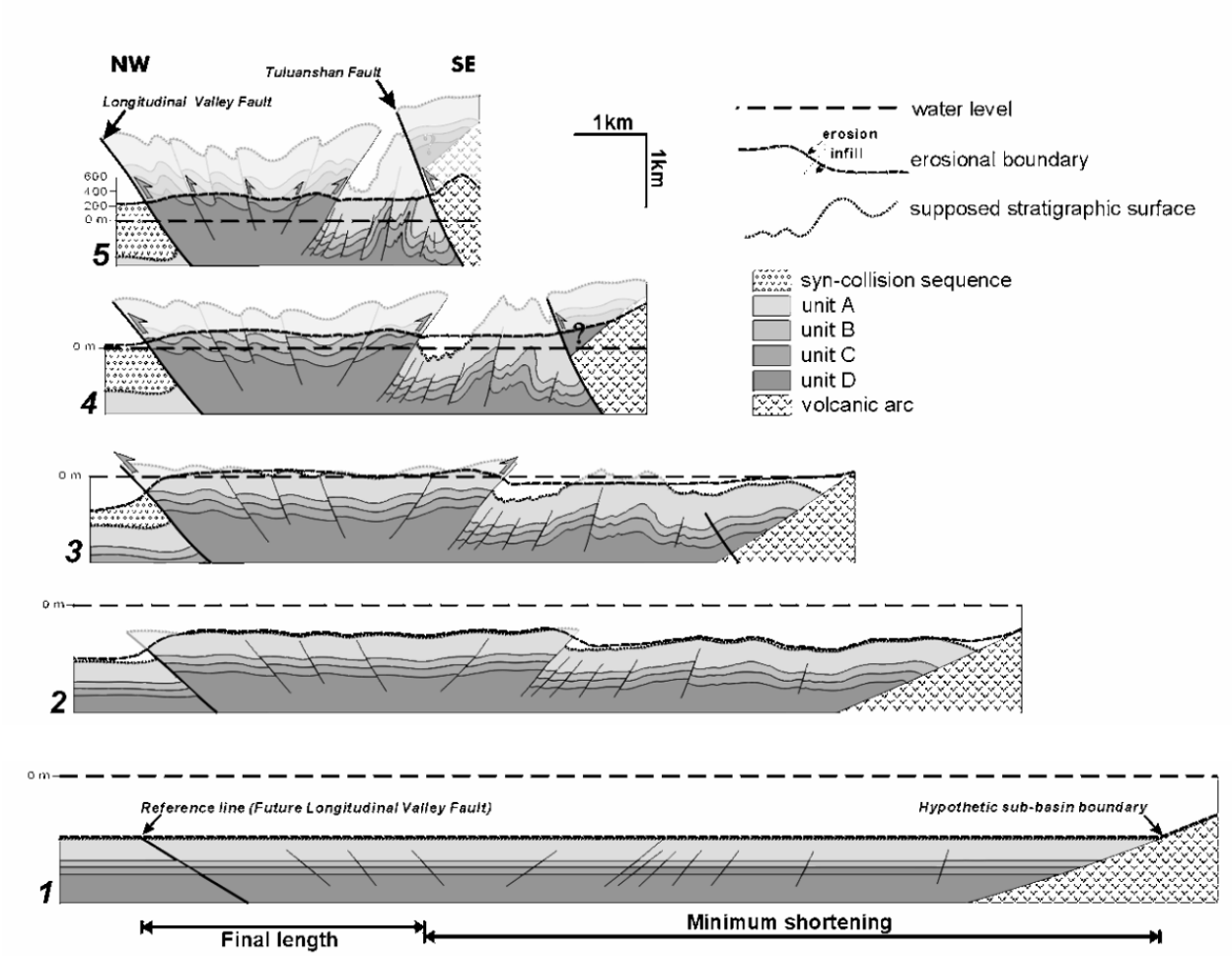


Fig. 5. Structural evolution of the Biehhsi profile. Geometrical assumptions and limitations are discussed in text. The initial configuration for the bottom of the forearc basin is considered as a simple horizontal plane. Units A, B, C and D (from top to bottom) represent the original position of forearc basin sequences at the first period (stage 1). For the last period (stage 5), these units are equivalent with the four units α, β, γ and δ discussed in the text and shown in Fig. 3. Geometrical restoration was carried out based on consideration of length of bedding interfaces. Because of the lack of subsurface data (drill-holes or seismic reflection profiles) in the area investigated, de´collement surfaces could not be located. To account for compaction and water escape in compressed mudstones, and also for non-planar shear deformation, a surface reduction of about 20% is applied between stage 1 and stage 5. According to this reconstruction, extensively sheared mudstones came from the lowest position in the basin, whereas weakly sheared mudstones came from the uppermost position and underwent a shorter extrusion path. The minimum shortening between the Longitudinal Valley Fault and the Tuluanshan Fault is about 10 km.

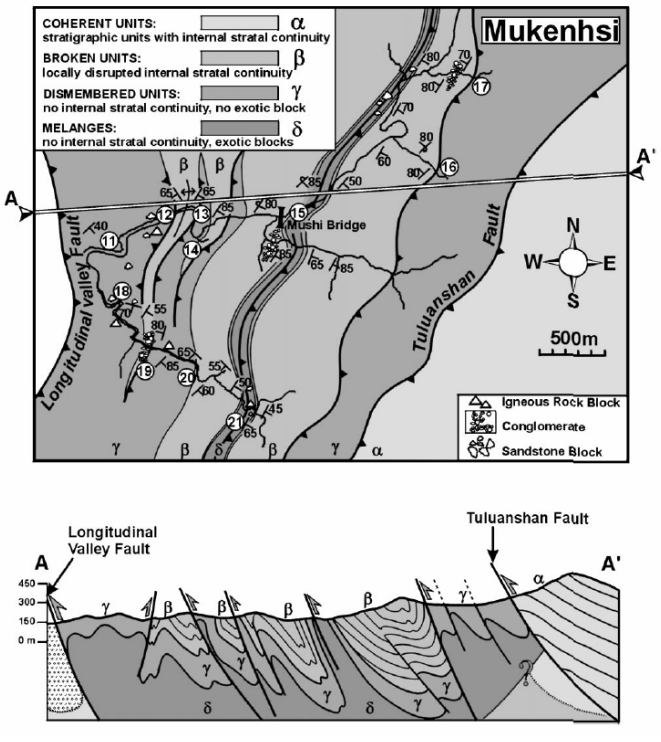


Fig. 4. Detailed geologic map of the Mukenhsi valley area and geologic cross-section. Circled numbers 11–21 refer to sites of brittle tectonic analysis in the Lichi Mélange (stereoplots in Fig. 7).




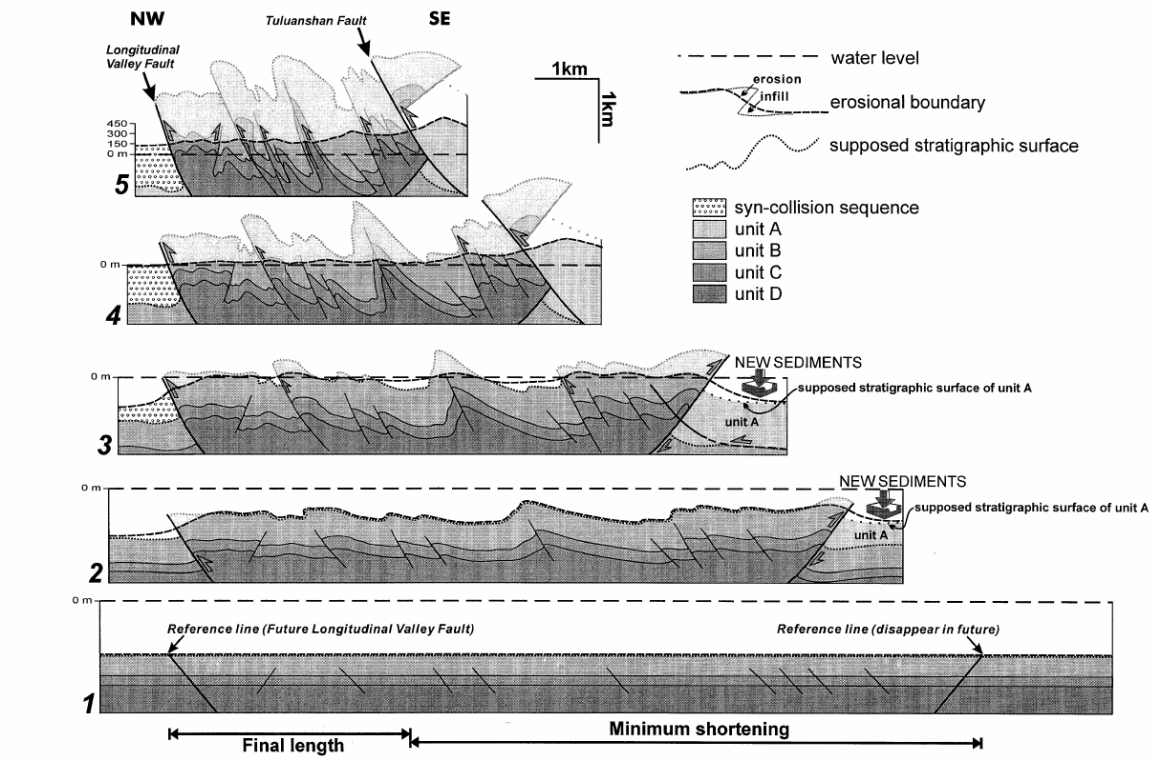


Fig. 6. Structural evolution of the Mukenhsi profile. Principle of restoration as for Fig. 5. Between the Longitudinal Valley Fault and the Tuluanshan Fault, the minimum shortening is about 9 km. Note the particular evolution of the backthrust, which explains the final structure with the younger Takankou Formation (unit A) overriding the older Lichi Mélange (unit C and unit D) across the Tuluanshan Fault.

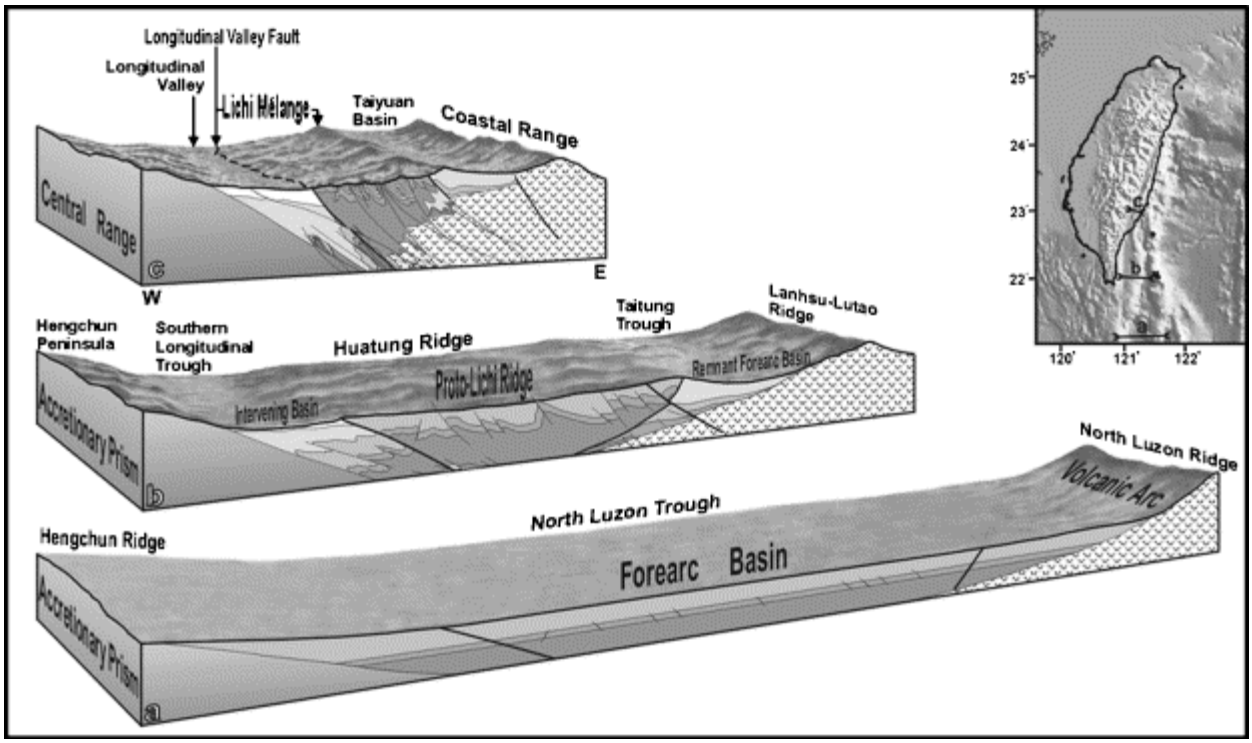


Fig. 9. Structural evolution of the Lichi Mélange and the Longitudinal Valley Fault. Three bars in the topographical map (upper right inset) indicate the approximate locations of staged evolution profiles a, b and c. Because the Taiwan arc–continent collision is a typical oblique collision, the collision and Taiwan orogen propagate southward, so that one reconstructs the tectonic evolution by comparing geological cross-sections at different latitudes. Thus, for stages A and B, some names of geomorphologic units located off southeastern Taiwan at the present are used to support the explanation. Stage C is directly observed in the study area of this paper. The topography shown in figure does not completely fit the present real topography: to illustrate the structural evolution better, the topography and geographic distribution of the Lichi Mélange were exaggerated; and the geographic extent of the undeformed domain of the forearc basin was underestimated. According to this model, the Longitudinal Valley Fault originated as an arc–prism boundary and because of arc–continent collision, developed as the main plate boundary in the weak zone between the accretionary prism (the Central Range derived from the Eurasian continent) and the Luzon arc (the Coastal Range on the Philippine Sea plate side).

**(2) Active faults along the southernmost Longitudinal Valley**.

Text and figures from Shyu, J. B. H., K. Sieh, Y.-G. Chen, R. Y. Chuang, Y. Wang, and L.-H. Chung (2008), Geomorphology of the southernmost Longitudinal Valley fault: Implications for evolution of the active suture of eastern Taiwan, Tectonics, 27,


**Abstract**

In order to understand fully the deformational patterns of the Longitudinal Valley fault system, a major structure along the eastern suture of Taiwan, we mapped geomorphic features near the southern end of the Longitudinal Valley, where many well-developed fluvial landforms record deformation along multiple strands of the fault. Our analysis shows that the Longitudinal Valley fault there comprises two major strands. The Luyeh strand, on the west, has predominantly reverse motion. The Peinan strand, on the east, has a significant left-lateral component. Between the two strands, late Quaternary fluvial sediments and surfaces exhibit progressive deformation. The Luyeh strand dies out to the north, where it steps to the east and joins the Peinan strand to become the main strand of the reverse sinistral Longitudinal Valley fault. To the south, the Luyeh strand becomes an E-W striking monocline. This suggests that the reverse motion on the Longitudinal Valley system decreases drastically at that point. The Longitudinal Valley fault system is therefore likely to terminate abruptly there and does not seem to connect to any existing structure further to the south. This abrupt structural change suggests that the development of the Longitudinal Valley suture occurs through discrete structural ‘‘jumps,’’ rather than by a continuous northward maturation.


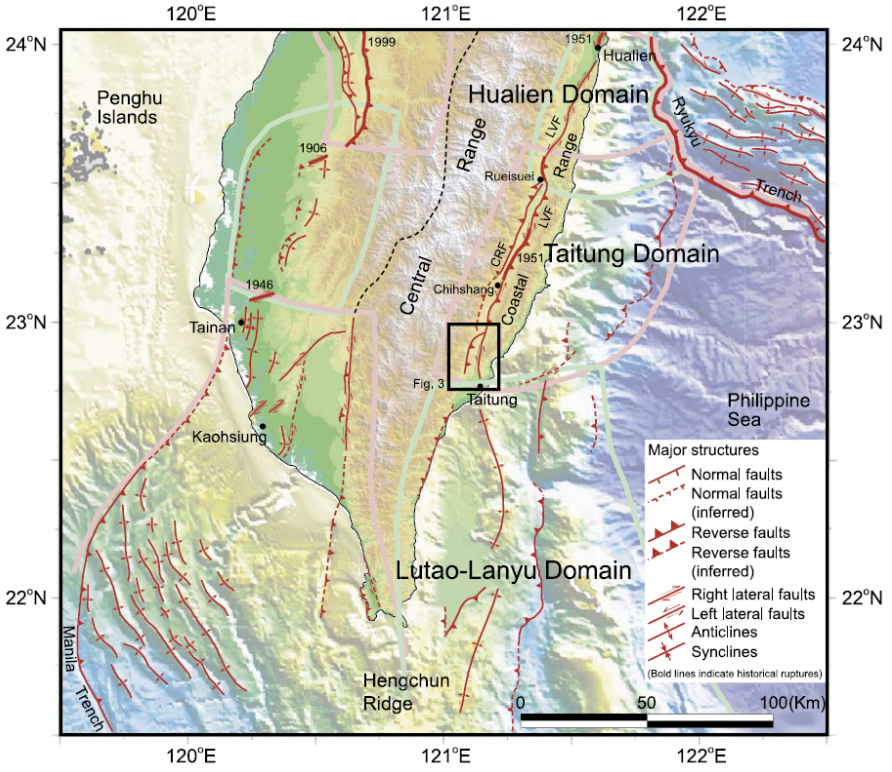


**Figure 2**. Map of neotectonic domains of southeastern Taiwan, modified from Shyu et al. [2005b]. Each domain contains a distinct assemblage of active structures. Two domains, the Hualien and Taitung Domains, are present in eastern Taiwan along the Longitudinal Valley suture. LVF: Longitudinal Valley fault; CRF: Central Range fault. Bold light green and pink lines are boundaries of domains.

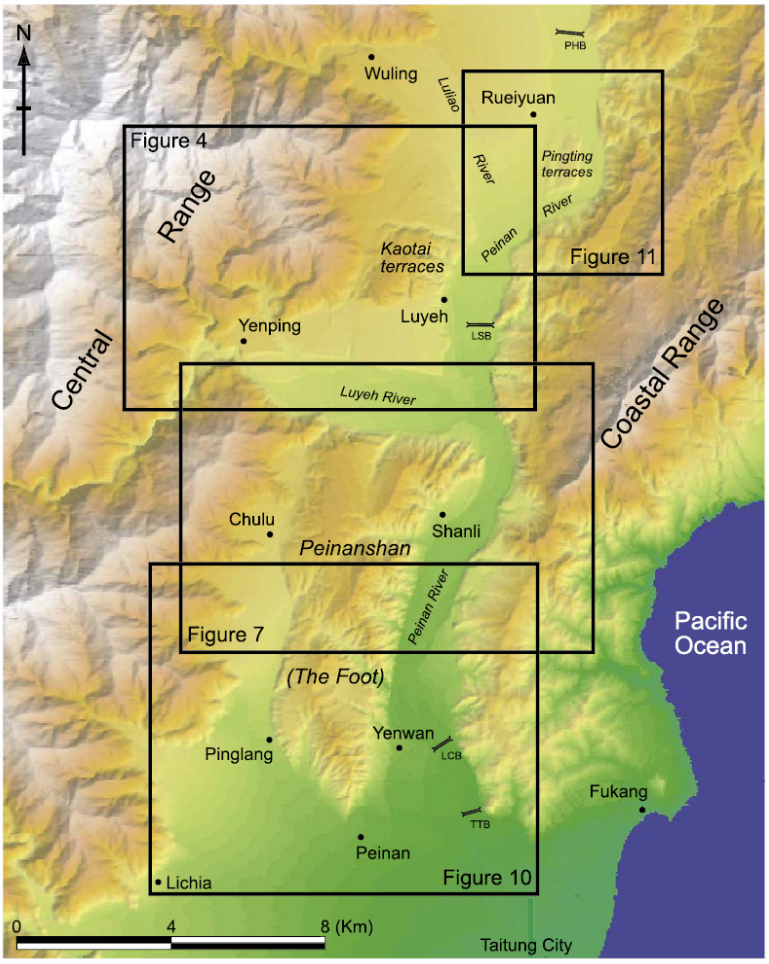


**Figure 3**. Major fluvial landforms near the southernmost Longitudinal Valley. Between the Central and Coastal Ranges are several uplifted fluvial surfaces. South of the Luyeh River, the Peinanshan is an elongate hill underlain by fluvial Peinanshan Conglomerate and capped by lateritic fluvial terraces. North of the Luyeh River, the Kaotai terraces are lateritized fluvial surfaces that may be correlative with the highest surfaces of the Peinanshan. East of the Luliao River, the lower Pingting terraces are underlain by young, thin uplifted Peinan River gravels deposited on Lichi Formation.

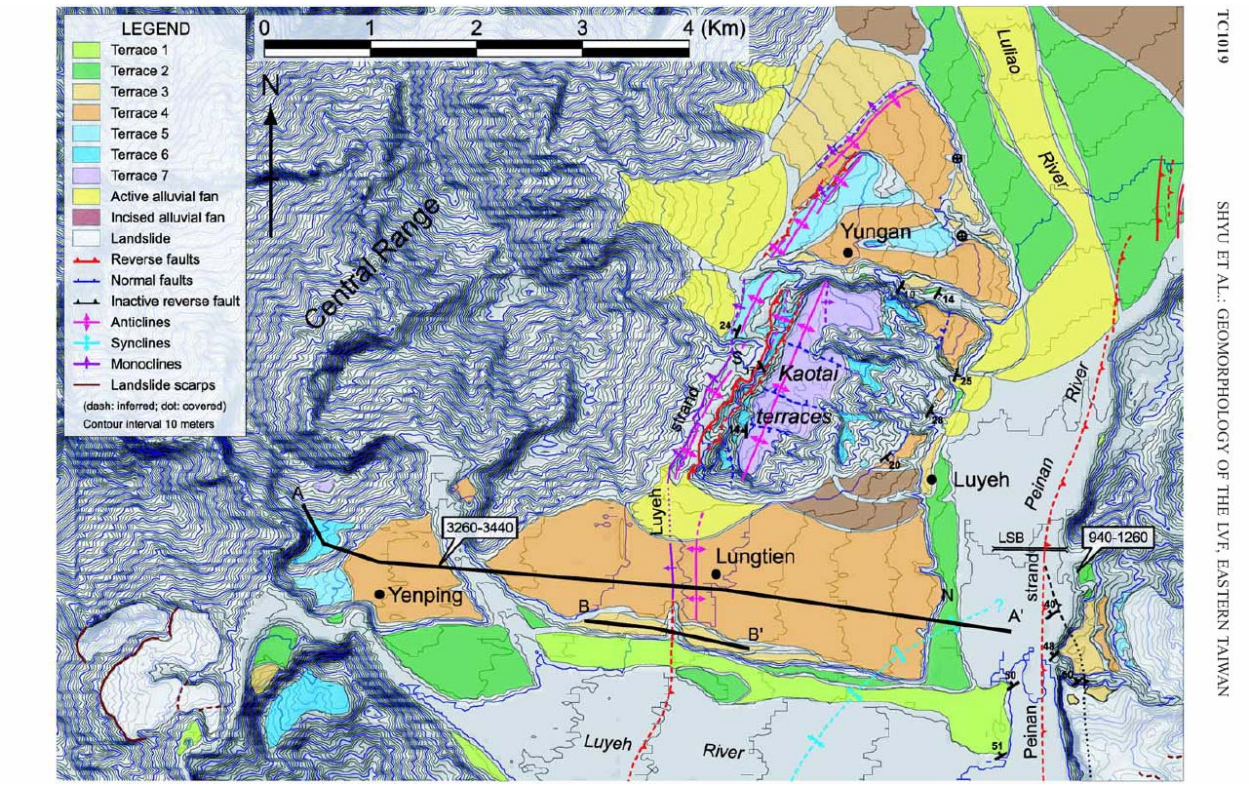


**Figure 4.** Detailed map of geomorphic features and active structures of the Kaotai terraces area. Note that the names of terraces indicate only the relative ages of the terraces and do not imply correlation of the terraces; that is, terrace 4 north of the Luyeh River may not be the same age as terrace 4 elsewhere. The Luyeh strand, a major strand of the Longitudinal Valley fault, runs along the western edge of the Kaotai terraces and has produced a monoclinal scarp on the Lungtien terrace to the south. To the north, the Luyeh strand dies out just south of the Luliao River. The other strand of the Longitudinal Valley fault, the Peinan strand, runs within the Peinan River valley and through the Luanshan Bridge (LSB) about 200 m from the eastern end of the bridge. Ages of terraces are calibrated ages (2s), in cal BP.


**Figure 6**. Field photographs of several deformed bridges across the Peinan River. (a) About 200 m from its eastern end, the Luanshan Bridge has been fractured, with its eastern part displaced relatively westward. View is toward the south. (b) Near the eastern end of the Lichi Bridge, an eastern section of the bridge appears to have moved upward and caused deformation of its contact with its neighboring section to the west. The lower part of the contact appears to have opened and the upper part of the contact appears to have narrowed. View is toward the north. (c) About 100 m from its eastern end, the Paohua Bridge has been deformed by the Longitudinal Valley fault. The eastern part of the bridge has moved upward with respect to its western part. View is toward the west.

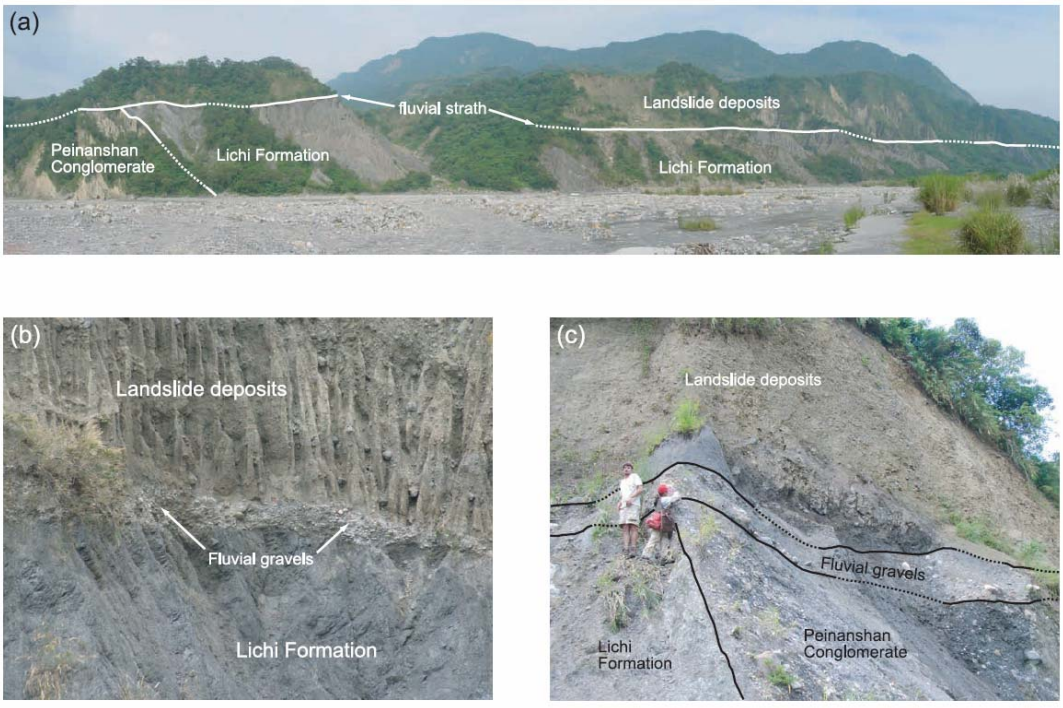


**Figure 9.** Photos of the landslide deposits on the eastern bank of the Peinan River. (a) The landslide sits on a fluvial strath, now 80 m above the modern Peinan River bed, on rocks of the Lichi Fm. and the Peinanshan Conglomerate. The location from which the photo was taken and its view direction are shown in Figure 7. (b) A thin layer of rounded fluvial gravels, about 1–2 m thick, lies between the strath and the landslide deposits. The photo was taken at point G in Figure 7, looking to the north. (c) The contact between the Lichi Formation and the Peinanshan Conglomerate, which may be an old fault, is covered by the fluvial gravels and the landslide deposits. No offset along this contact is present in the fluvial gravels or the landslide deposits. The photo was taken in a small westward flowing canyon, at point K in Figure 7, looking to the south.

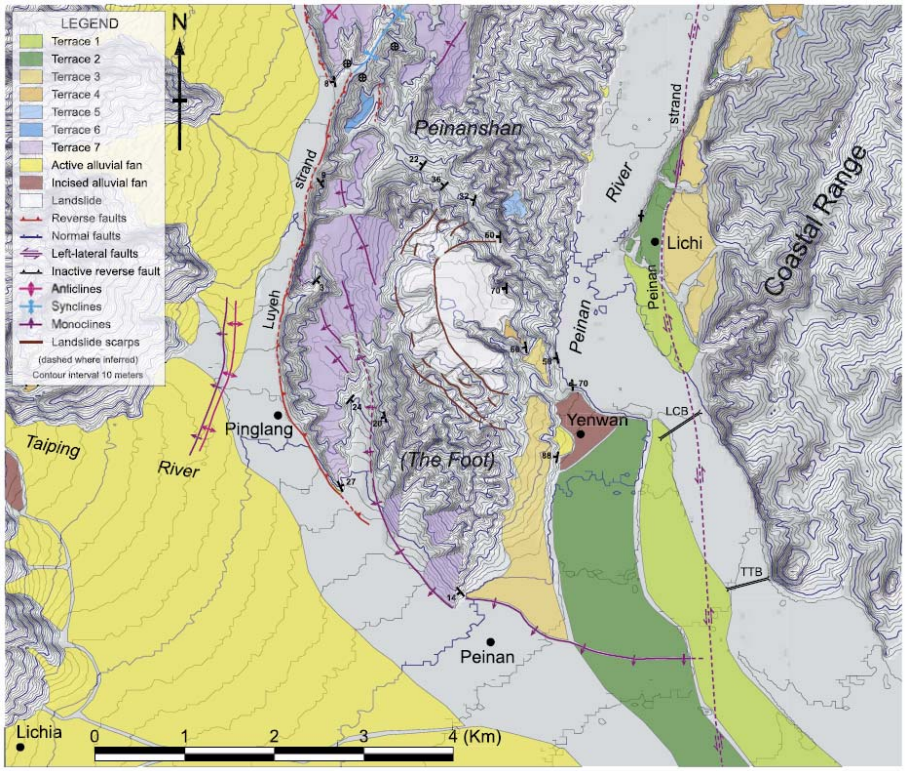


**Figure 10.** Detailed map of geomorphic features and active structures of the southern Peinanshan area. The Luyeh strand runs along the western front of the Peinanshan, but becomes an E-W striking monocline that wraps around the southernmost part of the Peinanshan. The Peinan strand traverses the Peinan River valley, but produces a small N-S scarp on the terraces near Lichi.



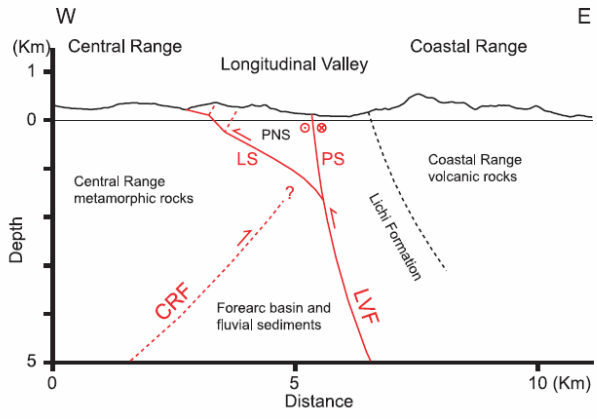


**Figure 13.** A schematic tectonic E-W cross section at the latitude of the Peinanshan shows the proposed tectonic model for the southern end of the Taitung Domain. The east-dipping Longitudinal Valley fault (LVF) branches into the Luyeh strand (LS) and the Peinan strand (PS), between which late Quaternary fluvial surfaces and the Peinanshan Conglomerate (PNS) are progressively deformed. The Luyeh strand crops out along the western edge of the Peinanshan, while the Peinan strand traverses the Peinan River valley. The west-dipping Central Range fault appears to be blind in this area and is overridden by the Longitudinal Valley fault. However, the uplifted and deformed terraces along the upper reach of the Luyeh River suggest the Central Range fault is also active.

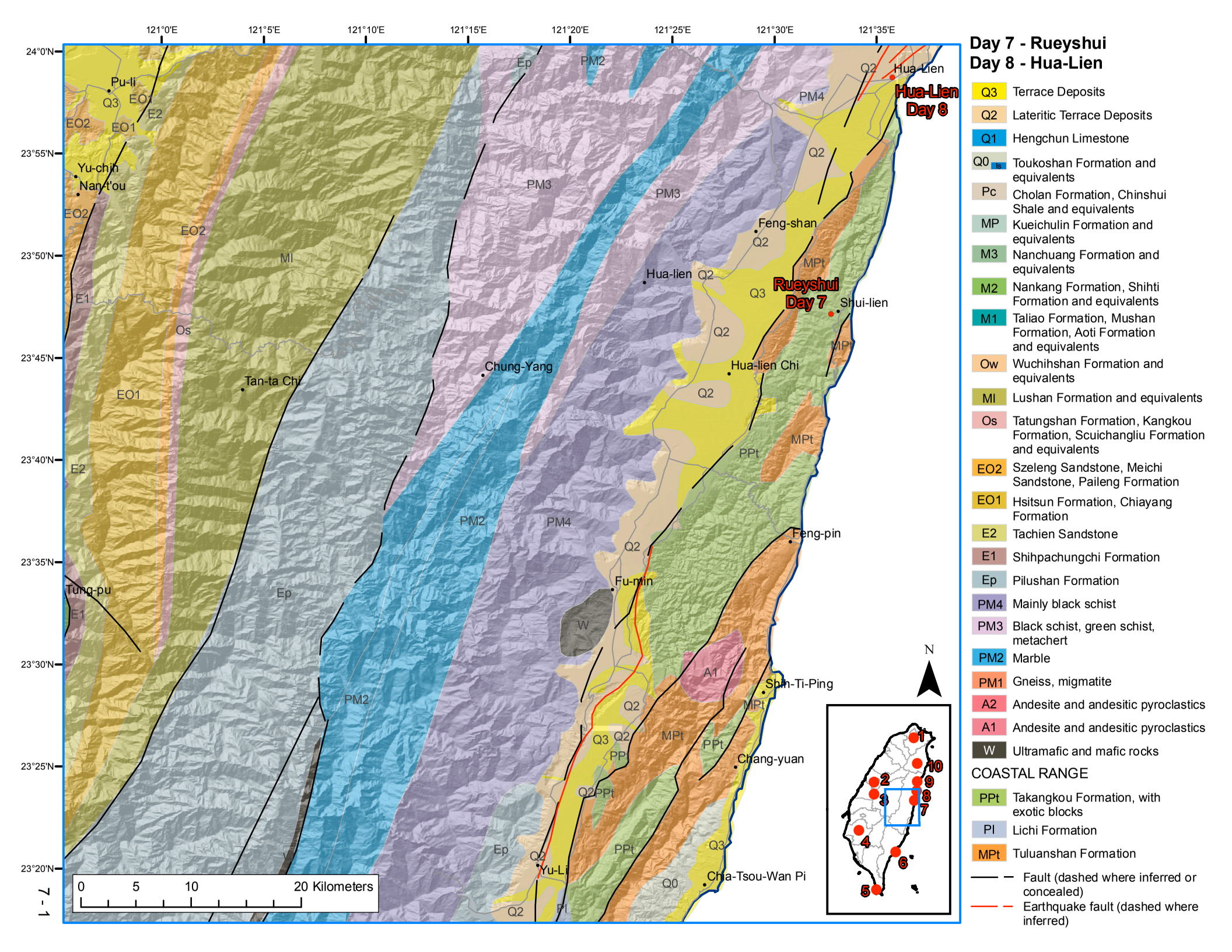
121°0'E
121°5'E
121°10'E
121°15'E
121°20'E
121°25'E
121°30'E
121°35'E
24°0'N
23°55'N
23°50'N
23°45'N
23°40'N
23°35'N
23°30'N
23°25'N
23°20'N
Pu-li
Yu-chih
Nan-t'ou
Tan-ta Chi
Chung-Yang
Hua-lien
Feng-shan
Hua-Lien
Hua-Lien Day 8
Rueyshui Day 7
Shui-lien
Hua-lien Chi
Feng-pin
Fu-min
Shih-Ti-Ping
Chang-yuan
Yu-Li
Chia-Tsou-Wan Pi
Tung-pu
Ep
PM2
PM4
PM3
Q2
Q3
EO2
EO1
E2
E1
Os
MI
MPt
PPt
A1
W
Q0
Pl
0 5 10 20 Kilometers
N
Day 7 - Rueyshui
Day 8 - Hua-Lien
Q3 Terrace Deposits
Q2 Lateritic Terrace Deposits
Q1 Hengchun Limestone
Q0 Toukoshan Formation and equivalents
Pc Cholan Formation, Chinshui Shale and equivalents
MP Kueichulin Formation and equivalents
M3 Nanchuang Formation and equivalents
M2 Nankang Formation, Shihti Formation and equivalents
M1 Taliao Formation, Mushan Formation, Aoti Formation and equivalents
Ow Wuchihshan Formation and equivalents
MI Lushan Formation and equivalents
Os Tatungshan Formation, Kangkou Formation, Scuichangliu Formation and equivalents
EO2 Szeleng Sandstone, Meichi Sandstone, Paileng Formation
EO1 Hsitsun Formation, Chiayang Formation
E2 Tachien Sandstone
E1 Shihpachungchi Formation
Ep Pilushan Formation
PM4 Mainly black schist
PM3 Black schist, green schist, metachert
PM2 Marble
PM1 Gneiss, migmatite
A2 Andesite and andesitic pyroclastics
A1 Andesite and andesitic pyroclastics
W Ultramafic and mafic rocks
COASTAL RANGE
PPt Takangkou Formation, with exotic blocks
Pl Lichi Formation
MPt Tuluanshan Formation
Fault (dashed where inferred or concealed)
Earthquake fault (dashed where inferred)
1
2
3
4
5
6
7
8
9
10

# Active Faults at the Plate Suture Along the Longitudinal Valley

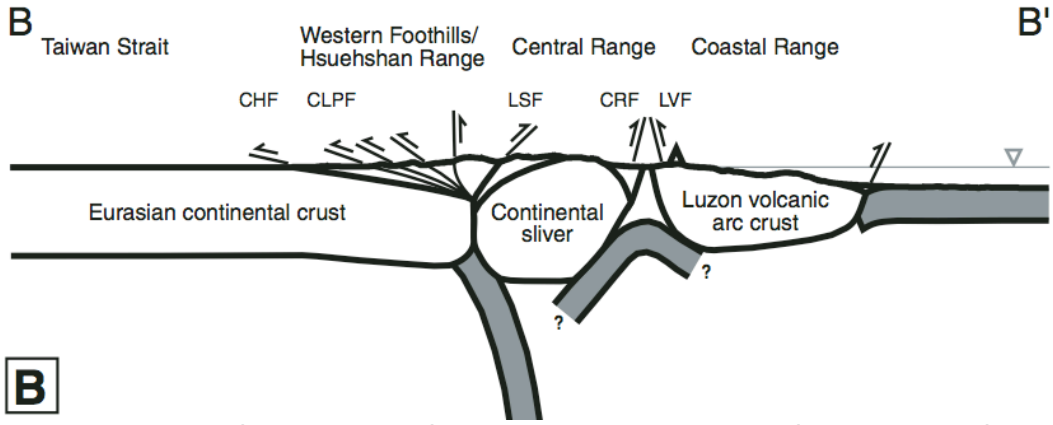


**Figure 1.** A NW–SE schematic crustal cross section across central Taiwan, . . . showing relationship of the three terraines during suturing. CHF–Changhua fault; CLPF—Chelungpu fault; LSF—Lishan fault; CRF—Central Range fault; LVF—Longitudinal Valley fault. No vertical exaggeration (Shyu et al., 2006)

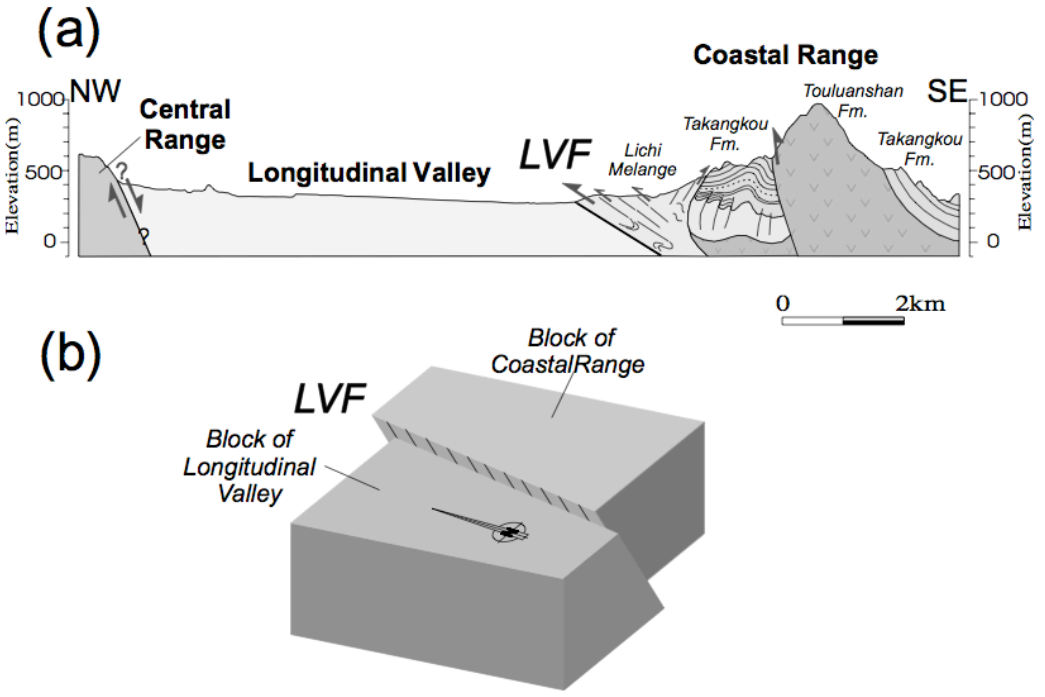


**Figure 2.** (a) General cross-section of the Longitudinal Valley. The Coastal Range along the Longitudinal Valley Fault (LVF) overthrusts to the Longitudinal Valley. (b) 3D reconstruction of the Longitudinal Valley Fault. (Lee et al., 2001)

## Overview shamelessly borrowed from some references,

The Longitudinal Valley Fault is "the present-day plate suture between the Eurasian and the Philippine Sea plates in eastern Taiwan." The Chihshang thrust fault is the most active segment of this suture. Through creep meter monitoring from 1998 to 2001, Lee et al. determined that creep on the Chihshang thrust fault is seasonal and moves steadily during the rainy season yet remains dormant through the rest of the year. "Through comparison with daily precipitation data, they inferred that moderate rainfall triggers or facilitates slippage on the surface fault. However, recurrent earthquakes occur regardless of season, indicating that the stress relaxation associated with seismicity in the seismogenic zone [does] not transfer immediately up to the surface" (Lee et al., 2003).

"The earthquakes of November 1951 constitute the most destructive seismic episode in the recorded history of the Longitudinal Valley, eastern Taiwan.. . . We divide the surface ruptures from south to north into the Chishang, Yuli, and Rueisuei sections. The first shock of the 1951 series probably resulted from the Chihshang rupture, and the second shock probably resulted from the Yuli and Rueisuei ruptures. The lengths of these ruptures indicate that the two shocks had similar magnitudes. The Chihshang and Rueisuei ruptures are along segments of the Longitudinal Valley fault, a left-lateral oblique fault along which the Coastal Range thrusts westward over the Longitudinal Valley. The Yuli rupture, on the other hand, appears to be part of a separate, left-lateral strike-slip Yuli fault, which traverses the middle of the Longitudinal Valley" (Shyu et al., 2007).

"Numerous landforms along the Longitudinal Valley suture of eastern Taiwan indicate that two opposing reverse faults currently dominate the suturing process between the Luzon volcanic arc and the Central Range of Taiwan. The east-dipping Longitudinal Valley fault, on the eastern flank of the valley, is well known. The west-dipping Central Range reverse fault, on the western flank of the valley, is more obscure. Nonetheless, it has produced many uplifted lateritic fluvial terraces along the eastern flank of the Central Range in the central reach of the valley, from just north of the Wuhe Tableland to near Chihshang. The fault appears to be active but blind south of Chihshang and inactive along the northern part of the Longitudinal Valley. The late Quaternary slip rate of the fault is less than 12.8 mm/yr. This constraint means that the fault is absorbing far less than half of the horizontal shortening across the Longitudinal Valley suture. However, the late Quaternary slip rate along the fault may be comparable to the uplift and exhumation rate of the Central Range. This suggests that localized brittle slip along the Central Range fault is an important component of crustal thickening and uplift of the range, even though additional shortening and crustal thickening may be occurring because of pervasive deformation beneath the range" (Shyu et al., 2006).

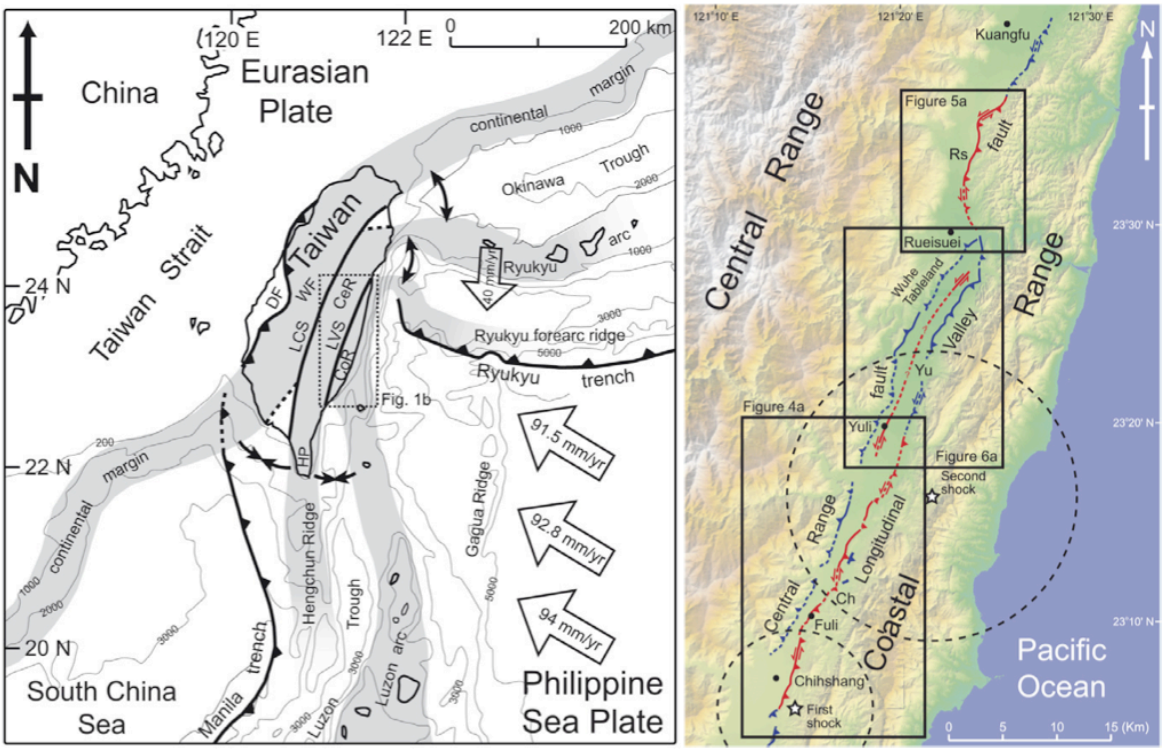


**Figure 3.** (left) Taiwan is experiencing a transitory tandem suturing of a volcanic arc and a sliver of continental crust to the Asian continental margin. The 1951 earthquakes resulted from failure of faults along the Longitudinal Valley suture (LVS), the eastern of the two sutures. This suture is developing by the oblique collision of the Luzon volcanic arc into a narrow strip of continental crust. Adapted from Shyu etal. (2005a). DF, deformation front; LCS, Lishan-Chaochou suture; WF, Western Foothills; CeR, Central Range; CoR, Coastal Range; HP, Hengchun Peninsula. (right) Shaded relief map showing the active structures in the middle part of the Longitudinal Valley, between the Central and Coastal Ranges. Our estimate of the extent of the November 1951 ruptures is shown in red. Major active reverse faults and Xexures that did not rupture in 1951 are shown in blue. ModiWed from Shyu etal. (2002, 2005b) and unpublished results of J.B.H. Shyu and L.-H. Chung. Ch, Chihshang rupture; Yu, Yuli rupture; Rs, Rueisuei rupture. Dashed faults are inferred. White stars are relocated epicenters of the November 1951 earthquakes, after Cheng etal. (1996), with their uncertainties shown as dashed circles. (Shyu et al., 2007)

Lee, J.C., Angelier, J., Chu, H.T., Hu, J.C. and Jeng, F.S., 2001. Continuous monitoring of an active fault in a plate suture zone: a creepmeter study of the Chihshang Fault, eastern Taiwan. Tectonophysics, 333(1-2): 219-240.

Lee, J.C. et al., 2003. Active fault creep variations at Chihshang, Taiwan, revealed by creep meter monitoring, 1998-2001. Journal of Geophysical Research-Solid Earth, 108(B11).

Shyu, J.B.H., Chung, L.H., Chen, Y.G., Lee, J.C. and Sieh, K., 2007. Re-evaluation of the surface ruptures of the November 1951 earthquake series in eastern Taiwan, and its neotectonic implications. Journal of Asian Earth Sciences, 31(3): 317-331.

Shyu, J.B.H., Sieh, K., Chen, Y.G. and Chung, L.H., 2006. Geomorphic analysis of the Central Range fault, the second major active structure of the Longitudinal Valley suture, eastern Taiwan. Geological Society of America Bulletin, 118(11-12): 1447-1462.

## Day 8 - 6/23 Rueyshui to Hualien

Transect and cross section of the Coastal Range along the Hsiuguoluan River: deformed Luzon Volcanic arc and the intra-arc basins

### Stops: Siou-Gu-Luan-Ci

(2) "The Taiwan orogen is the product of a tandem suturing and tandem disengagement of the Asian continental margin, the Luzon volcanic island arc, and a thin intervening continental sliver [Shyu et al., 2005b] (Figure 1). In the south, the three lithospheric blocks have begun colliding. Bothcollisions mature northward, creating the main body of the island and the numerous active thrust faults and folds that are manifestations of the double suturing. A tandem disengagement occurs in the northeastern quarter of the island above the Ryukyu subduction zone, where normal faulting is dominant and the three lithospheric blocks are separating along the two sutures. The Central Range, Taiwan's mountainous backbone, is the exhumed portion of a sliver of continental lithosphere, flanked on the east by the Coastal Range, the attached part of the Luzon volcanic arc. Between these two linear mountain ranges is the Longitudinal Valley, the locus of the suture between the continental sliver and the collided volcanic arc."

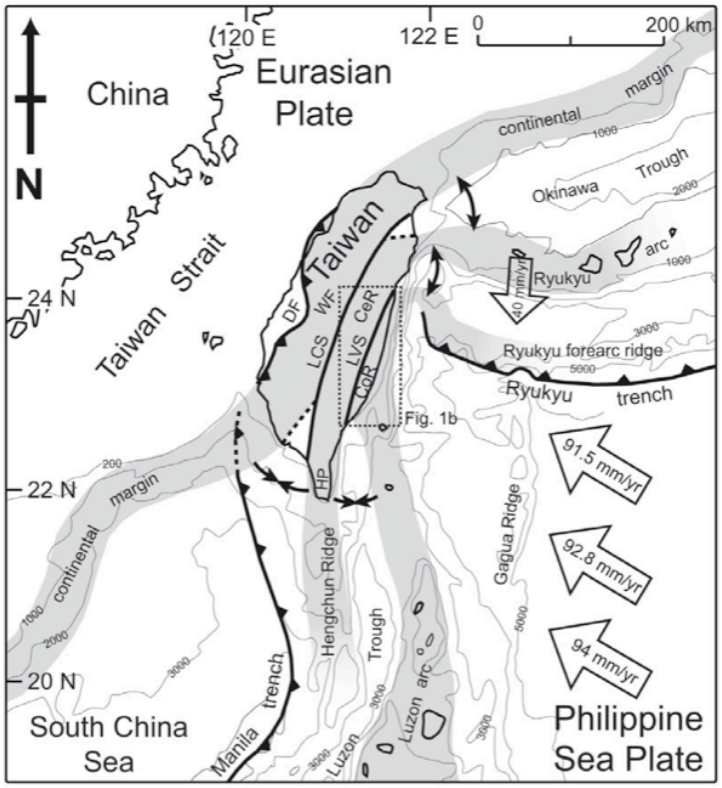


FIGURE 1
(2) "*Taiwan orogen being created by a tandem suturing of the Luzon volcanic arc and a sliver of continental crust to the Chinese continental margin. The Longitudinal Valley suture (LVS), in eastern Taiwan, represents the eastern of the two sutures, joining the Coastal Range (CoR) and the Central Range (CeR) blocks. Current velocity vectors of the Philippine Sea plate relative to south China, at 124_E and 20_, 21_, and 22_N, are calculated using the Recent plate velocity model (REVEL) of Sella et al. [2002]. Current velocity vector of the Ryukyu arc is adapted from Lallemand and Liu [1998]. Black dashed lines are the northern and western limits of the Wadati-Benioff zone of the two subduction zones, taken from the seismicity database of the Central Weather Bureau, Taiwan. DF, deformation front; LCS, Lishan-Chaochou suture; WF, Western Foothills; HP, Hengchun Peninsula. Adapted from Shyu et al. [2005b] with permission from Elsevier.*"

(2) "The Coastal Range is the shortened and accreted part of the Luzon volcanic arc and its forearc basin [e.g., Huang et al., 1997; Chang et al., 2001]. It is composed of an assemblage of young (Miocene through early Pliocene) volcanic arc rocks and associated turbidite deposits, me'lange, and fringing-reef limestones [e.g., W.-S. Chen, 1988; Ho, 1988] (Figure 5). The major geologic unit of the range is the Tuluanshan Formation, mostly andesitic volcanic sediments, such as breccias and tuffs. It forms the highest peaks and ridges of the range. Bordering the volcanic sediments are deep-marine turbidites, including the Fanshuliao and Paliwan formations [Teng, 1980; Teng et al., 1988]. The latter has abundant metamorphic rock fragments derived from the Central Range, which indicate the exposure and proximity of the Central Range during its deposition in a forearc basin [Teng, 1982]. In the southern part of the Coastal Range, the Lichi Formation, with its highly sheared clays and severely fragmented sedimentary sequences, is likely to be a highly shortened section of the forearc basin. Pieces of mafic and ultramafic rocks within the Lichi Formation may be remnants of the forearc oceanic crust [e.g., Chang et al., 2001]."

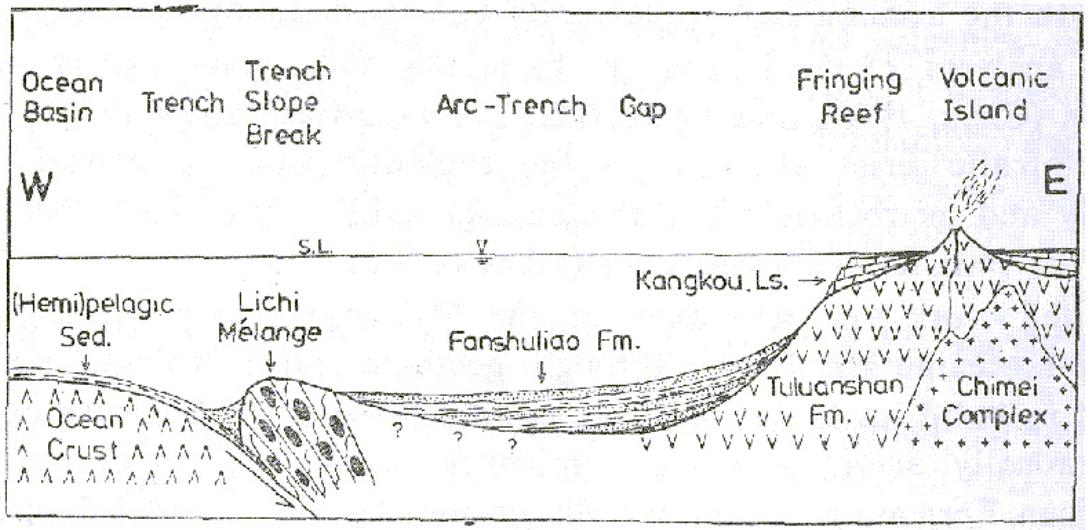


Fig. 4. Arc-trench settings of the Coastal Range before collision.

FIGURE 2
(4) *"Arc-trench settings of the Coastal Range before collision"*

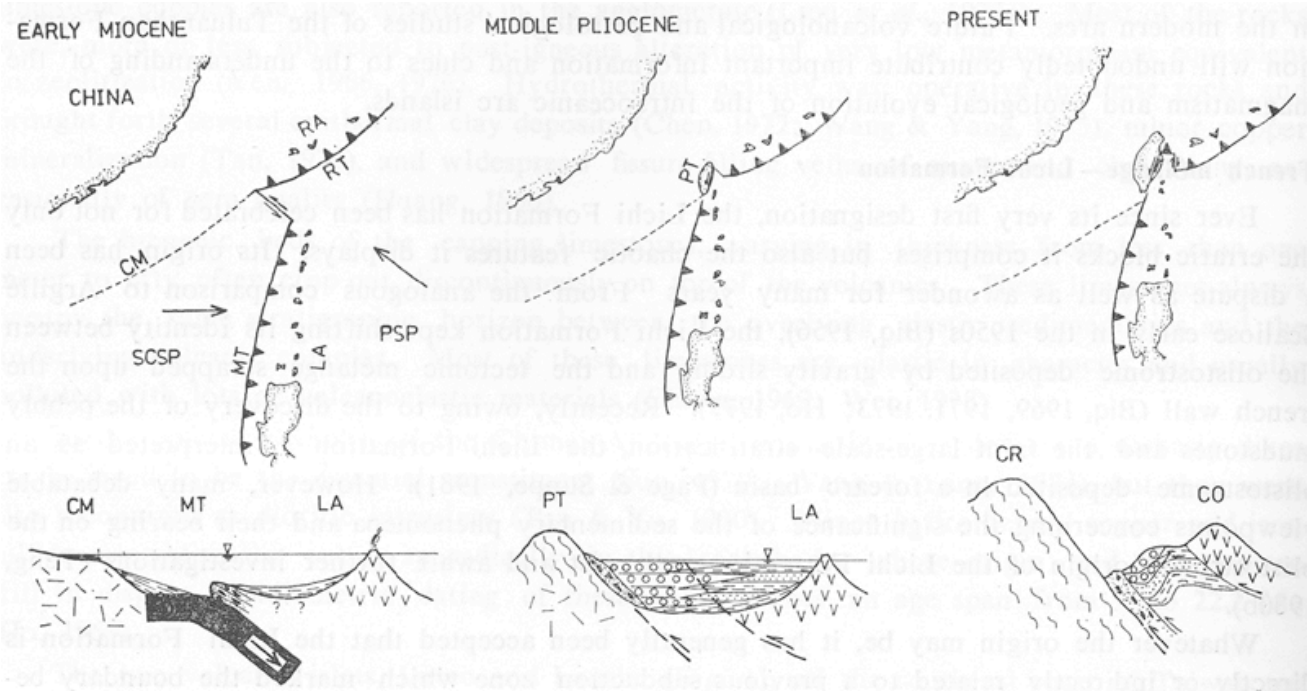


Fig. 5. Tectonic evolution of the Coastal Range arc system. CM, continental margin; CO, Coastal Range; CR, Central Range; LA, Luzon Arc; MT, Manila Trench; PSP, Philippine Sea Plate; PT, Proto-Taiwan; RA, Ryukyu Arc; RT, Ryukyu Trench; SCSP, South China Sea Plate.
Early Miocene: initiation of subduction; build-up of the island arc system.
Middle Pliocene: initial collision; deposition of the continental lithofacies.
Present: collision propogating southward; deformation of the whole Coastal Range.

FIGURE 3
(4) *"Tectonic evolution of the Coastal Range arc system. CM, continental margin; CO, Coastal Rang; CR, Central Range; LA, Luzon Arc; MT, Manila Trench; PSP, Philippine Sea*
*Early Miocene: initiation of subduction; build-up of the island arc system.*
*Middle Pliocene: initial collision; deposition of the continental lithofacies.*
*Present: collision propogating southward; deformation of the whole Coastal Range.*

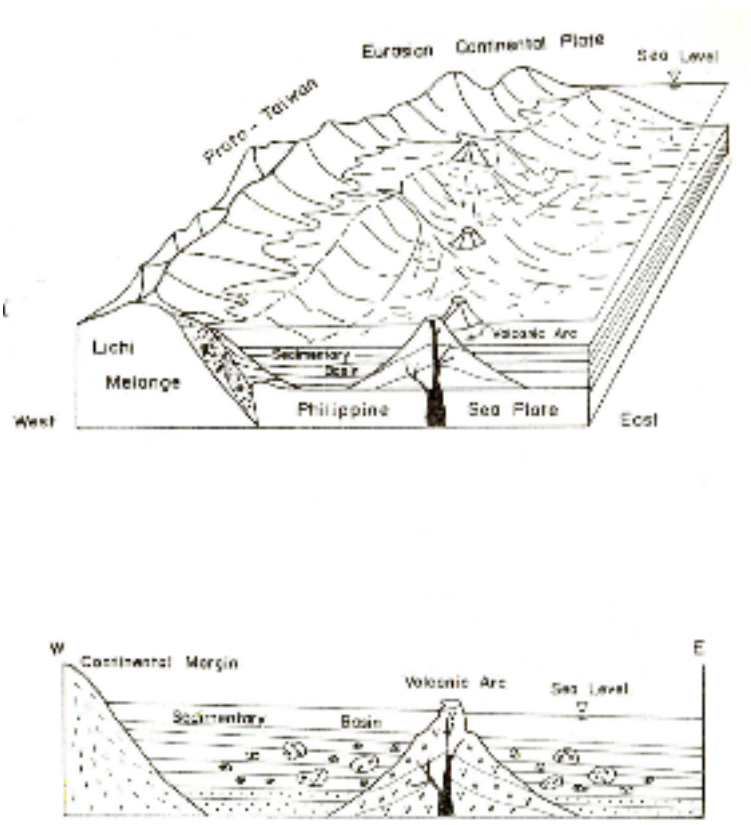


FIGURE 4
(3) *"(A) Sketch diagram indicating the depositional environments during the arc-continent collision. (B) Cross-section showing the vertical and horizontal relationship of sedimentary basin and the volcanic arc, and distributions of the slide volcanic blocks."*

(3) "A group of vertical clastic dikes has recently been found in the volcanic blocks at Chichi in the Coasta Range, eastern Taiwan. These dikes pinch out upwards and show a thickness variation from 10 to 30 centimeters. The dike rocks consist essentially of quartz, feldspar and lithic fragments, all being similar to those constituents of the sandstones in the Paliwan Formation. The volcanic blocks are considered slide blocks, produced through the block glide of the Tuluanshan volcanic. The clastic dikes are accordingly interpreted as the products of the upward in jection of unconsolidated sediments into the volcanic blocks due to liquefaction caused by an abrupt increase in pore-fluid pressure in the sediments induced by the block glide of the volcanic during the deposition of the Paliwan Formation. The slide volcanic blocks ranging from several centimeters to hundreds of meters in size are widely distributed in the Coasta Range. It is believed that the block glide of the volcanic rocks and the slumping of sediments were very common in the Coastal Range during the arc-continent collision."

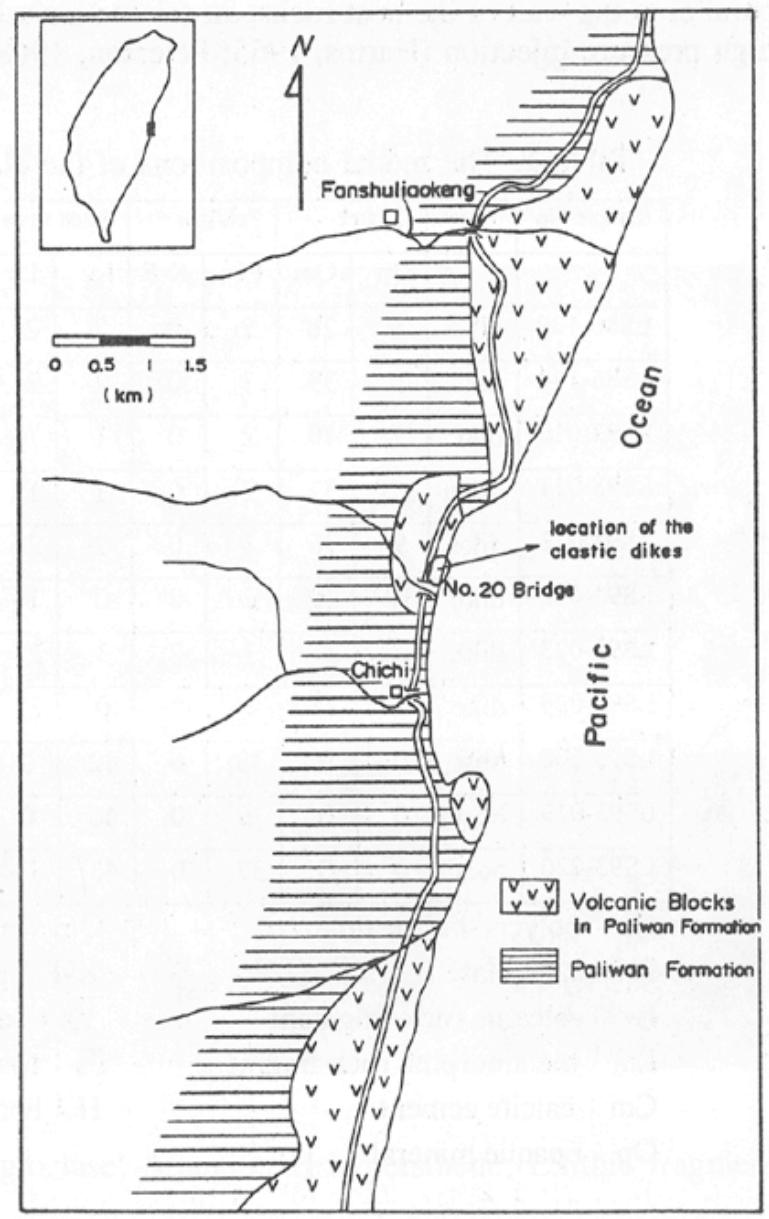


FIGURE 5
(3)*"Geological map of the Chichi area of the Coastal Range, eastern Taiwan showing the location of the clastic dikes and the relationship between the volcanic blocks and Paliwan Formation"*

(2) "Near the middle of the Longitudinal Valley, the Hsiukuluan River cuts through the Coastal Range and flows eastward to the Philippine Sea. Along this segment of the river (hereafter referred to as Hsiukuluan canyon) are many levels of fluvial terraces [e.g., Chang et al., 1992] (Figure 4), which provide a record of fluvial incision. Since the Hsiukuluan River is the only river that flows through the Coastal Range, these fluvial terraces provide a unique opportunity to assess long-term patterns and rates of uplift of the range. "

## REFERENCES

(1) Hsu, T.L. (1976) Neotectonics of the Longitudinal Valley, Eastern Taiwan, Bull. Geol. Sur. Taiwan, 25, 43-53.
(2) Shyu, J.B.H.*, Sieh, K., Avouac, J-P., Chen, W.S., Chen, Y.G. (2006) Millennial slip rate of the Longitudinal Valley fault from river terraces: Implications for convergence across the active suture of eastern Taiwan. *J. Geophys. Res.* 111, B08403, doi:10.1029/2005JB003971.
(3) Song, S.R., Lo. H.J. and Chen, W.S. (1994) Origin of clastic dikes in the Coastal Range, eastern Taiwan with implications for sedimentary processes during the arc-continent collision: J. Geol. Soc. China 37, 407-424.
(4) Teng, L.S., and Y. Wang (1981) Island arc system of the Coastal Range, eastern Taiwan, Proc. Geol. Soc. China, 24, 99-112.

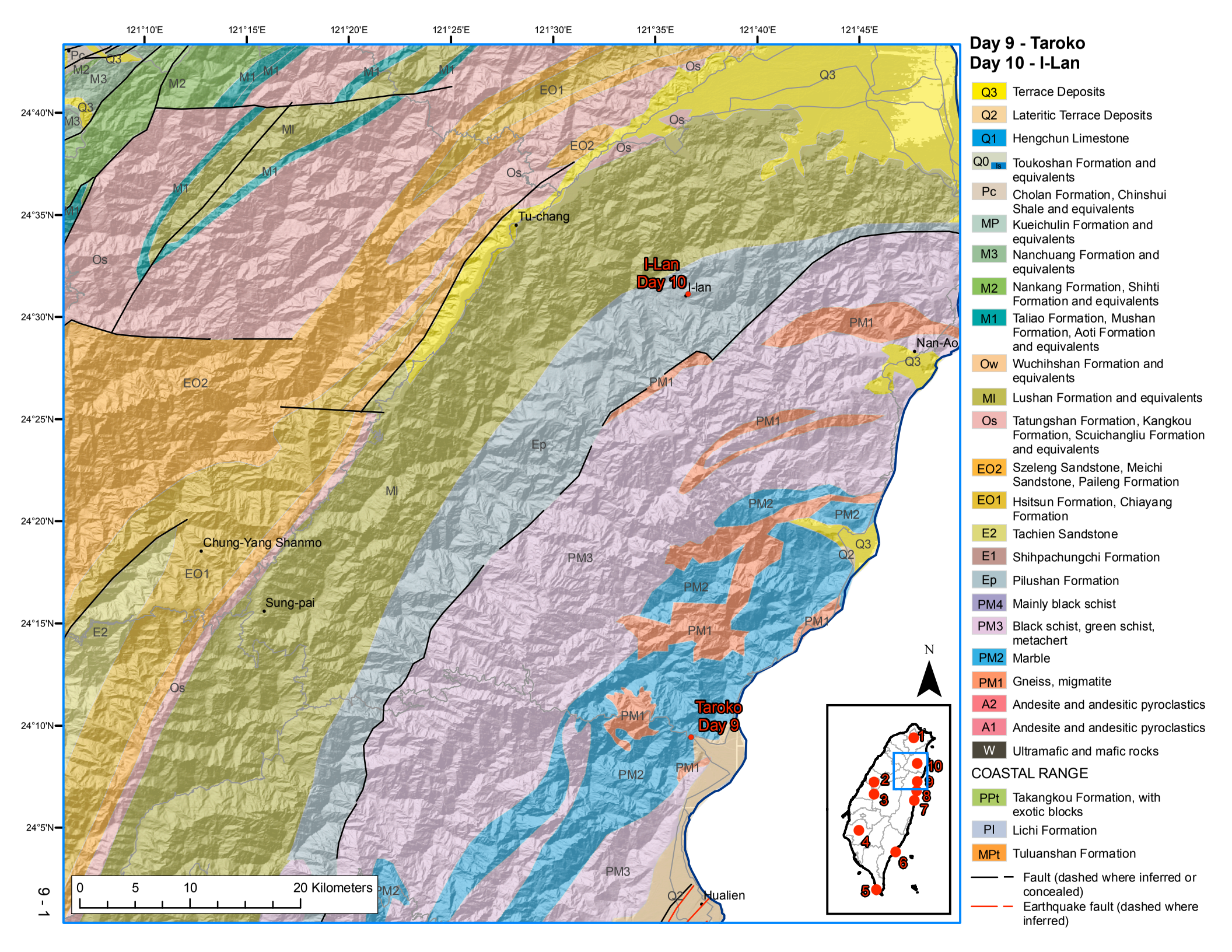


## Day 9 - Taroko
## Day 10 - I-Lan

- Q3 Terrace Deposits
- Q2 Lateritic Terrace Deposits
- Q1 Hengchun Limestone
- Q0 ls Toukoshan Formation and equivalents
- Pc Cholan Formation, Chinshui Shale and equivalents
- MP Kueichulin Formation and equivalents
- M3 Nanchuang Formation and equivalents
- M2 Nankang Formation, Shihti Formation and equivalents
- M1 Taliao Formation, Mushan Formation, Aoti Formation and equivalents
- Ow Wuchihshan Formation and equivalents
- Ml Lushan Formation and equivalents
- Os Tatungshan Formation, Kangkou Formation, Scuichangliu Formation and equivalents
- EO2 Szeleng Sandstone, Meichi Sandstone, Paileng Formation
- EO1 Hsitsun Formation, Chiayang Formation
- E2 Tachien Sandstone
- E1 Shihpachungchi Formation
- Ep Pilushan Formation
- PM4 Mainly black schist
- PM3 Black schist, green schist, metachert
- PM2 Marble
- PM1 Gneiss, migmatite
- A2 Andesite and andesitic pyroclastics
- A1 Andesite and andesitic pyroclastics
- W Ultramafic and mafic rocks

COASTAL RANGE

- PPt Takangkou Formation, with exotic blocks
- Pl Lichi Formation
- MPt Tuluanshan Formation

- Fault (dashed where inferred or concealed)
- Earthquake fault (dashed where inferred)

# Field Trip Guide to the Pre-Tertiary Tananao Metamorphic Complex Along the Eastern Part of the Central Cross-Island Highway, Taiwan

Yu-Chang Chan, Jian-Cheng Lee, Ching-Ying Lan, and Tzen-Fu Yui
Institute of Earth Sciences, Academia Sinica, Taipei, Taiwan, R.O.C.

## 1. Introduction

It is well known that the Taiwan mountain belt is resulted from the late Tertiary convergence between the Eurasian plate and the Philippine Sea plate. Because the convergence is oblique, the collision propagates southward and results in younger collisional features in deformation, metamorphism, and exhumation. The geology of Taiwan can be divided into six N-S trending tectonostratigraphic units (Ho, 1988): from west to east, the Coastal Plain, the Western Foothills fold-and-thrust belt, the Hsuehshan Range slate belt, the Backbone Range slate belt, the Tananao metamorphic complex, and the Coastal Range (Fig. 1). The Western Foothills, the Hsuehshan and Backbone Range slate belts, and the Tananao metamorphic complex belong to the late Tertiary accretionary prism, which exhibits increasing degree of deformation and metamorphism toward the east. The Tananao metamorphic complex consists of voluminous schist and marble as well as scattered bodies of granitic rocks and amphibolite. The metamorphic complex is commonly considered to represent an exposed portion of the Asian continental crust (Ho, 1988). The purpose of this field trip is to show some geologic features of the Tananao metamorphic complex along the eastern part of the Central Cross-Island Highway (Figs. 2 and 3).

## 2. Road Log

Note: these stops may not coincide with those taken on the 2008 trip, but are representative of the area.

**Stop 1: Tienhsiang (天祥)**

The Tienhsiang Formation is very well exposed along the Liwu river bed. At least two or more generations of folding can be observed in this area. Interlayered quartz-mica schist and phyllite are commonly observed with layer disruptions. Pinch-and-swell or boudinage structures are widely present in the multiple deformed rocks. Furthermore, exotic blocks of diverse lithology are recognizable in the Tienhsiang Formation. The rock type of the exotic blocks includes quartzite, marble, greenschist, metasandstone, and metaconglomerate. Based on the occurrence of the exotic blocks, the Tienhsiang Formation was interpreted to be a Mesozoic melange unit.

**Stop 2: Chiuchutung (九曲洞)**

At this stop a spectacular gorge is carved completely within the Chiuchu marble along the Liwu river. The highway passes through the massive marble and is highly scenic in the area. The Chiuchu Marble is composed of mainly calcite marble and locally dolomitic lenses of marble. Numerous approximately N-S trending normal faults can be observed along the road. Analyses of these normal faults suggest the latest tectonic environment is characterized by strike-perpendicular extension in the hinterland of Taiwan.

**Stop 3 : Yentzekou (燕子口) to Paishachiao (白沙橋)**

Deformed granitic rocks of granodiorite origin are exposed from Paishachiao to Yentzeko along the highway. The granitic rocks consist mainly of albite-oligoclase, quartz, biotite with accessories such as titanite, zircon, and opaques. Stretching lineations are well developed and plunge gently toward the northeast. The contact between the granitic rocks and marble is very irregular in the Paishachiao area. Some contact surfaces show features of mylonitization likely due to later deformation. Marble and schist enclaves are commonly observed within the granitic rocks. Previous workers have suggested that the granitic rocks intruded the Changchun and the Chiuchu Formations during late Cretaceous. In the Yentzekou area, the massive marble of the Chiuchu Formation shows an impressive cliff and gorge feature.

**Stop 4: Changchunchiao (長春橋)**

At this stop, we will examine various rock types and structures in the Changchun Formation and discuss the deformation and metamorphism of the Tananao metamorphic complex based on the observations. The Changchun Formation is composed of marble, cherty marble, metachert, quartzite, chlorite schist and amphibolite. Recumbent folds and sheath folds composed of marble and chlorite schist are commonly observed along the river bed and cliff. The sheath fold axes trend about northeast and are consistent with the NE-trending stretching lineations. Some minor recumbent folds can be observed along the road cut. Landslides have caused serious damages at this famous tourist spot during the past few years.

**Stop 5: Tailuko (太魯閣) (National Park Tourist Center)**

The tourist center provides valuable information about the Tailuko national park and is worthwhile visiting for an overview of the spectacular park.

# 3. Notes on the Geologic Background of Pre-Tertiary Tananao Basement Complex of Taiwan

## A. Stratigraphy

The age of the basement rocks was assigned to be pre-Tertiary. Based on lithologic characteristics, the basement rocks were divided into the following five units (Wang Lee, 1979):

1. the Yuli Formation
   - black schist, greenschist, ophiolitic blocks
2. the Changchun Formation
   - greenschist/thin marble layer/metachert interlayer
3. the Chiuchu Formation
   - massive marble
4. the Tienhsiang Formation
   - black schist, metasandstone, metaconglomerate
5. late Cretaceous granitic intrusions

The Yuli Formation forms the Yuli belt, while the rest four units form the Tailuko belt. Fossils are rare. A few Permian fusulinids and corals (Yen et al., 1951; Yen, 1953) and middle Jurassic to early Cretaceous dinoflagellates (Chen, 1989) were recovered from the Changchun Formation and the Tienhsiang Formation, respectively. Stratigraphic correlation is difficult, if not impossible. The above classification, therefore, is only a lithostratigraphic scheme.

## B. Metamorphism

Most of the rocks have greenschist facies mineral assemblages. Rocks near the granitic intrusions may contain amphibolite facies minerals. Ophiolitic rocks, however, still retain some subduction records, which were interpreted resulting from late Cretaceous and mid-Miocene subductions (Liou and Ernst, 1984). The time of metamorphism (thermal-tectonic event) was compiled by Lan et al. (1996) (Fig. 4).

## C. Structure Characteristics

Most deformation structures, such as foliations and lineations, were commonly interpreted to have resulted from the late Tertiary tectonic event that exhumed the Tananao metamorphic complex (e.g., Stanley et al., 1981; Chan, 1990; Faure et al., 1991; Clark et al., 1992; Byrne, 1995). In the Tailuko region, the structures are

characterized by a gently to moderately dipping foliation and a NE-plunging stretching lineation. Lu and Wang Lee (1986) documented sheath folds with NE-plunging fold axes in schists and marbles. Abundant shear structures, such as S-C fabrics in the granitic rocks, indicate a top-to-the northeast sense of shear.

**D. Mesozoic Tectonic Model**

Mesozoic tectonic history of this basement has been a debate for years due to the short of constraints. Two types of tectonic model have been proposed: the subduction type (Yui et al., 1988; Fig. 5A) and the collision type (Wang Lee and Wang, 1987; Fig. 5B).

**E. Cenozoic Exhumation Model**

The basement complex was covered by younger sediments during the Cenozoic rifting. Due to the Plio-Pleistocene to present arc-continental collision, the basement rock exhumed to the surface. Several mechanisms have been postulated to account for this exhumation (mountain building) process (Fig. 6): the critical wedge model (e.g., Davis et al., 1983), the discrete sequential thrusting model (Hwang and Wang, 1993), the lateral extrusion and normal faulting model (Byrne, 1995; Crespi et al., 1996), the lithospheric collision (Wu et al., 1997) and the subduction/extrusion model (Lin et al., 1998).

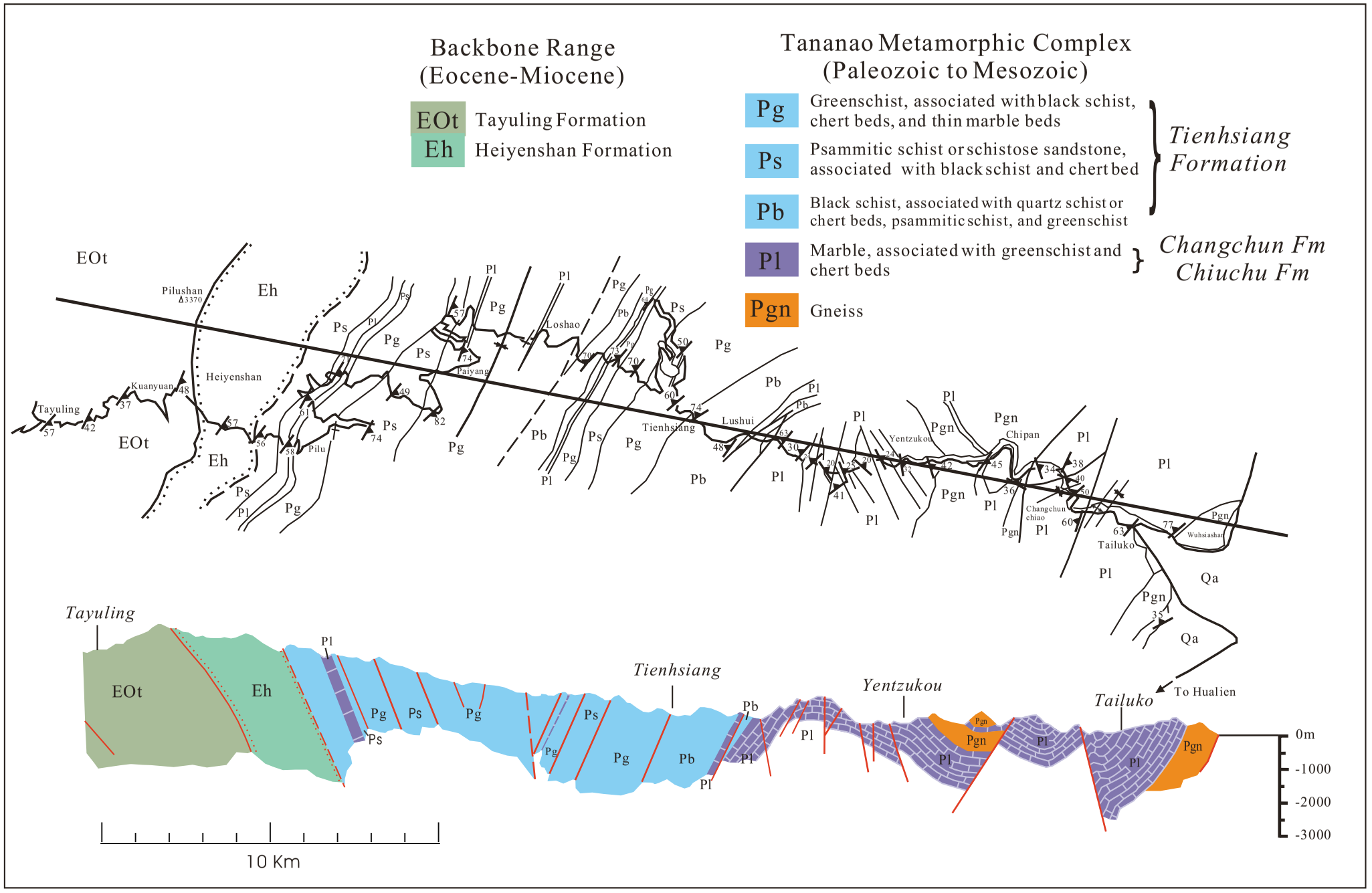


Figure 2. Geologic road map of the eastern part of the Central Cross-Island Highway (After Chen, 1979)

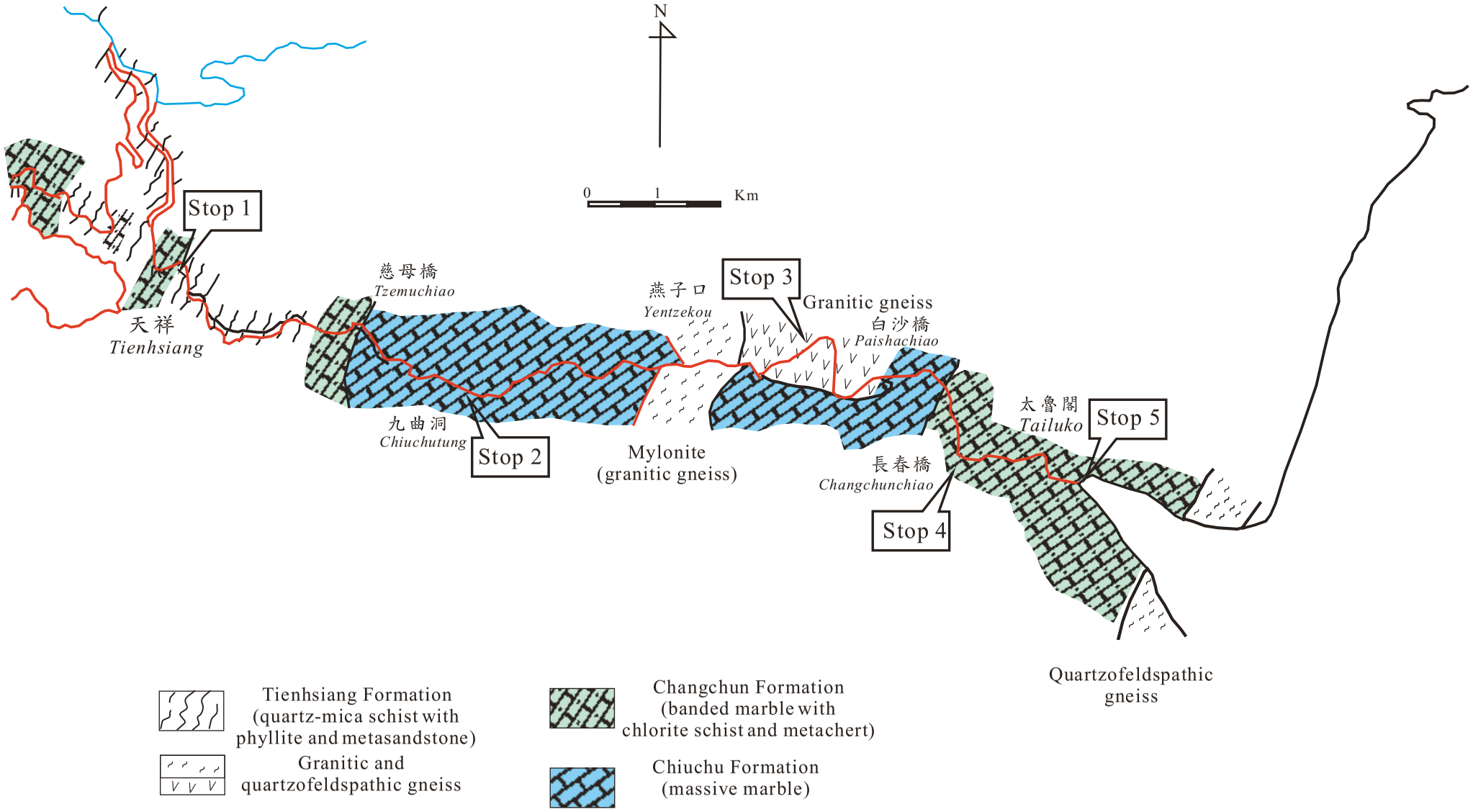


Figure 3. Geologic road map with marked field trip stops from the Tailuko to Tienhsiang area.

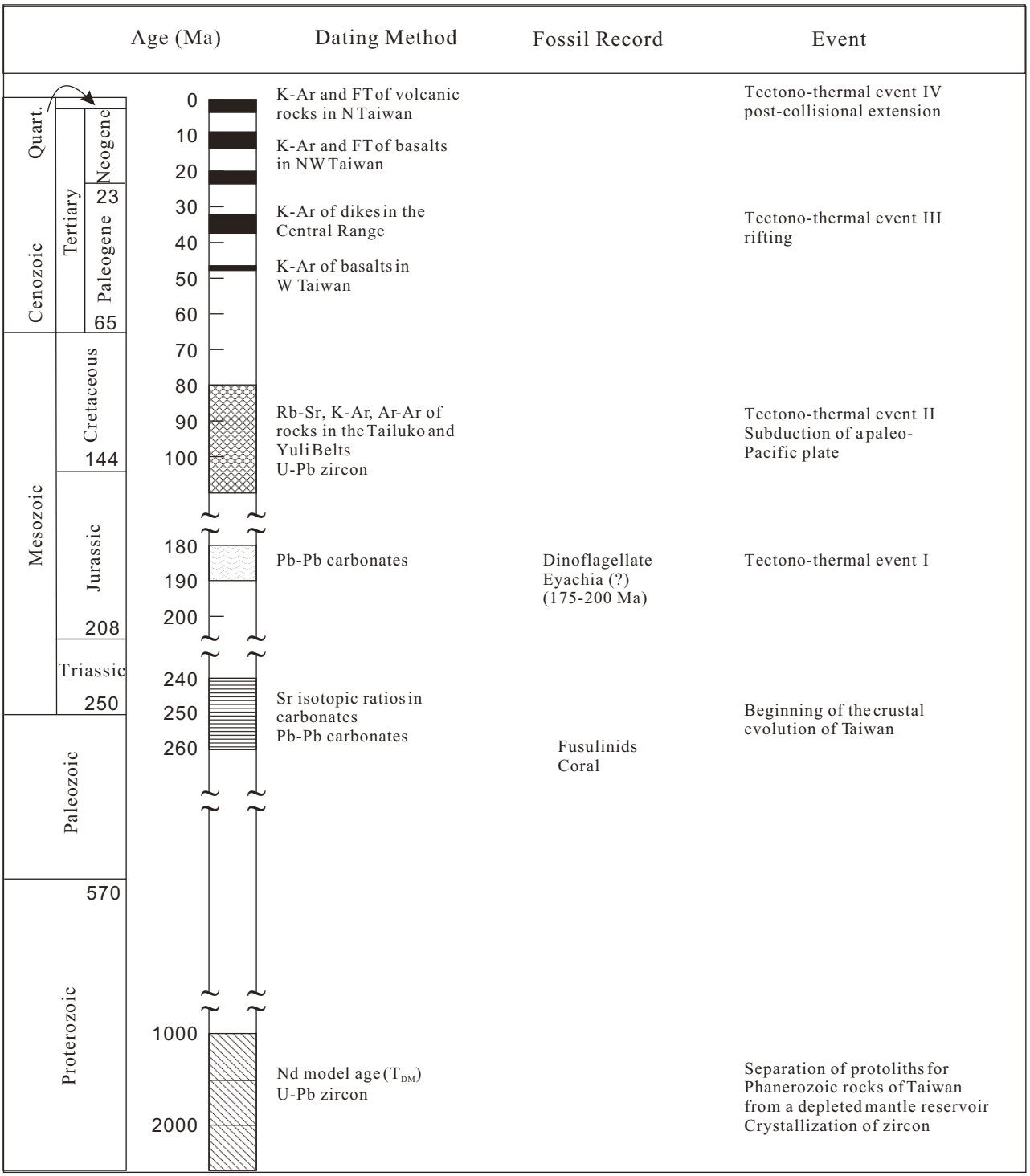


Figure 4. Summary of important tectono-thermal event in Taiwan (Lan et al., 1996)

(A)

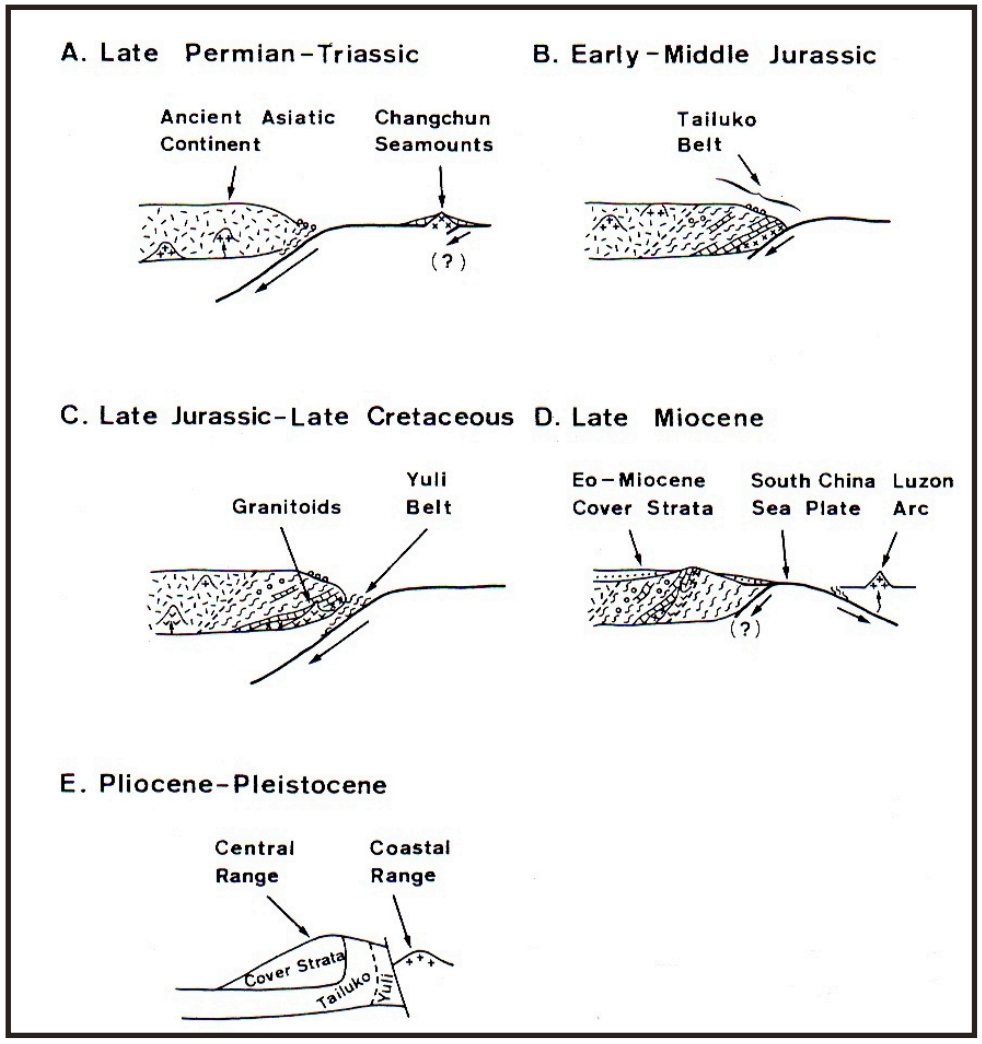


(B)

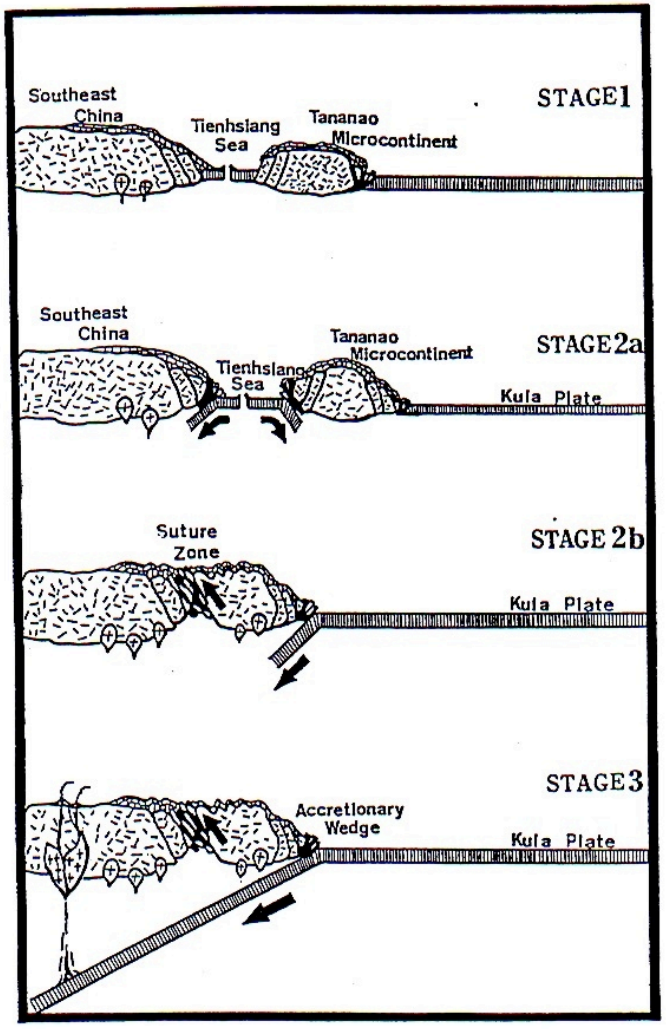


Figure 5. Two proposed tectonic models for the evolution of the Tananao metamorphic complex. (A) is from Yui et al.(1988) and (B) is from Wang Lee and Wang (1987).

(A) Davis et al. (1983)

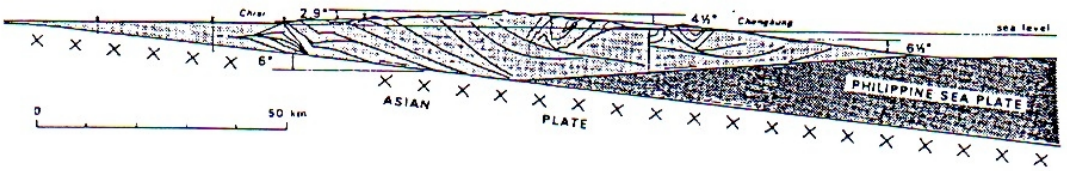


(B) Hwang and Wang (1993)

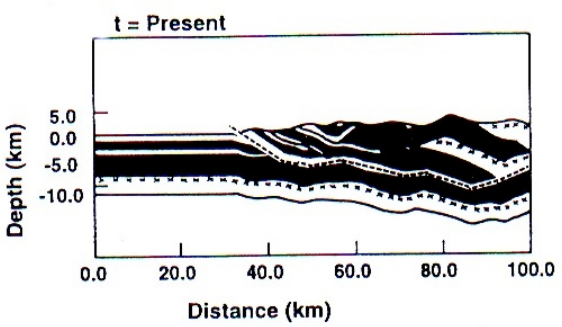


(C) Crespi et al. (1996)

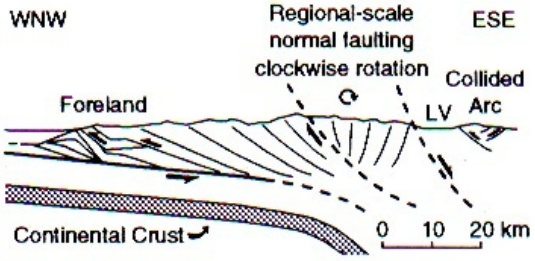


(D) Byrne (1995)

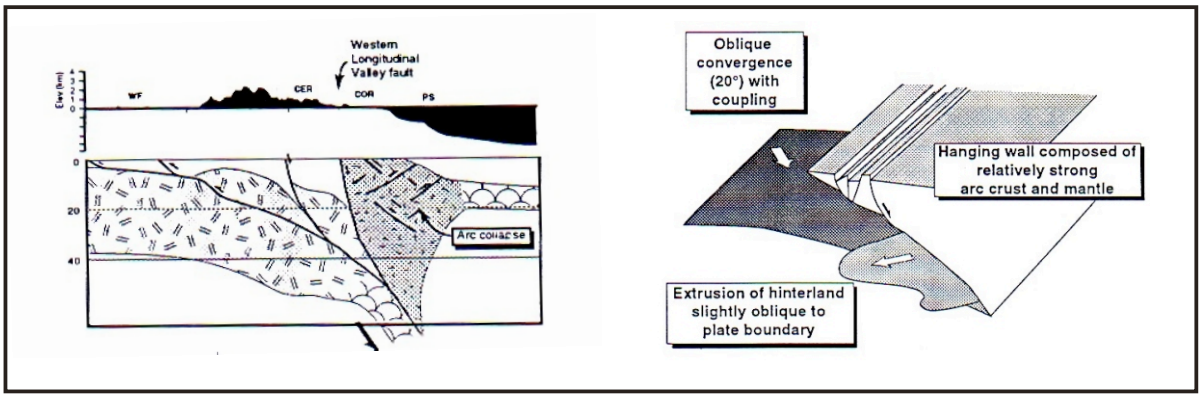


(E) Wu et al. (1997)

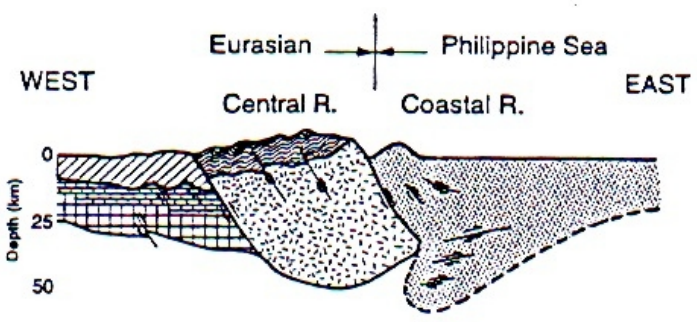


(F) Lin et al. (1998)

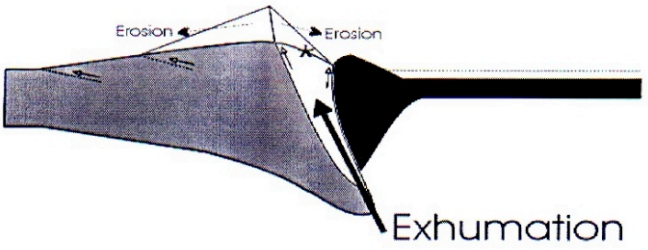


Figure 6. Models for the regional structure of the Taiwan mountain belt.

**Day 10: Hualien to Ilan**

(1) Transect of ductile deformation of the poly-metamorphosed basement and the slate belt along the Coast Road.

(2) Visit western extremity of the Okinawa Trough: the Ilan Plain

Sibuet, J. C., and Hsu, S. K.: How was Taiwan created?, Tectonophysics, 379, 159-186, 2004.

## How Taiwan was Created (A Summary)

- Since 9 Ma, the formation of Taiwan is controlled by the westward migration of the Philippine (PH) Sea plate within the torn Eurasia (EU) plate supposed to be fixed.
- 2. The PH Sea plate boundary A, which bounds to the west the Ryukyu subduction one, corresponds in the overlying terranes to a diffuse crustal boundary feature which limits present-day extensional processes east of A (northern Taiwan and Okinawa Trough) from contractional processes west of A. The westward motion of the PH Sea slab triggered the development of a tear fault inside the Eurasian continent. East of A, EU is torn and thus has two boundaries (relict T1). One is the upper plate, trench edge of the Ryukyu forearc; the other is the northern boundary of the deeply subducted EU slab underlying the PH Sea plate.
- 3. B corresponds to the limit between the oceanic and continental portions of the EU slab. The intraoceanic Luzon arc formed south of B above the oceanic portion of the subducting Eurasian lithosphere. North of B, the already formed Luzon arc collided with Eurasia, simultaneously with the subduction of a continental portion of Eurasian lithosphere. East of A, we suggest that the upper part of the Luzon arc accreted against the Ryukyu forearc while its lower part subducted beneath Eurasia.
- 4. The consequences of such a geodynamic model are:
  - The widely accepted notion of continuum from subduction to collision and finally to collapse might be taken with caution. The crustal strain changes from extension to compression across A might be linked to the presence of the underlying PH Sea slab edge. However, only faint strain and tectonic changes occur on each side of B, the ocean–continent boundary of the EU slab.
  - During the formation of the Okinawa Trough, its western tip moved simultaneously with A. The Okinawa Trough propagated westward in the proto-Taiwan orogen at the assumed 4.5 cm/year westward velocity, giving rise to the triangular shape of its southwestern extremity.
  - The bending of the southwestern Ryukyu subduction zone is due to the combination of two factors: the subduction of a portion of Eurasian continental lithosphere whose width increased through time and the westward propagation of the Okinawa Trough backarc basin.
  - Miocene arc volcanic rocks were never found in the southwestern part of the Ryukyu arc. We suggest that the portion of EU continental lithosphere, which subducted south of relict T1, included the portion of Miocene Ryukyu volcanic arc previously formed west of 126jE longitude.
  - The 150-km-wide oceanic domain located south of B between the Luzon arc and the Manila trench was progressively incorporated into the Eurasian plate north of B and then subducted beneath the Coastal Range simultaneously with the adjacent EU continental lithosphere.
  - The collision of the Luzon arc with EU triggered the development of a tear fault within the EU lithosphere and the initiation of continental subduction. Today, the slab pull force exerted by the continental subduction might be the fundamental mechanism giving rise to the Taiwan uplift, mostly by thinned-skinned tectonics.



AG

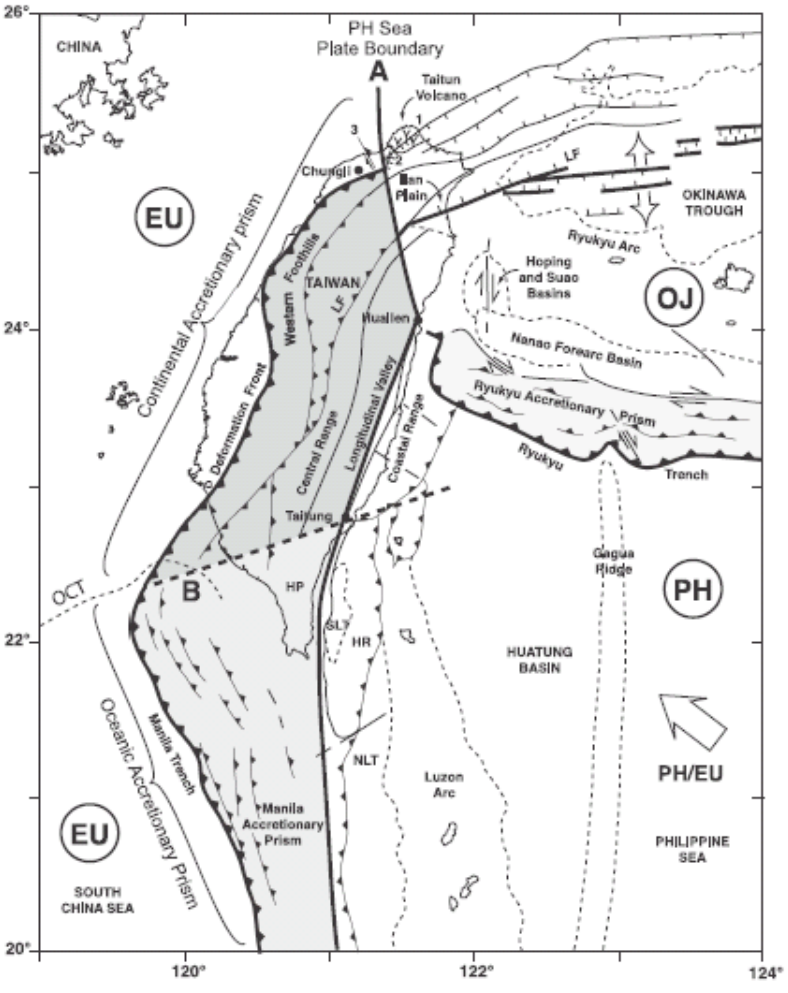


Fig. 4. Geodynamic context of the Taiwan area for northern Taiwan. A is the western boundary of the PH Sea plate and B is the ocean–continent transition (OCT) zone within the EU subducted slab (in the prolongation of the South China Sea OCT). East of A, in northern Taiwan and on the northeastern continental shelf, normal faults are reactivated thrust faults. Between A and B and south of B, all features are contractional. In light gray, Manila oceanic accretionary prism above the EU oceanic slab. In dark gray, Taiwan continental accretionary prism above the EU continental slab; HP, Hengchun peninsula; HR, Huatung ridge; IP, Ilan Plain; LF, Lishan fault and its extension in the Okinawa Trough. 1, Chinshan fault; 2, Shanjiao fault; 3, Nankan fault.

Fig. 5. 3-D Sketch of southern Taiwan. A is the western boundary of the PH Sea plate (thick lines). B is the boundary between the oceanic and continental parts of the EU slab located in the prolongation of the South China Sea ocean– continent transition (OCT) zone. The Manila oceanic accretionary prism and the Taiwan continental accretionary prism are in light and dark gray, respectively. CR, Coastal Range; HP, Hengchun peninsula; LA, Luzon arc; LV, Longitudinal Valley.

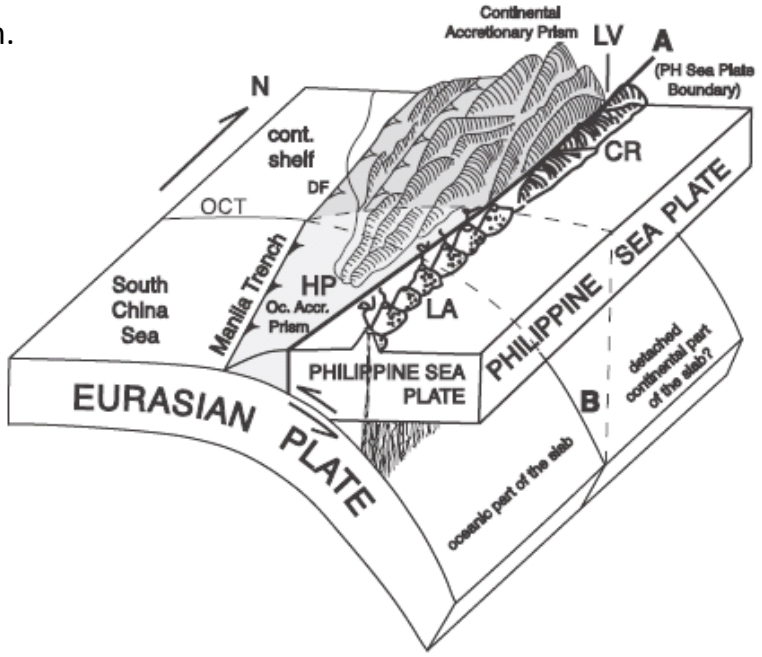

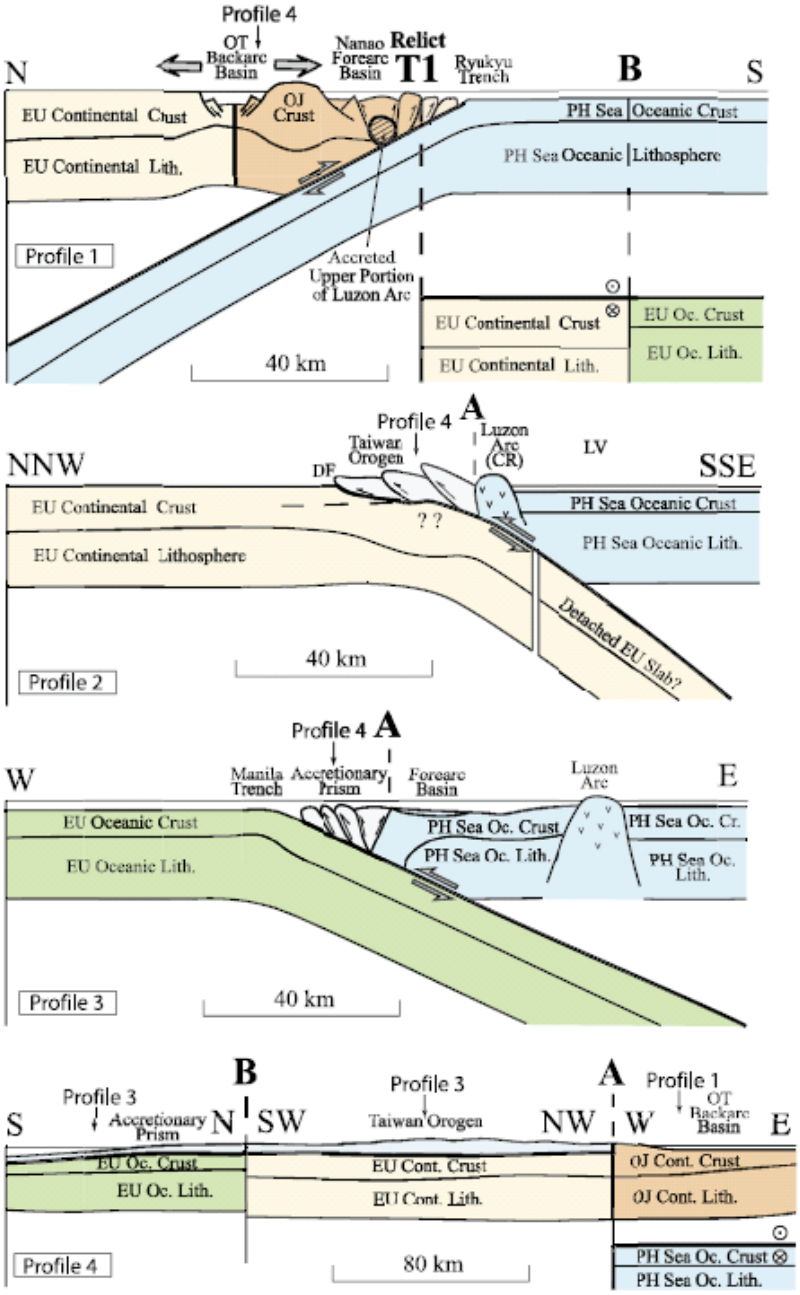


Fig. 8. Synthetic profiles located in Fig. 7 (dashed green lines) showing the nature and boundaries of Eurasia (EU), Philippine (PH) Sea and Okinawa-Japan (OJ) plates. In green, EU oceanic lithosphere; in yellow, EU continental lithosphere; in blue, PH Sea oceanic lithosphere, in orange, OJ lithosphere. In light blue, Philippines to northern Taiwan accretionary prism; in light orange, Ryukyu accretionary prism. The scale of profile 4 is half the one of other profiles.

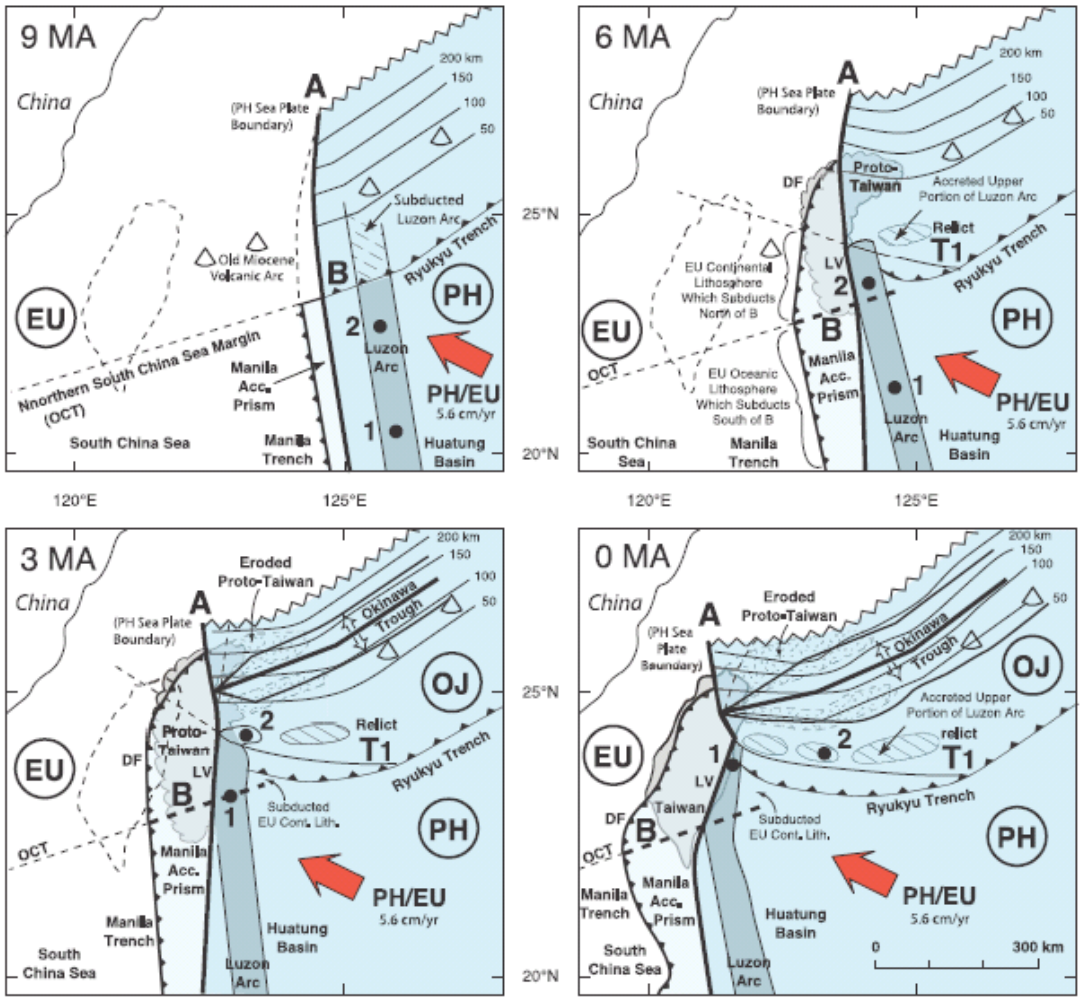


Fig. 10. Sketch of the geodynamic evolution of Taiwan. Eurasia (EU) is fixed. A is the western boundary of the Philippine (PH) Sea plate. Since 9 Ma, the PH Sea plate moved in the N307j direction at a constant 5.6 cm/year velocity. The uplift of proto-Taiwan is controlled by the westward motion of the PH Sea plate conveying the Luzon arc. The westward displacement of the PH Sea slab with respect to EU triggers the development of a tear fault inside the EU lithosphere. East of A, EU is torn and has two boundaries (relict T1). B is the boundary between the oceanic and continental parts of the EU slab [in the prolongation of the South China Sea ocean– continent transition (OCT) zone]. Thin continuous lines indicate depths of the Ryukyu slab (in km). Since 6 Ma, the beginning of Okinawa Trough (OT) opening, the OT tip is located above A and moves simultaneously with A, explaining the development of the southwestern OT within proto-Taiwan and the triangular shape of its western extremity. 1 and 2 are two fixed points of the Luzon arc whose tracks can be followed through time. As soon as a portion of the Luzon arc enters in the Ryukyu subduction zone, its upper part is accreted against the Ryukyu forearc while the lower part is subducted beneath EU. Volcanoes of the old Miocene volcanic arc located south of relict T1 have subducted simultaneously with the underlying EU continental lithosphere. DF, deformation front; LV, Longitudinal Valley; OJ, Okinawa-Japan plate. PH Sea plate in blue and Philippines to northern Taiwan accretionary prism in light blue.

## (1) Thrust, strike-slip and rotational tetonics of the northeastern coast

Taiwan Mountain Belt (Fig. 1) is an active curved collisional mountain belt and thrust wedge. It developed as a result of the late Cenozoic oblique convergence between the Philippine Sea plate and the Eurasian plate. The ENE-WSW-trending segment of northeastern Taiwan is composed of a mosaic of stratigraphic units which belong to the northern Hsiiehshan Range, the Western Foothills, the Coastal Plain, and the Pleistocene volcanics (Fig. 2). The late Cenozoic structure of this area is characterized by numerous NE trending folds and thrust faults, which developed together but were generally deformed by broadly spaced strike-slip faults and some normal fault systems. Plio-Quaternary normal faults are present in several basins and depression structures within the compressional mountain chain, such as the Taipei Basin, the Ilan Basin, and the Yenliao Depression together with the Chinkuashih goldcopper field (Fig. 2).

According to the slip line theory applied by geologists to collision with a wedge-shped indenter, based on field observations and tectonic analysis, and taking geophysical data and experimental modeling into account, Lu et al. (1995) interpret the curved belt of northern Taiwan in terms of contractional deformation (with compression, thrust-sheet stacking, folding and transcurrent faulting) combined with increasing block rotation, bookshelf-type strike-slip faulting and extension. Their tectonic model of northern Taiwan is summarized in Fig. 3A. The sketch of Fig. 3B illustrates the relationship between the major regional deformation modes, within the framework of oblique collision between the Chinese margin and an asymmetric wedge indenter representing the northwestern corner of the Philippine Sea plate (Fig. 1A).

They consider that the two conjugate strike-slip fault domains are the result of an indentation by a wedge-shaped backstop (Fig. 3). This indentation results not only in contractional tectonics across the belt, but also in divergent strike-slip components and block rotation, and in local occurrence of extension roughly parallel to the trends of the major units of the belt. They conclude that extensional structures such as the Taipei Basin developed in response to increasing belt curvature and related block rotations. Although the senses of strike-slip components and rotations are symmetrically distributed on both sides of the Tanshui River axis (Fig. 3A), due to the asymmetry of the collision, amounts of dextral strike-slip and clockwise rotation (to the east) are larger than amounts of left lateral strike-slip and anticlockwise rotation (to the southwest) (Fig. 3B). Contraction, transcurrent faulting, block rotation and even extension are four essential tectonic mechanisms dominating oblique convergence and collision tectonics.

Their major conclusion is that although significant changes have taken place during the Plio-Quaternary evolution of the Taiwan mountain belt (Fig. 1), most structures of the northeastern crescent-shaped belt (compressional, transcurrent and extensional) developed within a single overall tectonic mechanism (Fig. 3) that rotational tectonics and related space problem made complex.

## (2) Quaternary Tatun andestite volcanoes with hot spring and solfataras

The Tatun volcano group (TVG) is located in the northernmost part of Taiwan (Fig. 2) and was a result of episodic volcanisms between 2.8 and 0.2 Ma. It is a series of andesitic stratovolcanoes and lava



11 - 1

domes. About 20 volcanoes, the southernmost of which is only 15 km north of the capital Taipei, are included in the group. The highest and youngest volcano in TVG is Chisingshan (1120 m, Fig. 4). Hot springs, fumaroles, and solfataras are found over wide areas, and exploration for geothermal resources has been carried on for many years.

Earthquake data of over 30 years are analyzed to explore seismicity patterns and their associated mechanisms of faulting in the area. The focal mechanism solutions in TVG region are dominated by normal faulting, and most high frequency seismicity appeared to be concentrated near the areas of hydrothermal activity, forming tight clusters at depths shallower than 4 km. The occurrence of spasmodic bursts, mixed/low frequency events and a high *b*-value indicate that a magma chamber may still exist beneath TVG and that a future eruption or period of unrest should not be considered unlikely.

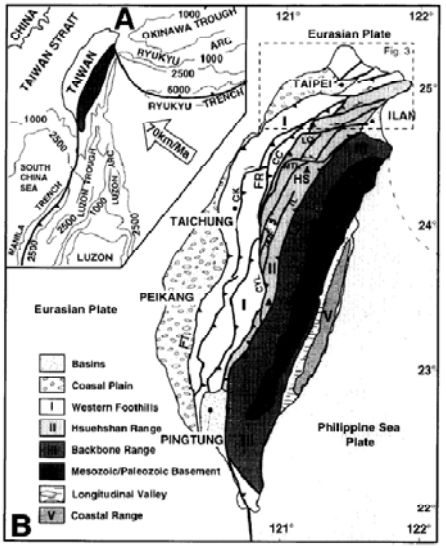


Fig. 1. Geodynamic setting (A) and tectonic map (B) of Taiwan. In (A), isobaths are in meters, and large open arrow shows the direction of convergence (Philippine Sea Plate relative to Eurasia). In (B), main tectonic units are shown following Ho (1986b) and Biq (1989). Major thrust faults are indicated as heavy lines with triangles on the upthrust side. *CC* = Chiuchih Fault; *CK* = Chukou Fault; *CYL* = Chenyulanchi Fault; *FR* = Frontal Range Thrust (Chishan-Chinkuashih line); *FT* = Foothill Thrust (Kaohsiung-Tanshui Dine); *LO* = Loshan Fault: *LS* - Plate Boundary Fault (Hungchun llan line); *MTL* = Matalanchi Fault; *TL* = Tili Fault; *YS* = Yushan.

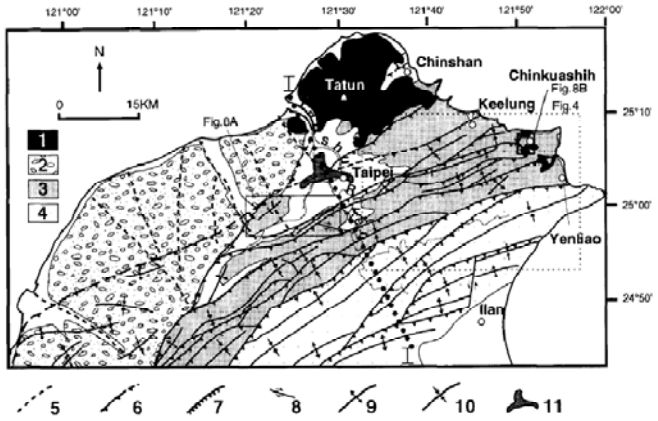


Fig. 2. Location map and general structures interpreted from the geological maps (Ho, 1986a,b) and SLAR (Side Looking Airborne Radar) image of Taiwan (Mars Inc., 1981). Keys: 1 = Pleistocene volcanic rocks; 2 = Pleistocene conglomerate; 3 = Western Foothills; 4 = Hsiiehshan Range; 5 = major fracture; 6 = thrust fault; 7= strike-slip fault; 8 = normal fault; 9 = anticline axis; *10* = syncline axis; *11* = T-shaped Taipei Basin indicated by the 250-m isopach of the Tertiary basement (after Wang Lee et al., 1978 and Consulting Engineers, 1989).

**(Fig. 1, Fig. 2 and Fig. 3 are taken from Lu et al. (1995), and Fig. 4 is from Konstantinou et al. (2007))**



11 - 2

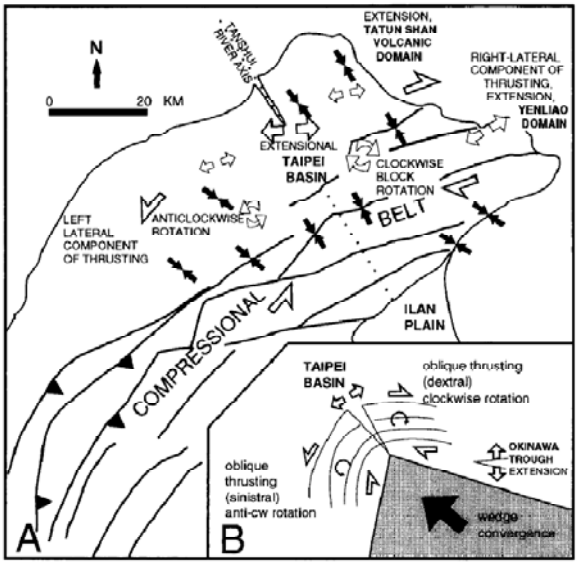


Fig. 3. Model of Plio-Quaternary tectonic deformation in the foreland thrust belt of northern Taiwan, as reconstituted in this paper. Note the existence of three major domains: (1) the eastern domain characterized by oblique-slip thrusts superimposed by major right-lateral strike-slip and bulk clockwise rotation deformation; (2) the central domain characterized by indentation and extensional deformation; (3) the western domain where major left-lateral oblique thrusting superimposed by right-lateral bookshelf-type strike-slip and bulk anticlockwise rotation dominates. (A) Interpretative map. (B) Explanatory sketch.

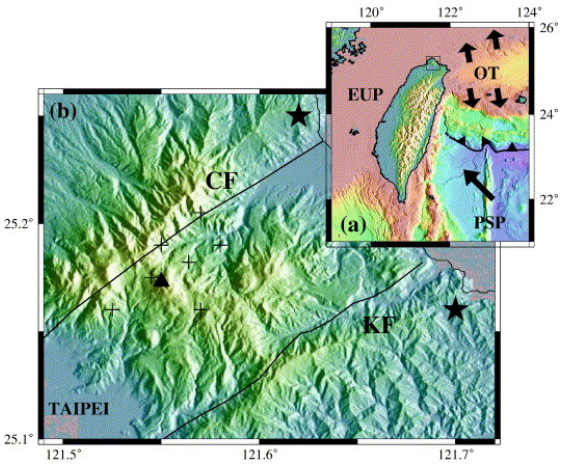


Fig. 4. (a) Map showing the regional tectonic setting and relative motion between the Philippine Sea plate (PSP) and the Eurasian plate (EUP) indicated by an arrow, as well as the opening of the Okinawa Trough (OT) backarc basin. The square in northern Taiwan shows the area of interest. (b) Map showing the area of the Tatun Volcano Group (TVG). The thick line to the south indicates the Kanchiao fault (KF), while that in the north the Chinshan fault (CF). The triangle represents the peak of the Chihsinshan volcanic cone (1120 m), the crosses indicate the place of hot spring/fumarole activity after Yang et al. (1999) and the stars show the positions of the two nuclear power plants. Part of the Taipei sedimentary basin can be seen at the lower left corner of the map.

## Reference

Kim, K. H., C. H. Chang, K. F. Ma, J. M. Chiu and K.C. Chen (2005). Modern seismic observations in the Tatun volcano region of northern Taiwan: seismic/volcanic hazard adjacent to the Taipei metropolitan area. Terr. Atm. Ocean. Sci., 2005, 16: 579–594.

Konstantinou, K. I., C. H. Lin and W. T. Liang (2007). Seismicity characteristics of a potentially active Quaternary volcano: The Tatun Volcano Group, northern Taiwan. *Journal of Volcanology and Geothermal Research,* 2007, 160: 300-318.

Lu, C.Y., J. Angelier, H.T. Chu, (1995). Contractional, transcurrent, rotational and extensional tectonics: examples from Northern Taiwan. *Tectonophysics*, 1995, 246: 129-146

http://www.moeacgs.gov.tw/english/twgeol/twgeol_western_27.jsp